Development of a Fast and Efficient Liposomal Drug Loading Technology for Poorly Water Soluble Drugs: Formulation, Characterization, and Potential Applications

by

Wei-Lun Tang

B.Sc., National Taiwan University, 2009

A THESIS SUBMITTED IN PARTIAL FULFILLMENT OF

THE REQUIREMENTS FOR THE DEGREE OF

Doctor of Philosophy

in

THE FACULTY OF GRADUATE AND POSTDOCTORAL STUDIES

(Pharmaceutical Sciences)

The University of British Columbia

(Vancouver)

October 2018

The following individuals certify that they have read, and recommend to the Faculty of Graduate and Postdoctoral Studies for acceptance, the dissertation entitled:

Development of a Fast and Efficient Liposomal Drug Loading Technology for Poorly Water Soluble Drugs: Formulation, Characterization, and Potential Applications

submitted by Wei-Lun Tang in partial fulfillment of the requirements for the degree of Doctor of Philosophy in Pharmaceutical Sciences

Examining Committee:

Dr. Shyh-Dar Li, Faculty of Pharmaceutical Sciences
Supervisor

Dr. Christian Kastrup, Department of Biochemistry
Supervisory Committee Member

Supervisory Committee Member

Dr. Harvey Wong, Faculty of Pharmaceutical Sciences
University Examiner

Dr. Jayachandran Kizhakkedathu, Department of Pathology & Laboratory Medicine
University Examiner

Abstract

More than 70% of drugs exhibit poor water solubility, thereby limiting their clinical applications. Formulating these drugs into liposomes is a feasible approach to increase their solubility and improve the therapeutic efficacy. However, encapsulating hydrophobic drugs into the lipid bilayer of liposomes often results in burst drug release and liposomal instability, due to the weak association between the drugs and the lipid bilayer. Additionally, the capacity of the lipid bilayer is limited, leading to inefficient drug loading. To address this issue, this thesis focused on developing a new loading technology, called **Solvent-assisted Active Loading Technology** (SALT), to allow stable and efficient loading of poorly water-soluble drugs into the aqueous core of liposomes.

This technology involved the addition of a certain amount of a water-miscible organic solvent into the mixture of a poorly soluble drug and preformed liposomes incorporated with a trapping agent inside the aqueous core. The solvent was not only used to help drug dissolution, but also to facilitate drug permeation into the liposomal core to form drug complexes with the trapping agent by increasing the membrane permeability during the drug loading. We have generated multiple examples to demonstrate the robustness and potential utilities of this technology.

As a proof-of-principle, the first part of the thesis focused on developing the SALT for stable loading of a model drug, staurosporine (STS, insoluble weakly basic drug), into liposomes and optimizing the fabrication of a liposomal STS formulation for *in vivo* therapy of tumor.

The second part of this dissertation was to explore whether the SALT is a flexible platform for formulating other types of poorly soluble drugs such as gambogic acid (GA, insoluble weakly

acidic drug) into liposomes. We also examined whether other miscible solvents (other than DMSO) could be utilized in the system and their roles in promoting drug loading.

The third part of this thesis was to demonstrate another utility of the SALT for preparing an oral pediatric formulation of mefloquine with bitterness masking.

This thesis work demonstrated that SALT was a robust drug loading technology to develop stable liposomal formulations for poorly soluble drugs with practical utilities.

Lay Summary

Drugs need to be solubilized in order to be absorbed by human body. Many developing or clinically used drugs are poorly water soluble, limiting their clinical efficacy. In this thesis, we developed a new technology to formulate these drugs to improve their solubility. Different drugs, various preparation procedures and multiple formulation parameters were investigated to optimize this technology. Multiple examples of drug formulations were generated to demonstrate the robustness and utility of this platform technology, including more effective and safer formulations for anticancer drugs and a platform for producing child-friendly oral formulations.

Preface

The studies presented in this dissertation were conceived and designed by myself and Li SD. Development and analysis of all liposomal formulations, and all the subsequent *in vitro* experiments were performed by myself. I was responsible for preparing all the manuscripts included in this dissertation.

The portion of the content in Chapter 1 was revised and adapted from the following reviews:

> Tang WL, Li SD (2018). Encapsulation Methods of poorly water soluble drug into liposomes, in preparation.
>
> **Tang WL**, Tang WH, Li SD (2018). "Cancer Theranostic Applications of Lipid-based Nanoparticles". 2018, ***Drug Discovery Today***, 2018 May;23(5):1159-1166.

The research described in Chapter 2 has been published in ***Pharmaceutical Research***:

Tang WL, Chen WC, Roy A, Undzys E, Li SD (2016). "A Simple and Improved Active Loading Method to Efficiently Encapsulate Staurosporine into Lipid-Based Nanoparticles for Enhanced Therapy of Multidrug Resistant Cancer." 2016 May;33(5):1104-14.

Animal studies were conducted with the assistance of Dr. Weihsu Claire Chen, Dr. Aniruddha Roy, and Mr. Elijus Undzys. CryoTEM imaging was performed by Mr. Jayesh Kulkarni (a PhD student from Dr. Pieter Cullis' laboratory).

The study in Chapter 3 has been published as a research article in ***Biomaterials***:

Tang WL, Tang WH, Szeitz A, Kulkarni J, Cullis P, Li SD (2018). "Systemic Study of Solvent-Assisted Active Loading of Gambogic Acid into Liposomes and its Formulation Optimization for Improved Delivery." 2018 Jun;166:13-26.

Ms. Wei-Hsin Tang assisted me to prepare liposomal formulations for the *in vivo* study. CryoTEM imaging was performed by Mr. Jayesh Kulkarni (a PhD student from Dr. Pieter Cullis' laboratory). The analytical method for gambogic acid was developed by **myself with the assistance of** Mr. Andras Szeitz.

The research described in Chapter 4 has been published as a research article in ***Molecular Pharmaceutics***:

Tang WL, Tang WH, Chen WC, Diako C, Ross CF, Li SD (2017). "Development of a Rapidly Dissolvable Oral Pediatric Formulation for Mefloquine Using Liposomes." 2017 Jun 5;14(6):1969-1979. Wei-Hsin Tang assisted me in preparing liposomal formulations for the *in vivo* studies. Oral administration for the PK study was assisted by Dr. Weihsu Claire Chen. Bitterness masking measurement was performed by Dr. Charles Diako from Dr. Carolyn Ross's laboratory, School of Food Science at the Washington State University, Pullman, Washington, USA.

Some of the contents presented in Chapter 5 have been published as a review in ***Drug Discovery Today***:

Tang WL, Tang WH, Li SD (2018). "Cancer Theranostic Applications of Lipid-based Nanoparticles". 2018 May;23(5):1159-1166.

All procedures involving animals presented in this dissertation were approved by the Animal Care Committee at The University of British Columbia and were performed in accordance with guidelines established by the Canadian Council on Animal Care.

Animal Care and Ethics Protocol: A14-0198-A003

Animal Care and Ethics Training Certificate: 6682-14, RBH-932-10, RA-133-11, RSx-71-12

Table of Contents

List of Tables

List of Figures

List of Abbreviations

Abbreviation	Definition
API	Active pharmaceutical ingredient
AUC	Area under the concentration-time curve
BCl-2	B-cell lymphoma 2
BPCA	Best Pharmaceuticals for Children Act
Chol	Cholesterol
CIHR	Canadian Institutes of Health Research
CL	Clearance
C_{max}	Maximum concentration in plasma
Cryo-TEM	Cryo-transmission electron microscopy
DMF	Dimethylformamide
DMSO	Dimethyl sulfoxide
DOPC	1,2-dioleoyl-sn-glycero-3-phosphocholine
DSPC	1,2-distearoyl-sn-glycero-3-phosphocholine
DSPE-mPEG$_{2000}$	1,2-distearoyl-sn-glycero-3-phosphatiylethanol-amine-N-[methoxy (polyethyleneglycol)-2000
DTX	Docetaxel
EPR	Enhanced permeability and retention
E-tongue	Electronic tongue
EtOH	Ethanol
GA	Gambogic acid
GA-Lipo	Gambogic acid encapsulated liposomes
HBS	HEPEs buffered saline
H&E	Hematoxylin and eosin
HEPEs	4-(2-hydroxyethyl)-1-piperazineethanesulfonic acid
IC_{50}	Half maximal inhibitory concentration
i.p.	intraperitoneal

i.v.	Intravenous
LNPs	Lipid nanoparticles
Mef	Mefloquine
Mef-Lipo	Mefloquine encapsulated liposomes
MeOH	Methanol
MPS	Mononuclear phagocyte system
MRT	Mean residence time
MTDs	Maximum tolerated doses
MSPC	1-myristoyl-2-stearoyl-sn-glycero-3-phosphocholine
NF-kb	Nuclear factor-κB
NMP	N-Methyl-2-pyrrolidone
PEG	Polyethylene glycol
RBCs	Red blood cells
RES	Reticulo-endothelial systems
SALT	Solvent-assisted active loading technology
SBE-β- CD	Sulfobutyl ether-β-cyclodextrin
s.c.	Subcutaneous
STAT3	Signal transducer and activator of transcription 3
STS-Lipo	Staurosporine encapsulated liposomes
$t_{1/2}$	Half-life
UPLC	Ultra-performance liquid chromatography
VEGF-A	Vascular endothelial growth factor A
Vss	Estimated volume of distribution at steady state
w/w	Weight/weight

Acknowledgements

I would like to express my sincere gratitude and appreciation to my supervisor, Dr. Shyh-Dar Li, for his enormous motivation, continuous support, and mentorship throughout my graduate studies and research career. He is not only my supervisor, but also my life mentor, inspiring and helping me navigating my career, such as communication and interpersonal skills, project management, scholarship applications, etc, by sharing his experience and wisdom without hesitation. The most important thing that I learn from him is "never give up and always have faith in myself". Over the past 4 years, I have been through many setbacks and failures in my research or scholarship/award applications. Thanks to his encouragement and inspiration, these failures did not affect my determination to keep trying. Instead, those experiences have taught me that success requires persistence and strong belief. I am very fortunate and grateful to have him as my supervisor.

I am also extremely grateful for the kind academic support and invaluable scientific advice from Dr. Marcel Bally, Dr. Urs Hafeli, and Dr. Christian Kastrup, during my graduate studies. I greatly appreciate them for the opportunities to practise my presentation in their labs and attend their group meetings, in order to learn how to improve my presentation skills and to discuss collaboration possibility between the labs, related to research expertise in the field of drug delivery, particularly in drug encapsulation using liposomes. I would also like to thank Dr. Judy Wong and Dr. Adam Frankel for organizing every committee meeting. Without their help, I could not host committee meeting smoothly in time.

I also would also like to acknowledge the financial support from the Canadian Institutes of Health Research (CIHR) with Banting and Charles Best Canada Graduate Scholarship, and the

University of British Columbia with Four Year Fellowship (4YF) Tuition Award. These financial supports allowed me to focus on completing my PhD study without financial concern.

Next, thanks to our collaborators' contributions and cooperation, the thesis could be finished as scheduled. Their scientific contributions are acknowledged at the end of each chapter of this thesis.

I am thankful for the lab members whom I have worked for their constructive suggestions on my research projects in every group meeting and their friendship.

I also would like to express my appreciation and gratitude to the Faculty of Pharmaceutical Sciences, UBC for providing me an excellent environment with numerous collaboration opportunities and strong technical and research supports.

Lastly, I would like to thank my family. To my parents and my sister, Sophia, thank you for all your support throughout my life and more specifically during the past four years. I know I could not have done it without your continuous encouragement and support.

The thesis is dedicated to my parents and my sister

Chapter 1: Introduction

1.1 Challenges in Delivery of Poorly Water Soluble Drugs

More than 70% of drugs exhibit poor water solubility, which largely limit their clinical applications. A few strategies have been implemented to improve drug solubility, including pH adjustment [1], amorphous solid dispersion methods [2], inclusion of co-solvents and surfactants in the formulation [3], and nano- or micro-technology [4, 5]. The solubility of ionizable drugs can be increased by adjusting the pH of the solution to promote ionization. However, the pH should be in the range of 5-9 to ensure safe administration. It is also crucial that the drug remains soluble after it is administered to ensure safety and efficacy [6]. Maintaining drug in its amorphous state improves its solubility and dissolution rate, leading to improved oral absorption. The solubility of a compound in the amorphous form is higher than that in the crystalline form, due to the higher Gibbs energy, which allows the drug to disperse in an aqueous solution in a supersaturation state [7]. Several water-soluble polymers, such as PEG, HPMC and PVP, have been used as an excipient to maintain the supersaturated state in the gastrointestinal (GI) tract. There are several approaches to prepare amorphous solid dispersions (ASDs), including fusion method spray drying, solvent evaporation method, and hot melt extrusion [8]. However, ASDs are only suitable for oral formulations due to the relative instability of amorphous form in a liquid [9]. The use of water-miscible solvents and surfactants can also improve drug solubility, including propylene glycol, polyethylene glycol, ethanol, polysorbate 80, and Cremophor EL (CrEL). However, one of the major risks of using these solvents and surfactants is that they may provoke hemolysis and hypersensitivity reactions, leading to severe side effects, such as vascular irritation, anemia, phlebitis, and acute renal failure [10, 11]. For instance, Taxol®, an i.v. formulation of paclitaxel, prepared in CrEL and EtOH, was reported to cause significant

hypersensitivity reactions, which are primarily ascribed to CrEL [12]. Similarly, hypersensitivity reactions were also observed in patients treated with Taxotere®, a docetaxel formulation prepared with polysorbate 80 [13]. Therefore, the type of excipients used for i.v administration need to be carefully considered. Micro/nanotechnology has been extensively utilized to improve delivery of poorly water-soluble drugs with clinically approved products [14]. Insoluble drugs are encapsulated in the hydrophobic compartment of small particles to improve the solubility and dissolution. These formulations include microparticles, polymeric micelles, solid lipid nanoparticles, micro- or nano-emulsions, polymer-lipid hybrid nanoparticles, and liposomes [15, 16]. Among these micro/nanoparticulate systems, liposomes are the most established drug delivery vehicle. In the following section, liposomal drug delivery system is reviewed.

1.2 Liposomes for Drug Delivery

Liposomes are artificial vesicles with an aqueous core surrounded by a unilaminar or mutilaminar lipid membranes. This unique feature allows water-soluble and fat-soluble drugs to be entrapped within the aqueous core and the lipid bilayer, respectively. Liposomes have been widely used in pharmaceutical, cosmetic and food industry [17, 18]. There are more than 15 liposomal products on the market for several medical indications including cancer, infections, and eye diseases (**Table 1.1**). Most of them are employed for cancer therapy.

Table 1. 1 FDA approved liposomal Drugs

Brand name	API†	Approved date	Encapsulation method	Indications*
Abelcet	Amphotericin B	1992	Passive encapsulation	Invasive fungal infections
Ambisome	Amphotericin B	1992	Passive encapsulation	Invasive fungal infections
Doxil (U.S) /Caelyx (Canada)	Doxorubicin	1995	Active loading	Ovarian Cancer HIV-Associated Kaposi's Sarcoma Multiple Myeloma
DaunoXome	Daunorubicin	1996	Active loading	HIV-Associated Kaposi's Sarcoma
DepoCyt	Cytarabine	1999	Passive encapsulation	Lymphomatous meningitis
Visudyne	Verteporfin	2000	Passive encapsulation	Subfoveal choroidal neovascularization
DepoDur	Morphine	2004	Passive encapsulation	Pain pre/post-surgery
Exparel	Bupivacaine	2011	Passive encapsulation	Postsurgical analgesia
Marqibo	Vincristine	2012	Active loading	Philadelphia chromosome-negative acute lymphoblastic leukemia
Onivyde	Irinotecan	2015	Active loading	Pancreatic adenocarcinoma
Vyxeos	Daunorubicin cytarabine	2017	Active loading	newly-diagnosed therapy-related acute myeloid leukemia (t-AML) or AML with myelodysplasia-related changes (AML-MRC)

* indications were adapted from the Lexicomp database. †Active pharmaceutical ingredient

Liposomes can be produced using different techniques including sonication, thin-film hydration, reverse phase evaporation, and microfluidic mixing. The producing method influences liposome properties such as size, lamellarity, and drug encapsulation [19-21]. Thin-film hydration is the most commonly used method to prepare liposomes, due to its high reproducibility and simplicity. Lipids are dissolved in an organic solvent, such as chloroform and ethanol, followed by evaporation to form a dried thin film. Liposomes can self-assemble to form multilamellar vesicles after hydration of the thin film with an aqueous solution. Their

size, size distribution, and lamellarity can be further controlled by extrusion or sonication. Additionally, the liposomal surface can be modified for various purposes, including PEGylation (PEG, polyethylene glycol) for prolonged systemic circulation, attachment of a targeting ligand for cell-specific delivery, or an imaging agent for diagnosis or non-invasive monitoring of the biodistribution. The presence of PEG on the surface of liposomes introduces steric hindrance to reduce serum protein binding to the liposomes, thus minimizing the uptake by the mononuclear phagocyte system (MPS) and prolonging the circulating half-life [22, 23]. PEGylation also confers liposomes improved stability and resistance against aggregation. These features allow nano-sized liposomes (<200 nm) with extended circulation to passively accumulate in the tumor exhibiting a leaky vasculature and destructed lymphatic drainage. This phenomenon is called the enhanced permeability and retention (EPR) effect [24]. In contrast to tumors, the endothelial lining in most normal tissues is tight, preventing effective extravasation of liposomes.

Apart from parenteral delivery, liposomes have also been used to improve drug delivery through various administration routes, including oral, inhalation, and transdermal [25]. It is believed that liposomes can protect drugs at the absorption site and harness different absorption mechanisms to improve drug transport through the epithelial barrier [26].

1.3 Drug loading in liposomes

In general, drugs can be encapsulated into liposomes by either a passive or active (remote) loading method, as shown in **Figure 1.1**.

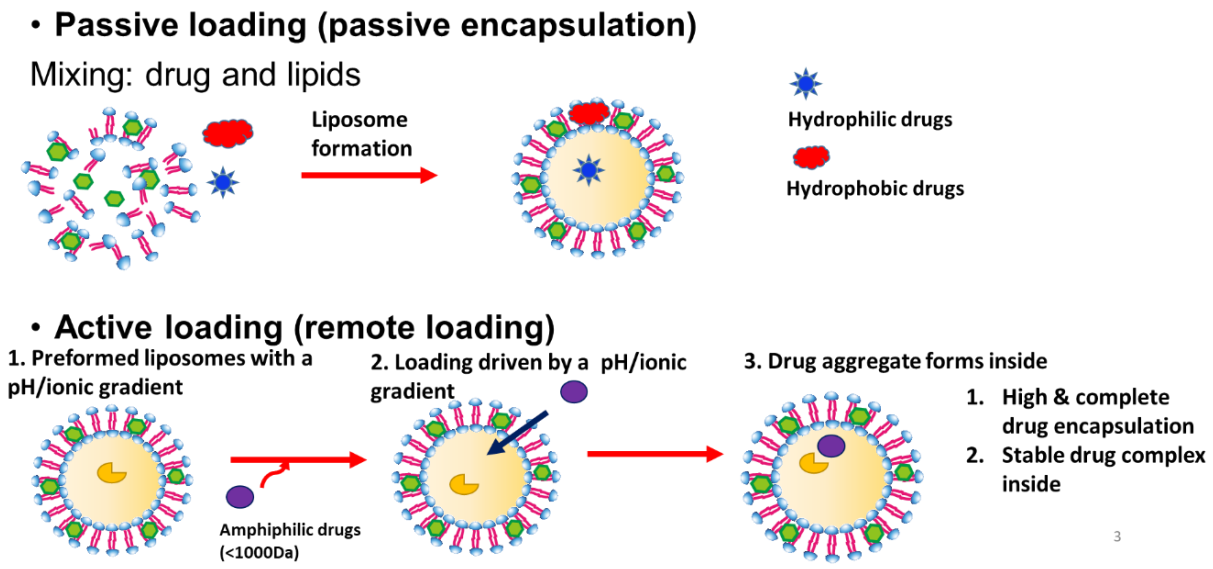

Figure 1. 1 Current drug loading methods used to encapsulate drugs into liposomes.

Passive loading includes the procedure where the lipid and drugs are dispersed in aqueous buffer to achieve drug entrapment while the liposomes are formed. In general, hydrophilic agents are passively incorporated into the aqueous core, whereas hydrophobic drugs are retained inside the lipid bilayer of liposomes, respectively. Specifically, hydrophobic drugs are first dissolved with lipids in an organic solvent, followed by solvent evaporation to prepare a drug containing thin film, which is later hydrated with an aqueous phase containing a water soluble drug to prepare liposomes. The trapping efficiency of this method varies due to several factors, including drug solubility, vesicle size, lipid concentration, and preparation procedure [27]. In most cases, the typical drug-to-lipid ratio (D/L) achieved by this passive loading technique is less than 0.05 (w/w) [28, 29]. In addition, the entrapped drugs often cannot be retained stably due to weak association between the drugs and the liposomes, resulting in poor drug retention and storage stability. On the other hand, active loading promotes formation of stable drug complexes inside the aqueous core of liposomes, thus providing improved drug

retention and formulation stability. In addition, it also allows complete drug encapsulation at a higher D/L (> 0.2, w/w).

In general, a water soluble amphiphilic weak base or acid with a logD (distribution coefficient between ionized form and un-ionized form) in the range of -2.5 to 2.0 at pH 7 [30] is a preferred candidate for active loading into cholesterol containing liposomes through a transmembrane gradient, such as pH (**Figure 1.2A**), ammonium sulfate (**Figure 1.2B**), metal salts (**Figure 1.3**), or other trapping agents such as EDTA, polymers, etc [31-35]. As shown in **Table 1.1**, about half of the clinically approved liposomal drugs are prepared using an active loading method. For instance, irinotecan can be efficiently and stably loaded into the preformed liposome with a metal ion gradient (inner: 300 mM $CuSO_4$ or $ZnSO_4$; external: neutral buffer at pH 7) at a D/L of 0.2 (mol/mol) after 10 min of incubation at 50 ºC with a high encapsulation efficiency of >98% [36]. Likewise, topotecan, doxorubicin, vincristine, and diclofenac could be actively loaded into liposomes containing a copper, manganese, and calcium gradient, respectively [37-39]. The actively loaded drug molecules form insoluble drug crystals or complexes with specific counter ions in the aqueous core of liposomes [33, 40-53]. This mechanism locks the drug molecules efficiently and stably inside the liposomes. Relative to passive loading, the formulation prepared with active loading displays an increased D/L [40] and extended PK [43, 54-56]. Doxil®(PEGylated liposomal doxorubicin) is the first FDA approved liposomal drug with prolonged PK and reduced toxicity, and has been used clinically and exploited as a prototype for developing liposomal formulations [57]. In this formulation, DOX, a weak base, is loaded into liposomes containing phospholipids and cholesterol (>40 %mol) via a transmembrane gradient of ammonium sulfate (**Figure 1.2B)**.

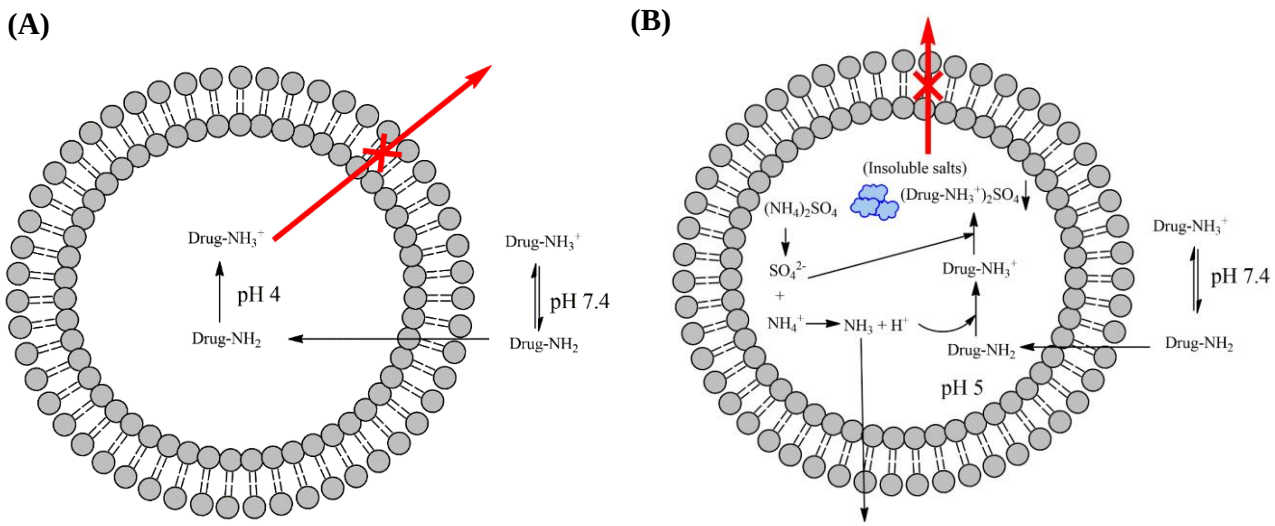

Figure 1. 2 Mechanism of active loading of a weakly basic drug into the intraliposomal aqueous phase by a (A) pH gradient or (B) ammonium sulfate gradient. An amphipathic weakly basic drug in the non-ionized form can diffuse through the lipid bilayer under heating (slightly above the transition temperature of the bilayer), and then be protonated in the low pH aqueous core (pH gradient) and form membrane impermeable aggregates with sulfate ions (ammonium sulfate gradient).

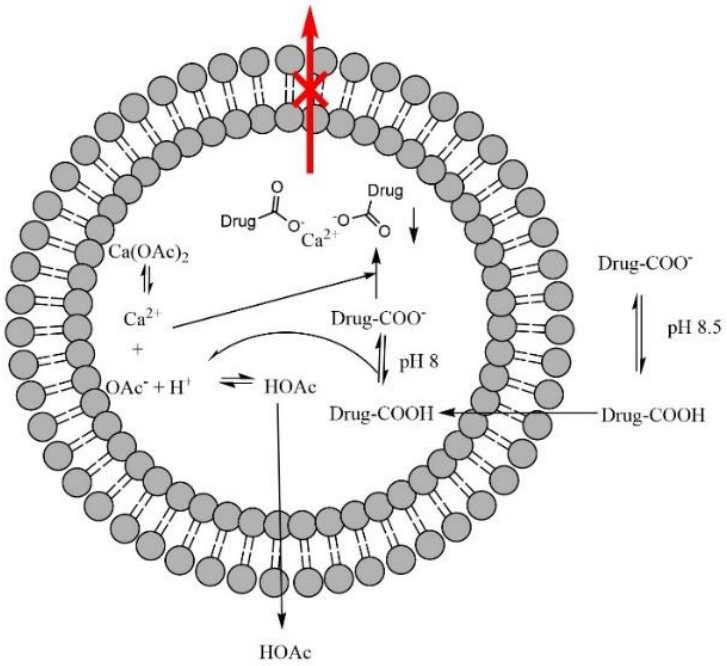

Figure 1. 3 Mechanism of active loading of a weakly acidic drug into the intraliposomal aqueous phase by a calcium acetate gradient. An amphipathic weakly acidic drug in the non-ionized form can diffuse through the lipid bilayer under heating (slightly above the transition temperature of the bilayer),

and then be deprotonated by donating a proton to an acetate ion. The deprotonated drugs subsequently form insoluble complexes with a calcium ion.

The standard active loading approaches only can be applied to *amphiphathic* drugs that are *soluble* in the outer aqueous phase of liposomes and are highly membrane permeable. Drugs must also possess a *functional group* that can interact with a trapping agent inside the liposomal core. This interaction can limit the drug leakage back to the outer phase and drive the uni-direction transport of the drug. [31, 33, 40]. Unfortunately, ~80% drugs are poorly water soluble and thus cannot be effectively loaded into liposomes by the standard active loading approaches [14].

1.4 Current approaches to improve active loading of hydrophobic drugs into liposomes

Several active loading strategies have been developed for hydrophobic drugs and are summarized in **Figure 1.4**. These techniques are mainly focused on improving the solubility of the poorly soluble compounds. A component is included in the loading mixture to increase the solubility of a hydrophobic compound during the active loading process, including a pH titrate, a solubilisation agent, a prodrug, and an ionisable carrier.

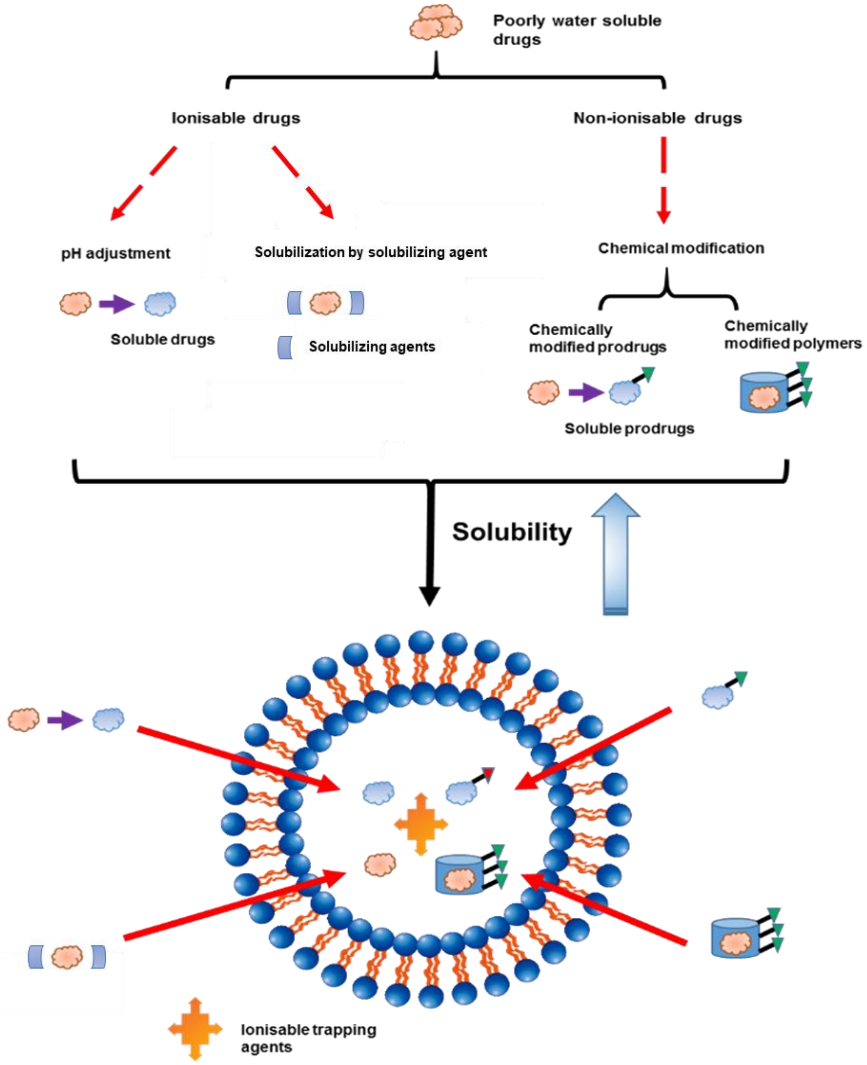

Figure 1. 4 Current strategies to actively encapsulate poorly water-soluble drugs into liposomes. A component is included in the loading mixture to increase the solubility of a hydrophobic compound during the active loading process, including a pH titrate, a solubilisation agent, a prodrug, and an ionisable carrier.

1.4.1 Solubility improvement by pH adjustment

The water solubility of an ionizable drug is highly dependent on the pH. For instance, ciprofloxacin is barely soluble in water at the range of pH 6-9 and cannot be actively loaded into liposomes with an external pH of 7. However, complete drug loading was achieved at a D/L of 0.3 (w/w) through an methylammonium sulfate gradient with an external pH of 3.5 [58].

A similar approach was applied to asulacrine,(ASL) a potent topoisomerase II inhibitor, which also exhibits an U-shape solubility profile (insoluble at the range of pH 6-9, yet increasingly soluble beyond that pH region); nevertheless, >90% of ASL could be remotely loaded into a preformed liposome entrapped ammonium sulfate with an external pH of 5.6 [59]. Another example is staurosporine (STS), a weak base, highly potent pan-protein kinase inhibitor. Rajesh et al. [60] proposed that STS could be actively loaded into liposomes via a reversed pH gradient (inner pH 8, outer pH 3). Under this extremely low pH condition, STS molecules would be solubilized in the outer phase and once it permeated into the liposomal core, the drug precipitated due to the increased pH. The encapsulation efficiency of STS with this method reached ~70% at a D/L of 0.09 (mol/mol), which was about 10-fold higher than the passive loading (~66 % at a D/L of 0.01 (mol/mol)) [61]. However, the formulation prepared with this method was not stable and nearly 90% of STS was released from the liposomes in human serum within 50 h. Bortezomib, the first therapeutic proteasome inhibitor that is soluble at a low pH, was actively loaded into the liposomes containing a reverse pH gradient and a polyol gradient [62]. As illustrated in Figure 1.5, bortezomib was soluble at pH 6.5 in the external phase and would permeate through the lipid bilayer and react with the free hydroxyl groups of the polyol molecule at a pH >7 for stable encapsulation. However, this pH adjustment method is not suitable for drugs that are not readily ionized or not stable under extreme pHs and those drugs cannot be solubilized at a higher concentration (>1 mg/mL) even after extreme pH adjustment, such as gambogic acid.

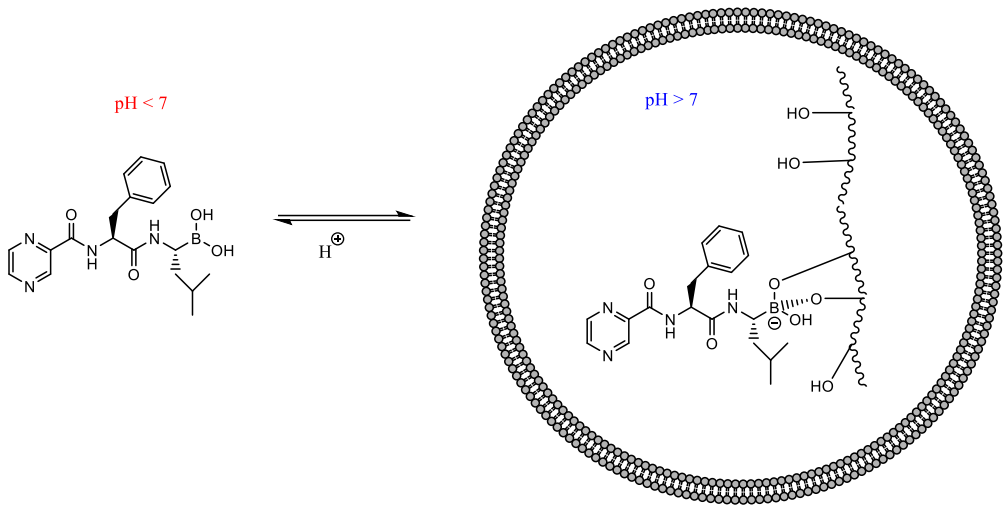

Figure 1. 5 Remote loading of bortezomib into liposomes containing a reverse pH gradient and a polyol gradient.

1.4.2 Chemical modification

In order to formulate docetaxel that contains no ionisable functional group into liposomes, Zhigaltsev et al. [63] developed a prodrug approach. A docetaxel prodrug was synthesized by conjugating an N-methyl-piperazino group to docetaxel through a cleavable ester bond, providing an ionizable tertiary amine to increase the water solubility at a lower pH (2.8 mg/mL at pH 4) as well as to promote the formation of drug complexes with a sulfate ion in the liposomal aqueous core. As a result, complete drug loading was obtained at a D/L of 0.4 (w/w) via an ammonium sulfate gradient. This liposomal formulation displayed prolonged PK and superior anticancer efficacy compared with Taxotere against a NDA435/LCC6 human breast carcinoma animal model. Subsequently, the similar concept was applied to geldanamycin, a poorly water-soluble HSP90 inhibitor [64]. Geldanamycin was conjugated with 3-(dimethylamino)-1-propylamine via an amide bond to synthesize 17-DMAPG that exhibited good water solubility of 4.6 mg/mL compared to its parent drug (<0.01 mg/mL). When 17-DMAPG was dissolved with the preformed liposomes containing a pH gradient (inner pH 4.0,

outer pH 7.4), the drug could permeate into the liposomal core to be ionized and locked inside the liposomes. To further improve the liposomal drug retention, acrylic acid was incorporated in the liposomal core to generate a pH gradient. Once 17-DMAPG was loaded, 2,2-diethoxyacetophenone and methylene-bis (acrylamide) were mixed with the liposomes to initiate polymerization of acrylic acid under UV irradiation to form lipogels that retained the drug even better (20% release at pH 7.4 after 24 h incubation) in comparison with 60% release obtained with the pH gradient only. Although chemical modification can assist active loading for water insoluble drugs, this strategy might alter the therapeutic potency and selectivity of the parent drugs. For this reason, modification of hydrophobic drugs with a functional group needs to be carefully designed and evaluated to minimize the undesirable effects.

1.4.3 Solubilizing agent

Cyclodextrin has been used as a solubilizing agent for poorly soluble drugs. Zhang *et al*. [65] synthesized sulfobutyl ether-β-cyclodextrin (SBE-β- CD) and included 5% of this solubilizer in the loading mixture of asulacrine (an insoluble weak base drug) and preformed liposomes containing an ammonium sulfate gradient. The results suggested that SBE-β-CD incorporated asulacrine in the hydrophobic chamber and thus increased the drug solubility. SBE-β-CD could also interact with the lipid bilayer to increase the membrane permeability to promote active loading of asulacrine. Complete drug loading was obtained at a D/L of 1:10 (w/w) [65]. In this study, they also identified an optimal range of SBE-β-CD content in the loading mixture for complete drug loading. When an insufficient amount of SBE-β-CD was used, drug precipitation occurred, limiting its loading into the liposomes. When excessive SBE-β-CD was included, liposomal integrity might be compromised, leading to reduced encapsulation efficiency. Sur et al. [66] developed a chemically modified cyclodextrin containing an ionisable functional group

(e.g. amino- or succinyl- moiety) on its surface, which could be ionized in response to the change of pH. The amino-cyclodextrin could shuttle a hydrophobic drug through the liposomal bilayer and became protonated and trapped inside the low pH core (pH 4.0) [66]. BI-2536, a highly selective inhibitor polo-like kinase-1 (PLK1) developed by Pfizer could be actively loaded into the liposomes using this method at a D/L of 0.4-0.6 (w/w). Mice treated with the liposomal BI-2536 exhibited reduced tumor growth and displayed improved safety profile in a xenograft colon cancer model compared to the free drug. This loading approach appears to be a platform technology that may be applicable for a wide range of drugs to improve administration safety and drug encapsulation.

1.5 Thesis Objectives

The thesis was focused on developing a robust platform technology that would allow active loading of poorly soluble drugs into liposomes and demonstrating how this technology could help resolve some unmet medical needs. We hypothesized that inclusion of a limited amount of water miscible solvent in the loading mixture that could completely dissolve an insoluble drug in the exterior phase of liposomes would help drug penetration into the liposomal aqueous core for active loading. This method is termed the **S**olvent-assisted **A**ctive **L**oading **T**echnology (SALT).

As a proof-of-principle, the first part of the thesis focused on developing the SALT for stable loading of a model drug, staurosporine (STS), into liposomes and optimizing the preparation parameters to fabricate a liposomal STS formulation for *in vivo* therapy of tumor. The second study of this dissertation was to explore whether the SALT is a flexible platform for loading other types of poorly soluble drugs into liposomes. We also examined whether all the miscible solvents could be utilized in the system and their roles in promoting drug loading. The third part

of this thesis was to demonstrate another utility of the SALT for preparing an oral pediatric formulation for a poorly soluble drug. The drugs candidates listed in **Table 1.2** were studied in this thesis.

Table 1. 2 Summary of drug candidates used to develop SALT through this thesis

Drug	Structure	Property	Indication	Solubility in water (μg/mL)	Delivery problem
Staurosporine (STS)	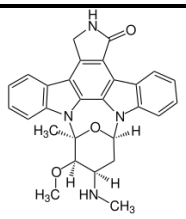 **M.W. 466.53 g/mol**	**Weak base**	**Anti-tumor (apoptosis)**	**< 5**	**1. Poor solubility 2. Short plasma half-life 3. Non-selective toxicity**
Gambogic acid (GA)	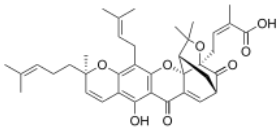 **M.W. 628.76 g/mol**	**Weak acid**	**Anti-tumor, anti-angiogenesis, anti-inflammation**	**< 5**	**1. Poor solubility 2. Short plasma half-life 3. Acute toxicity from hemolysis**
Mefloquine (Mef)	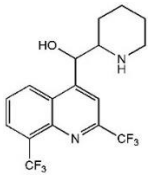 **M.W. 378.31 g/mol**	**Weak base**	**Antimalarial prophylaxis**	**< 500**	**1. Poor solubility 2. Strong bitterness**

Chapter 2: A Simple and Improved Active Loading Method to Efficiently Encapsulate Staurosporine into Liposomes for Enhanced Therapy of Multidrug Resistant Cancer

2.1 Project Summary

Stauroporine (STS), a universal protein kinase inhibitor, was impeded for clinical use due to its poor solubility and high toxicity despite its significant antitumor potency against a variety of cancers [67, 68]. We hypothesized that these critical issues with STS can be resolved with liposome delivery. However, a stable encapsulation method for this water insoluble drug is yet to be developed. In this chapter, a new drug loading method called **Solvent-assisted Active Loading Technology** (SALT) was developed by including a limited amount of DMSO to prevent STS precipitation, thereby facilitating the entry of individually solubilized STS into the aqueous core of liposomes via an ammonium sulfate gradient, to form stable drug crystalline inside, as revealed by cryo-transmission electron microscopy. Compared to the previous loading method [60], not only this new method could increase the drug loading efficiency by 3-fold (Drug/lipid=0.31, mol/mol, compared to 0.09), but also could improve drug retention in serum when incubated at 37°C (>95% retention compared to 25% in 24 h). With this new loading method, the loading efficiency of STS reached 100% within 15 min of incubation at room temperature in the presence of 5-60% DMSO, which was removed by gel filtration or dialysis to produce the final product, STS-Lipo (STS-encapsulated liposomes prepared by the SALT) that remained stable at 4 °C for >6 months with no significant size change or drug leakage. STS-Lipo exhibited comparable IC_{50} against a panel of tumor lines (3-70 nM), compared to free STS. The circulation half-life of STS delivered by STS-Lipo was significantly prolonged by 15-fold relative to free STS, dissolved in 100 mM acetate buffer (pH 5.5). A 3-fold higher dose of STS-Lipo could be tolerated by female BALB/c mice compared with free STS (9 vs 3 mg/kg, total dose), leading to near complete growth

inhibition of a multidrug resistant EMT6/AR1 tumor, while free STS given at its maximum tolerated dose only produced mild activity.

2.2 Introduction

Staurosporine (STS), a universal kinase inhibitor, exhibits potent activity against many tumor cells *in vitro* [69]. However, the clinical application of STS for cancer therapy has been hindered due to poor solubility and the lack of selectivity, which result in significant side effects [70]. To improve the solubility and specificity, STS derivatives have been synthesized such as UCN-01. Unfortunately, UCN-01 has failed clinical trials due to its narrow therapeutic window [71]. An alternative approach is to employ a nanoparticle (NP) system to carry STS in an aqueous medium as this enhances its tissue selectivity toward tumors via the enhanced permeability and retention (EPR) effect [24]. Liposomes are attractive systems for targeted delivery of drugs with a number of products approved clinically, including Doxil, Ambisome, DaunoXome and Marqibo [72]. As mentioned in the previous chapter, there are two major methods to encapsulate a drug into liposomes. First, a hydrophilic agent and a hydrophobic drug can be *passively* loaded into the aqueous core and the lipid bilayer of a liposome, respectively. Second, an amphiphilic weak base or acid can be *actively* loaded into the interior of liposomes through a chemical gradient such as pH, ammonium sulfate or calcium acetate [31-33]. The active loading method has been demonstrated superior to the passive loading method by providing improved drug loading efficiency (which refers to increased drug-to-lipid ratio) and enhanced stability *in vitro* and *in vivo* (which refers to reduced drug leakage during storage and prolonged blood circulation) [40]. This is due to the fact that the actively loaded drug molecules can form crystals or complexes with specific counter ions in the aqueous core of liposomes [33, 40-44, 46-53]. This mechanism leads to efficient and stable drug loading, which eventually prolongs the drug half-life [43, 54-56].

However, not all compounds are suitable for active loading. For instance, the drug has to be amphiphathic such as doxorubicin, as it should not only be soluble in the outer aqueous phase of liposomes, but also permeable through the lipid bilayer and interact with the counter ions or oligomer/polymer in the inner aqueous phase, in order to form stable crystals or complex. This particular formation limits the leakage of drug back to the outer phase (**Figure 2.1A.**). Furthermore, the drug needs to contain a functional group to interact with specific ions or molecules in the aqueous core, in order to take advantage of this active loading mechanism [31, 33, 40]. Active loading of STS into liposomes is challenging as STS exhibits little water solubility. Active loading of this drug was first pursued by Mukthavaram et al [60]. STS was dissolved in a liposome suspension exhibiting a reverse pH gradient (inner phase pH 7.4, outer phase pH 3), and incubated the mixture at 50 °C for 20 min. Approximately 70% drug encapsulation was achieved at a drug-to-lipid ratio (D/L) of 0.09 (mol/mol). In their loading method, a secondary amine group of STS was protonated at pH 3 to improve the solubility in the outer phase, yet precipitated inside the liposomes once penetrated into the inner phase (pH 7.4). However, the STS-liposomes (DSPC:DOPE:Chol:DSPE-PEG2000; 6:6:6:1, molar ratio) produced with this method only achieved a moderate drug loading efficiency, and the drug leakage was fast when incubated with PBS and serum (>70% in 24 h).

This study was focused on the development of a simple and improved active loading method for STS into liposomes. One of the critical challenges is that the active loading process requires the drug to be dissolved with the preformed liposomes containing a chemical gradient. However, STS is insoluble, and its solubility improvement at 1 mg/mL by lowering the pH is limited (**Figure 2.2A**). Herein, we hypothesized that introducing a limited amount of dimethyl sulfoxide (DMSO) to the liposomes could not only prevent precipitation of STS in the active loading process, but also

facilitate the permeation of the drug into the inner core of liposomes with increased membrane permeability. Additionally, STS containing a secondary amine could be actively loaded into liposomes via an ammonium sulfate gradient (inner aqueous phase) and complex with sulfate to form stable nano-aggregates (**Figure 2.1B.**), followed by removal of DMSO by gel filtration or dialysis to obtain the final product.

Herein, we report the development and optimization of this improved active loading method for STS. The drug retention in serum, the cytotoxic potency, the pharmacokinetics and the antitumor efficacy of STS-Lipo (STS-encapsulated liposomes prepared by the SALT) were determined and compared with free STS.

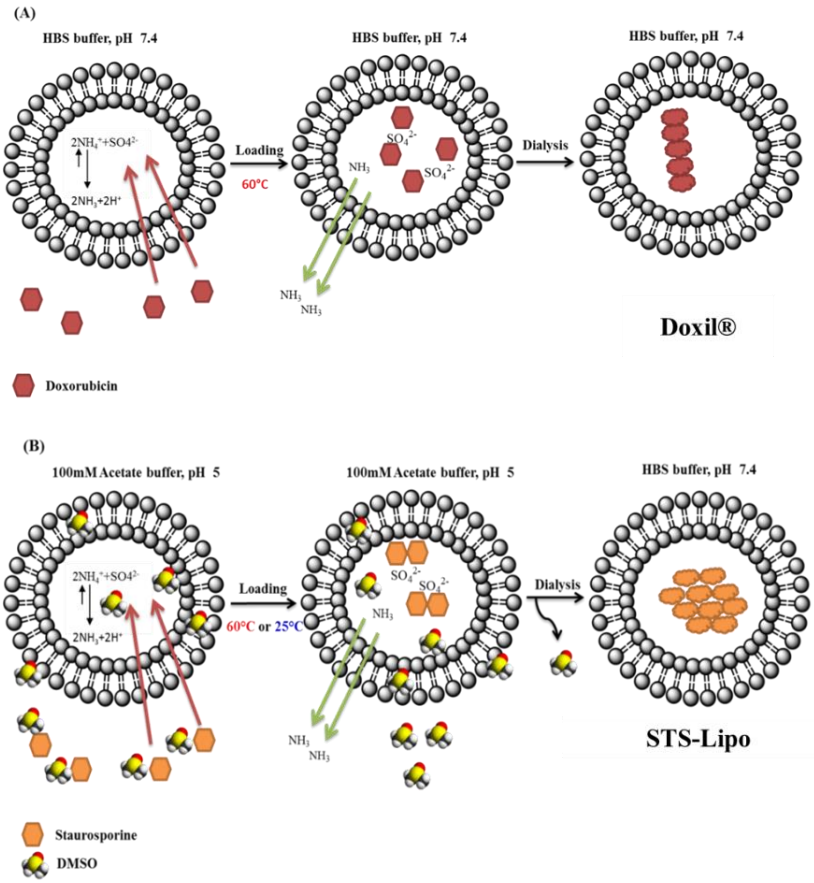

Figure 2.1 Schematic of active loading of weak base drugs into liposomes. A) Active loading of DOX into preformed liposomes with an ammonium sulfate gradient B) Active loading of STS into preformed liposomes with an ammonium sulfate gradient in the presence of 5% DMSO.

2.3 Materials and Methods

2.3.1 Reagents

1,2-Distearoy-sn-glycero-3-phosphatidylcholine (DSPC) and 1,2-distearoyl-sn-glycero-3-phosphatiylethanol-amine-N-[methoxy (polyethyleneglycol)-2000] (DSPE-PEG2000) were purchased from Avanti Polar Lipids (Alabaster, AL). Staurosporine (STS) was purchased from LC laboratories. Free cholesterol E assay kit was purchased from Wako Chemicals USA, Inc. To-Pro-3, was obtained from Life technologies. Cholesterol (Chol), dimethyl sulfoxide (DMSO), XTT reagent, formalin solution (10%), anhydrous ethanol and sodium acetate were purchased from Sigma-Aldrich (Oakville, ON). All other reagents were analytical grade.

2.3.2 Resistant cancer cell lines

PC-3 (human prostate cancer) cells were obtained from the American Type Culture Collection (ATCC), and the docetaxel (DTX)-resistant variant was generated by incubating the cells with gradually increasing concentrations of DTX until the cells were completely resistant to 100 nM DTX as described previously [73]. EMT6 (murine breast tumor) and the resistant variant, EMT6/AR1 cells overexpressing P-glycoprotein were a gift from Ian Tannock (Princess Margaret Hospital, Toronto) [74]. All cells were maintained in Dulbecco's Modified Eagle's Medium (DMEM) supplemented with 10 %vol fetal bovine serum (FBS), 1 %vol penicillin/streptomycin (P/S), and 100 nM DTX.

2.3.3 Mice

Female BALB/c mice (6-8 weeks old) purchased from the Jackson Laboratory (Bar Harbor, ME) were used for the in vivo study. All animal studies were conducted at the Animal Resources Centre at the University Health Network (Toronto, ON, Canada) with approved protocols in compliance with the guidelines developed by the Canadian Council on Animal Care.

2.3.4 Ultra-performance liquid chromatography analysis (UPLC)

Drug analysis in this chapter was performed with an ACQUITY UPLC System equipped with a Photodiode Array (PDA) detector, a binary solvent system and an auto-sampler. Diluted samples were injected into the UPLC system and separated on a Waters ACQUITY CSH™ C18 column (2.1 × 50 mm, 1.7 um) with mobile phase (A: MilliQ water with 0.1% formic acid**;** B: acetonitrile with 0.1% formic acid). The eluent was monitored at 291 nm at a flow rate of 0.4 mL/min with the following designed gradient (0 min: A/B (90/10), 1.8 min: A/B (90/10), 2.3 min: A/B (90/10), 2.5 min: A/B (90/10), 3 min: A/B (90/10)). [STS] was determined by integrating the peak area and compared with a standard curve.

2.3.5 Solubility of STS

Three mg STS was dissolved in 1 mL of acetate buffer (100 mM, pH 5), water or HEPES buffered saline (HBS, 25 mM HEPES, 0.9% NaCl, pH 7.4) in the absence or presence of 5% DMSO. The drug suspension was sonicated for 30 min and incubated for 30 min at room temperature. Drug precipitates were removed by 0.2 μm amicon centrifugal filter units (12,000 rpm, 15 min). The filtrate was diluted with methanol and analyzed by UPLC using the method described in 2.3.4.

2.3.6 Optimization of STS loading

One hundred mg of DSPC/Chol/DSPE-mPEG$_{2000}$ (55/40/5, mol%) was dissolved in 1 mL ethanol in a flask. Ethanol was removed by rotary evaporation at 60 °C to form a thin film. The thin film was dried under heavy vacuum overnight and then hydrated with 1 ml of 350 mM ammonium sulfate at 60 °C. The extruder was equilibrated at 70 °C and the lipid suspension was extruded through 200, 100, 80 nm stacked Nucleopore polycarbonate membranes 20 times each to control the size. The outer phase of liposomes was replaced with acetate buffer (100 mM, pH 5) by dialysis

(Slide-A-Lyzer Dialysis Cassettes 10kDa MWCO, Pierce Biotechnology, Rockford, IL). The size and zeta potential of preformed liposomes with an ammonium sulfate gradient were measured by a particle analyzer (Zetasizer Nano-ZS, Malvern Instruments Ltd, Malvern, UK) and stored at 4 °C. Various amounts of the preformed liposomes were mixed with 1 mg of STS in the presence of 5% DMSO in a total volume of 1 ml (diluted in 100 mM acetate buffer, pH 5). The mixture was incubated at 60 °C for 1 h and then quenched on ice. STS-Lipo was purified by a Sepharose CL-4B column, pre-equilibrated with HBS. To determine the drug loading efficiency, the following equation reported previously was applied [63].

$$Loading\ efficiency\ (\%) = \frac{[D]_{purified} / [Chol]_{purified}}{[D]_{initial} / [Chol]_{initial}} \times 100\%$$

To determine STS concentration ([D]) in the formulations, the liposomes were diluted with methanol to an adequate extent and the drug was quantified by UPLC using the method described in **Section 2.3.4**. Cholesterol concentration ([Chol]) was measured using a cholesterol E assay kit.

2.3.7 Loading kinetics

STS (1 mg) was incubated with the preformed liposomes containing 5 mg total lipid (D/L = 0.31/1, mol, L is referred as total lipid throughout the article) in the presence or absence of 5% DMSO at room temperature or 60 °C for 5-60 min. After incubation, non-encapsulated STS and DMSO were removed by gel filtration on a Sepharose CL-4B column. The eluted liposome fraction was analyzed for lipid and drug content as described earlier.

2.3.8 Active loading in the presence of various amounts of DMSO

One mg STS was incubated with preformed liposomes containing 5 mg of total lipids (D/L = 0.31/1, molar ratio) in the presence of 5-60% DMSO at room temperature for 1 h. After incubation,

non-encapsulated STS and DMSO were removed by gel filtration on a Sepharose CL-4B column. The eluted liposome fraction was analyzed for the lipid and drug content as described earlier.

2.3.9 Cryo-transmission electron microscopy (Cryo-TEM) imaging

The morphology of the preformed liposome and STS-Lipo was imaged by a FEI Tecnai G20 Lab6 200 kV TEM (FEI, Hillsboro, OR) following a previously described method [75]. The instrument was operated at 200 kV in bright-field mode. Digital images were recorded under low dose conditions with a high-resolution FEI Eagle 4 k CCD camera (FEI, Hillsboro, OR) and analysis software FEI TIA. A nominal underfocus of 2-4 μm was used to enhance image contrast. Sample preparation was performed using the FEI Mark IV Vitrobot. Approximately 2-4 μL of liposomes at 10-15 mg/mL total lipid was applied to a copper grid and plunge-frozen in liquid ethane to generate vitreous ice. The frozen samples were then stored in liquid nitrogen until imaged. All samples were frozen and imaged at the UBC Bioimaging Facility (Vancouver, BC).

2.3.10 Stability of STS-Lipo

Released STS from STS-Lipo was measured using the fluorescence de-quenching method as previously described with minor modifications [76, 77]. STS-Lipo (500 μg STS/ml in 200 μl of 50% FBS/50% HBS) were incubated at 37 °C at various time points, and were immediately cooled in an ice bath, diluted by 100-fold, and then transferred into a 96-well plate. The fluorescence of released STS was measured using a BioTek Synergy H1 Multi-Mode Reader (Ex 296 nm/Em 396 nm). The percentage of the released STS was calculated as $(I_T - I_0)/(I_{100} - I_0) \times 100\%$, in which I_T is the fluorescence at time point T, I_0 is the fluorescence at the start of the incubation time, I_{100} is the fluorescence after the addition of 10 μl of 5% Triton X-100.

2.3.11 *In vitro* cytotoxicity

EMT6/AR1 and PC-3-RES cells were plated in a 96-well plate (1000~5000 cells/well). After 24 h of incubation, the cells were treated with different concentrations of DTX (final DMSO <0.1%), free STS (final DMSO <0.1%) and STS-Lipo, respectively. After 72 h of treatment, cell viability was analyzed by the XTT assay as described previously [73]. The IC_{50} was determined by nonlinear regression analysis using GraphPad Prism Software (San Diego, CA).

2.3.12 Dose escalating study

A dose escalating study was performed to determine the maximum tolerated doses (MTDs) of STS-Lipo and free STS. Free STS was dissolved in acetate buffer (pH 5) containing 1% DMSO (v/v %). DMSO was included to solubilize free STS in the acetate buffer, increasing the viscosity of the STS solution, creating a significant challenge for consecutive i.v. injections. Alternatively, i.p. injections were employed for administrating free STS. On the other hand, STS-Lipo can be administrated intravenously to BALB/c mice. The mice treated different doses of free STS and STS-Lipo, respectively, were monitored in accordance with the established clinical health score chart [78]. This health score chart includes the change of body weight, and the mice status of activity, appearance, breathing, posture, hydration, and elimination. The health status of the mice was scored until they recovered to the baseline score, and mice that reached humane endpoints were euthanized. The MTD was defined as the maximum dose that did not induce any humane endpoints in the treated animals.

2.3.13 Pharmacokinetic study

A dose escalating study was first performed to obtain the maximum tolerated doses (MTDs) for STS and STS-Lipo, which were 0.6 and 3 mg/kg, respectively. Native STS dissolved in 1% DMSO /acetate buffer (pH 5) and STS-Lipo were i.v. administrated to BALB/c mice at their MTDs. Blood

was collected in EDTA-containing microtubes (Microvette® CB 300, Sarstedt, Germany) at selected time points (0.05, 0.16, 0.25, 0.5, 1, 2 h for free STS and1, 3, 8, 24 h for STS-Lipo), followed by drug concentration measurement by UPLC. Briefly, 100 µL of plasma was mixed with 200 µL methanol containing the internal standard (UCN-01, 25 ng/mL). The mixture was vortexed for 30 s and centrifuged at 5,000g for 7 min at 15 °C. Fifteen µL of the supernatant was injected into an Agilent 1290 infinity UPLC system (Waters Corp, Milford, MA) coupled with AB SCIEX 5500 QTRAP system (AB SCIEX, Foster City, CA). Samples were separated by a Waters ACQUITY BEH™ C18 column (2.1 × 100 mm, 1.7 µm, connected with vanguard column) with a mobile phase (A: MilliQ water with 0.1 % formic acid; B: Methanol with 0.1 % formic acid). Detection of STS and the internal standard were monitored in ES^+ mode using a daughter ion (m/z=467 for STS and m/z=483 for I.S.) at a flow rate of 0.2 mL/min with the designed gradient program (0 min: A/B (50/50), 2 min: A/B (5/95),4 min: A/B (5/95),4.1 min: A/B (50/50), 6 min: A/B (50/50)). Chromatographic data were acquired and analyzed using the Analyst v1.5.2 (AB SCIEX, Foster City, CA). The PK profiles of STS and STS-Lipo were analyzed by WinNonlin using a non-compartmental model.

2.3.14 *In vivo* efficacy study

The MTDs for i.v. DTX (dissolved in Tween80/ethanol/ 0.9% saline, and then diluted in normal saline), i.v. STS-Lipo and i.p. free STS (dissolved in DMSO and then diluted in 100 mM acetate buffer, pH 5) were 12 mg/kg (twice weekly for 3 doses), 3 mg/kg (twice weekly for 3 doses) and 0.6 mg/kg (5 consecutive days), respectively. The MTDs were obtained from the dose escalating study described above or reported previously [70, 79]. The right lateral flank of female BALB/c mice was shaved and s.c. inoculated with EMT6/AR1 cells (2×10^5 cells/injection, n = 10 mice per group). One week later, when tumors reached the size of about 50 mm^3, the mice were

randomly divided into 4 groups for drug treatments: 1) HBS (i.v., twice weekly for 3 doses), 2) DTX (12 mg/kg twice weekly for 3 doses, i.v.), 3) free STS (0.6 mg/kg, i.p., daily for 5 consecutive days), and 4) STS-Lipo (3 mg/kg twice weekly for 3 doses, i.v.). Tumor volume and body weight for each group were monitored every two days. Mice were euthanized when tumor volume reached the end point (>1,000 mm^3) or open tumors were discovered.

2.3.15 Storage stability

Sterile filtered STS-Lipo with a D/L of 0.31 (mol/mol) at 1 mg STS/mL was stored in a glass vial at 4 °C. At selected time points, an aliquot of STS-Lipo was collected, and the size and loading efficiency were measured following the methods described above.

2.3.16 Statistical analysis

All data are expressed as mean ± SD. Statistical analysis was conducted with the two-tailed unpaired *t* test for two-group comparison or one-way ANOVA, followed by the Tukey's multiple comparison test by using GraphPad Prism (for three or more groups). A difference with *P* value< 0.05 was considered to be statistically significant.

2.4 Results

2.4.1 Solubility of STS

STS was insoluble in water (pH 7.0) and HBS (pH 7.4) (solubility in both <0.78 μg/mL), and mildly soluble in acetate buffer (solubility ~ 120 μg/mL, pH 5.0) (**Figure 2A**). The solubility of STS in acetate buffer was improved in the presence of increased amount of DMSO (**Figure 2B**) and complete solubilization of STS in acetate buffer (1 mg/mL) was observed with 5 vol% DMSO involved (**Figure 2A&B**). However, addition of 5 vol% DMSO in water and HBS failed to increase the solubility of STS to a significant extent (<50 μg/mL, **Figure 2A**), suggesting complete solubilization is related to both the pH of aqueous solutions and the amount of DMSO included.

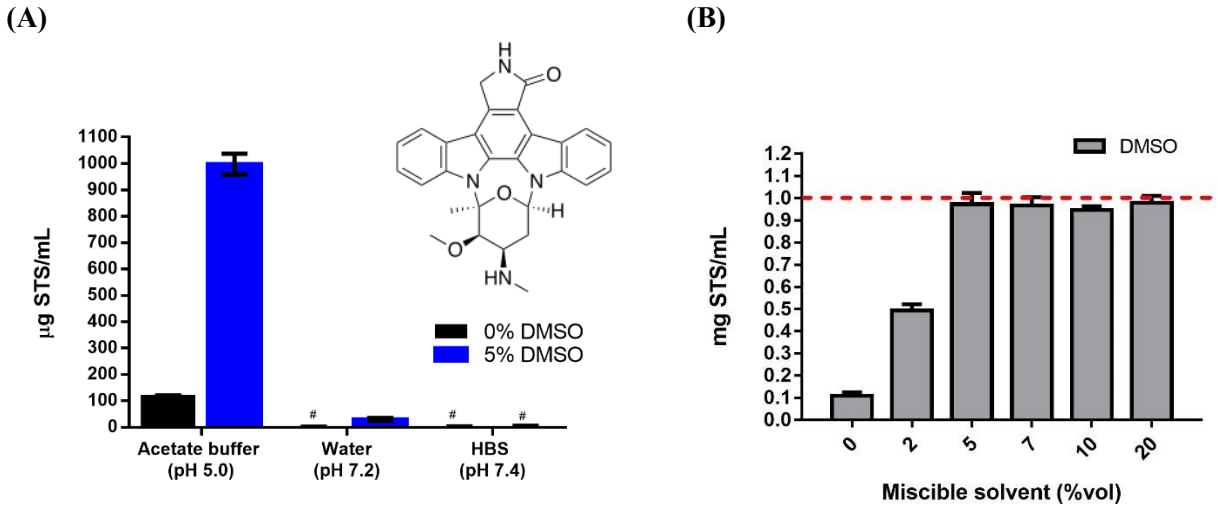

Figure 2.2 Structure and solubility of STS in various solvent systems.

Data = mean ± S.D., n=3. # [STS] is lower than the detection limit: 0.78 μg/mL.

2.4.2 Efficient active loading of STS in the presence of 5 vol% DMSO

We hypothesized that DMSO could be used as a solubilizing agent to prevent STS precipitation during the active loading process and increase the permeability of lipid membrane, allowing STS to pass through the lipid bilayer and get encapsulated more effectively. Next, we incubated STS with preformed liposomes (inner: 350 mM ammonium sulfate; outer: 100 mM acetate buffer, pH 5) in the presence of 5 vol% DMSO at 60 °C for active loading of STS. The highest drug-to-lipid ratio (D/L, mol/mol) to remain complete encapsulation at 1 mg/mL was 0.31. When the D/L increased to 0.39, the encapsulation efficiency was decreased to ~50% (**Figure 2.3**).

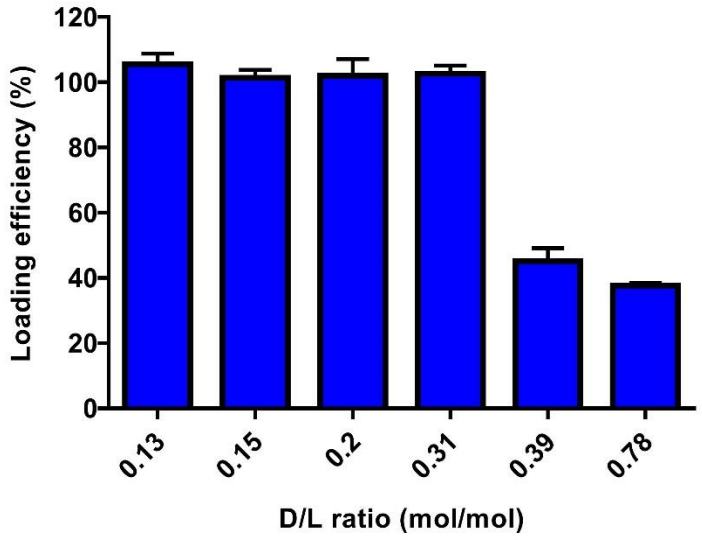

Figure 2.3 Loading efficiency with different drug-to-lipid (D/L) ratios. Data = mean ± S.D., n=3.

2.4.3 Loading kinetics of STS

We then studied the STS loading kinetics in the presence of 5 vol% DMSO at a D/L of 0.31 at either room temperature or 60 °C. As shown in **Figure. 2.4**, complete STS loading was achieved within 5 min of incubation at 60 °C, which is higher than the DSPC lipid transition temperature (T_m, 55 ^oC). Complete STS loading was also achieved at room temperature within 15 min (lower than the T_m of DSPC) despite slower drug loading rate, indicating the increased membrane permeability by added DMSO.

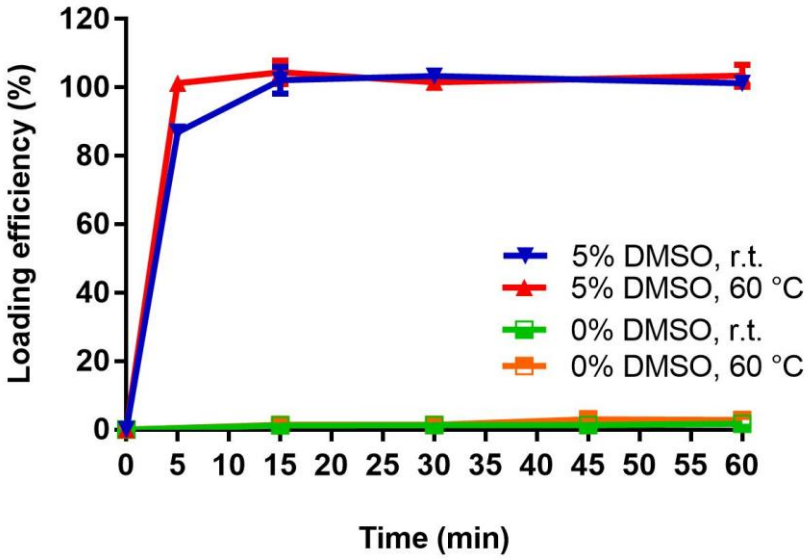

Figure 2.4 STS loading kinetics into the liposomes in the absence/presence of 5% DMSO at either room temperature (r.t.) or 60 °C. Data = mean ± S.D., n=3.

2.4.4 Drug loading in the presence of different amounts of DMSO

We also examined whether an excess amount of DMSO in the active loading system would adversely affect the drug loading. Although only 5 vol% DMSO was required to completely dissolve STS in this system shown in **Figure. 2.2B** (1 mg/ml), the presence of an excess amount of DMSO (up to 60 vol%) did not reduce the drug loading (**Figure 2.5**). Complete STS loading was produced via an ammonium sulfate gradient in the presence of 5-60 vol% DMSO at room temperature. Moreover, the size (~104 nm) and the polydispersity index (PDI < 0.06 for all samples) of the final STS-Lipo products produced with different amounts of DMSO were comparable and were unchanged compared to the empty liposomes before drug loading (0 vol% DMSO represent empty liposomes). However, when 2 vol% DMSO that is less the required amount for complete solubilization (5 vol%) was employed in the active loading process, the

loading was incomplete, yielding a significant amount of drug precipitate in the final product (data not shown).

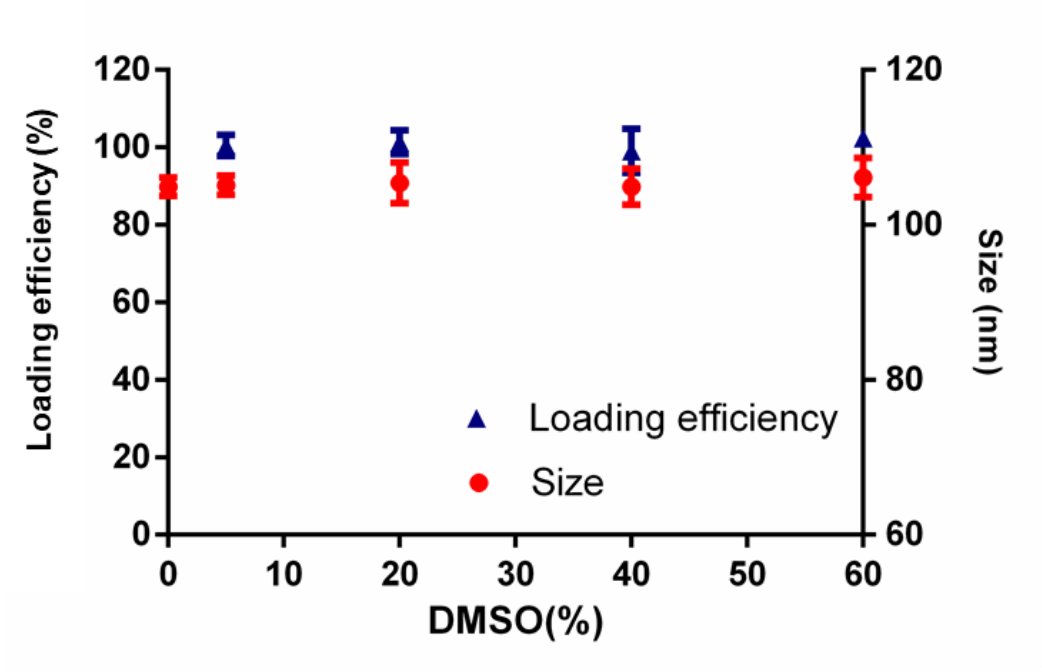

Figure 2.5 STS loading in to the liposomes in the presence of various amounts of DMSO (5-60 vol%) at room temperature. Data = mean ± S.D., n=3.

2.4.5 Characterization of STS-Lipo

STS-Lipo with a D/L of 0.31 (mol/mol) were further characterized and the key parameters of the formulation are reported in **Table 2.1**.

Table 2.1 Characterization of STS-Lipo. Data = mean ± S.D., n=3.

Lipid composition		Particle size (nm)	PDI	Zeta potential (mV)	Loading efficiency (%)	Drug/total lipid (mol/mol)*
DSPC/Chol/ DSPE-PEG2K (50:45:5)	before loading	104.9±1.1	0.043±0.017	-15.5(±0.28)	100.45±2.72	0.31:1
	after loading	105.1±1.2	0.035±0.011	-24.7(±1.41)		

* Drug/total lipid (w/w) = 0.2/1.

2.4.6 Nano-aggregates formed in the aqueous core of STS-Lipo

Empty liposomes and STS-Lipo prepared with a D/L of 0.31 in the presence of 5 or 60 vol% DMSO were imaged by Cryo-TEM (**Figure 2.6**). Nano-aggregates were clearly observed in the aqueous core of STS-Lipo. Higher amounts of DMSO present (60 vol%) during the drug loading, didn't affect the formation of nano-aggregates and the membrane integrity.

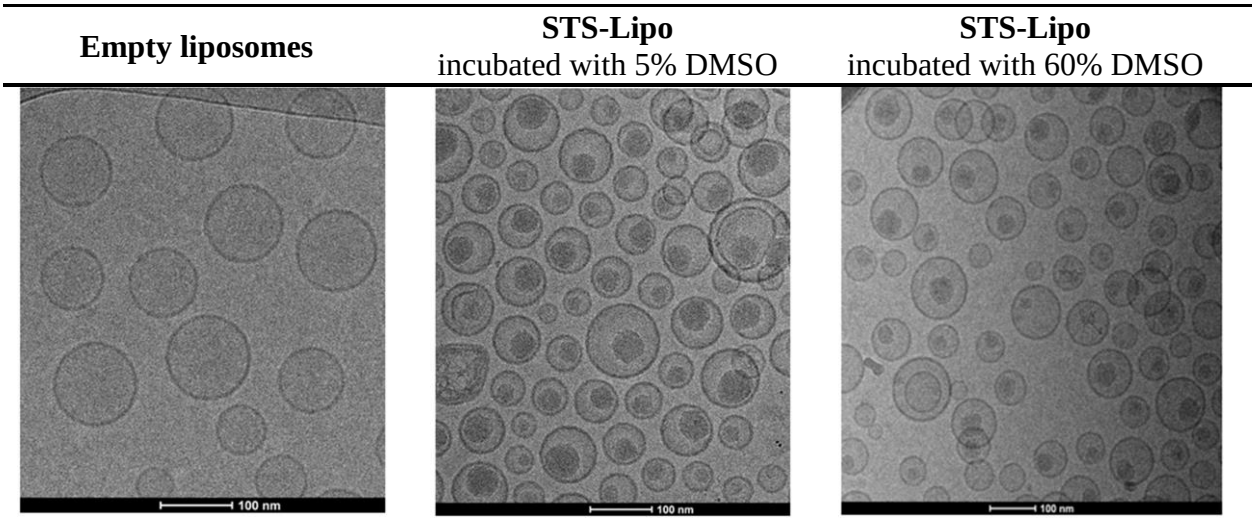

Figure 2.6 Cryo-TEM images of the empty liposomes (A) and STS-Lipo incubated with 5% (B) and 60% (C) DMSO during the STS loading with a D/L of 0.31 (mol/mol). Scale bar represents 100 nm.

2.4.7 Stability of STS-Lipo in HBS or 50% FBS

Released STS from STS-Lipo was determined by using the fluorescence de-quenching assay. The fluorescence intensity increased linearly while the drugs released from the liposomes. As shown in **Figure 2.7**, minimal drug leakage was found (<5% in 7 days) from STS-Lipo when incubated in HBS or 50% FBS at 37 °C.

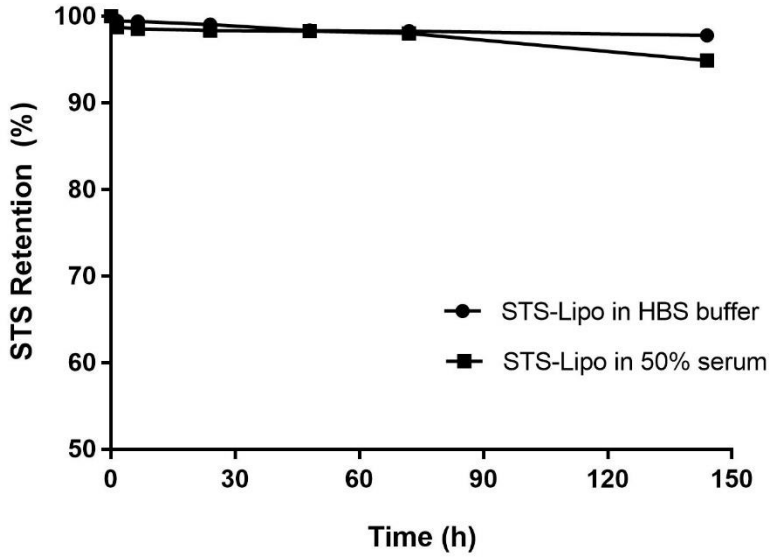

Figure 2.7 The stability of STS-Lipo when incubated in HBS (●) and 50% serum (■) at 37 °C. Data = mean ± SD (n=3)

2.4.8 IC_{50} analyses

We first demonstrated that the resistant cell lines used in the study were highly resistant to DTX with a 40- to 450-fold increased IC_{50}, compared to the parent lines (**Table 2.2**). Free STS and STS-Lipo exhibited comparable cytotoxic potency against EMT6/AR1 and PC-3-RES cells with IC_{50} value between 3 and 70 nM. STS and STS-Lipo were 2- to 300-fold more potent compared to DTX. EMT6/AR-1 cells were founded to be sensitive to STS and the STS-Lipo with an IC_{50} of ~3 nM. Therefore, EMT6/AR1 was selected for the following *in vivo* study.

Table 2.2 Cytotoxicity of different agents against resistant tumor cells. Data = mean (± SD), n=3.

IC_{50} (nM)	DTX	STS	STS-Lipo
EMT6/AR1	1,091(±45)	3.3(±0.5)	3.5(±0.8)
PC-3-RES	903(±50)	56(±5)	65(±2)

2.4.9 Pharmacokinetic analysis

The PK of STS and STS-Lipo was first compared at an equal dose at 0.6 mg/kg, the maximum tolerated dose (MTD) for free STS. However, STS-Lipo were cleared rapidly from the circulation (data not shown) possibly because the lipid dose injected was close to the threshold of ~1 μmol phospholipid/kg [80]. Utkhedd and Tilcock [80] showed that the blood circulation half-life of PEGylated liposomes was prolonged to 20 h and independent of dose when the lipid dose was above 1.30 μmol phospholipid/kg, while the half-life reduced to 4 and 2 h at a dose of 0.5 and 0.16 μmol phospholipid/kg. respectively. Therefore, we compared the PK of free STS and STS-Lipo at their MTDs, 0.6 and 3 mg/kg respectively, which were also the doses used for the efficacy study. As shown in **Figure 2.8**, the plasma drug levels in the STS-Lipo group were significantly higher compared to that of the free STS group. Free STS was cleared from the blood circulation within 2 h, while STS-Lipo displayed prolonged circulation with a moderate drug level (23 ng/ml) at 24 h post injection. The plasma PK profiles of STS-Lipo and free STS were fitted to the non-compartment model using WinNonlin to acquire PK parameters (**Table 2.3**). STS-Lipo displayed 25-fold increased area under the curve (AUC), 14-fold prolonged half-life, 10-fold increased mean resident time, and 5-fold reduced clearance.

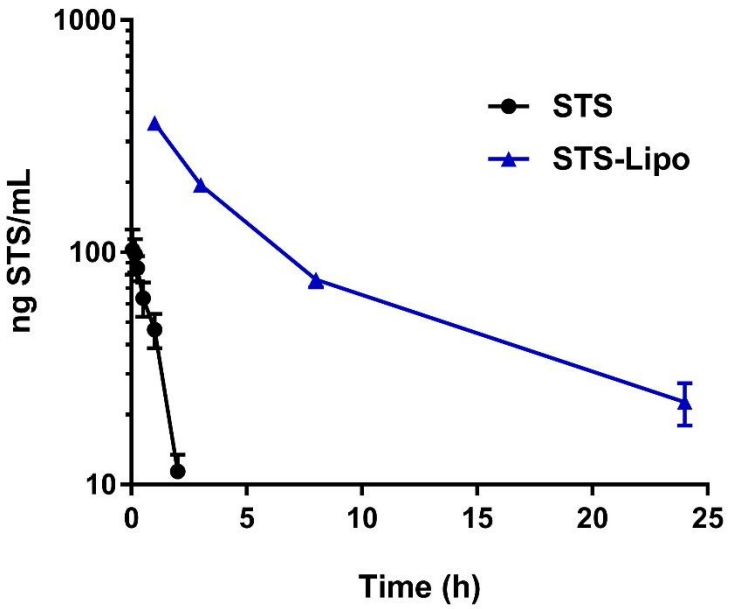

Figure 2.8 PK profiles of free STS (●) and STS-Lipo (▲) after i.v. injection. Data=mean± SD (n = 3)

Table 2.3. **Estimated plasma pharmacokinetic parameters of STS and STS-Lipo in BALB/c mice.**

	C_{max} (ng/mL)	AUC (ng/mL×h)	$t_{1/2}$ (h)	CL (mL/h)	Vss (mL)	MRT (h)
STS	102.86	109.48	0.59	109.60	91.81	0.83
STS-Lipo	360.81	2743.39	8.17	21.87	188.31	8.61

2.4.10 *In vivo* antitumor efficacy study

A dose escalating study was first performed to obtain the MTDs for STS and STS-Lipo (**Table 2.4)**. The MTDs for i.v. DTX (dissolved in Tween80/ethanol/saline, and then diluted in saline) and STS-Lipo were 12 mg/kg and 3 mg/kg (twice weekly for 3 doses), respectively. The dosing regimen for free STS (dissolved in DMSO and then diluted in acetate buffer) was adopted from the previous report [70], and the MTD for which was 0.6 mg/kg consecutively for 5 days by i.p. injection. The antitumor activity of DTX, free STS and STS-Lipo was compared at their MTDs in a rapidly growing EMT6/AR1 mouse breast cancer model in BALB/c mice (**Figure. 2.9A**).

This tumor model was highly resistant to DTX, which showed no antitumor activity. STS-Lipo exhibited significantly improved antitumor activity in this highly resistant breast cancer model compared with free STS and DTX. After 3 doses of STS-Lipo, the tumor growth was effectively impeded and the average tumor volume was controlled by 150 mm^3 in comparison to ~800 mm^3 in the free STS group by Day 18, while all tumors in the DTX and buffer treated mice all exceeded the endpoint size (1,000 mm^3) or displayed open ulceration before Day 14. STS-Lipo treatment did not cause significant body weight loss (**Figure 2.9B**). On the other hand, 3 mice in the free STS group reached humane endpoints on Day 9 possibly due to the drug toxicity as well as ~5% body weight loss.

Table 2.4 Dose escalating results of STS-Lipo and free STS. n = 3 in each group

	Dose (mg/kg)	**Survival rate**	**Maximum change of body weight (%)**
Free STS	0.6	3/3	-2.1±2.0
	0.8	0/3	-16.0±3.0
STS-Lipo	0.6	3/3	0.1±1.1
	3	3/3	0.8±1.4
	5	1/3	-8.0±2.1

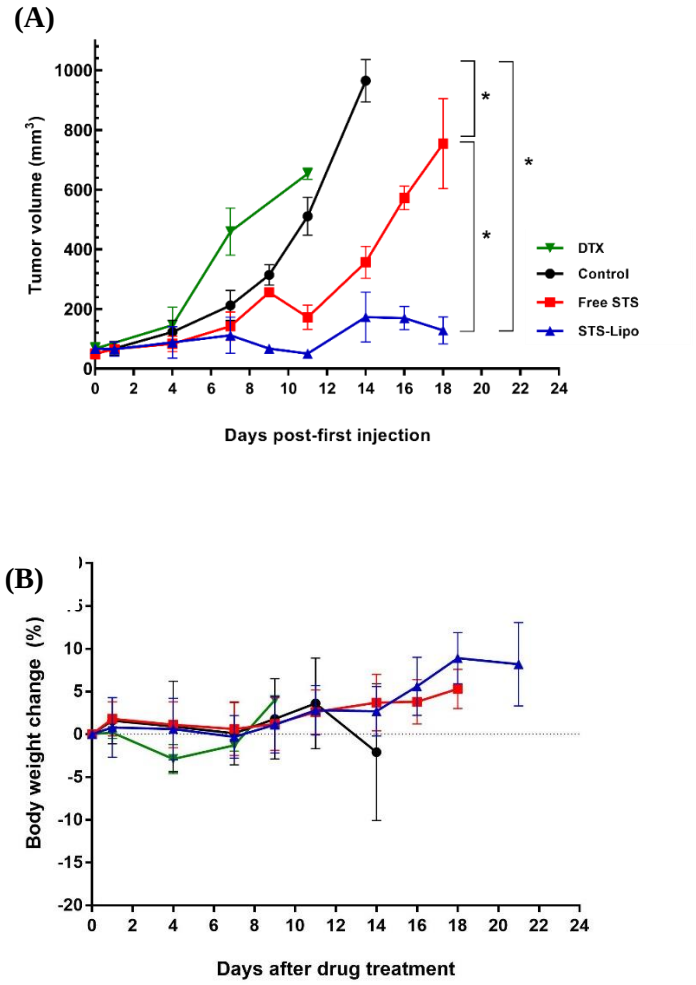

Figure 2.9 *In vivo* antitumor efficacy against murine EMT6/AR1 tumor. (A) tumor size; (B) body weight. The EMT-6-AR1 tumor cells were inoculated into the right flank of the BALB/c mice. One week later, the mice were i.v. injected with HBS (control), DTX (3 doses in 2 weeks; total dose: 36 mg/kg), or STS –Lipo (3 doses in 2 weeks; total dose: 9 mg/kg). Free STS was i.p. injected consecutively for 5 days by i.p. injection (total dose: 3 mg/kg). The tumor growth was measured using calipers. Data = mean ± SD (n = 10). * indicates p value< 0.05. Significant difference for the comparisons indicated on Day 18

2.4.11 Storage stability

STS-Lipo was stored at 4 ºC and the size and encapsulation efficiency were measured after 1, 4, and 6 months (**Table 2.5**). The samples did not show visible precipitates, and no apparent change in size or drug encapsulation was observed over the period of 6 months.

Table 2.5. Drug retention, size and polydispersity index (PDI) of the STS-Lipo upon storage at 4 °C. Data = mean ± SD (n = 3)

Month	Size	PDI	Loading efficiency (%)
0	96.71±1.01	0.023±0.032	100.44±2.55
1st	98.24±1.22	0.033±0.12	97.25±1.87
4th	100.5±0.151	0.030±0.023	98.12±3.10
6th	102.3±0.173	0.039±0.014	96.74±2.46

2.5 Discussion

Most of the clinically approved liposomal products employ the active loading approach to stably encapsulate the drug, including Doxil, DaunoXome and Marqibo. Taking Doxil as an example, doxorubicin (DOX) is actively loaded into the liposomes via an ammonium sulfate gradient, forming crystals with the sulfate ions inside the liposomal core. As a result, a high loading efficiency (D/L = 2/15, w/w) can be achieved, and the formation of drug aggregates inside the liposomes reduces the leakage of the drug, leading to improved PK and storage stability. This active loading method involves dissolving and incubating the drug with preformed liposomes containing a chemical gradient (i.e. the compositions of the inner and outer aqueous phases are different) at the temperature that is slightly above the transition temperature (T_m) of the lipid bilayer. The drug needs to be soluble in the outer aqueous phase first and permeable through the lipid bilayer into the inner phase to efficiently interact with the ions inside to form stable crystalline or complex. Therefore, the drug needs to possess specific properties to be a candidate for the active loading approach. First, the drug needs to exhibit good water solubility and membrane permeability. Second, the drug has to contain certain functional groups that can interact with specific ions for forming stable complex, for example, amino group and sulfate;

carboxylate and calcium. Like DOX, STS contains a weak base secondary amine group that may interact with sulfate to form stable complex, and its high lipophilicity (logP 4.17) suggests good membrane permeability. However, STS is not a good candidate for the active loading method as it is not water soluble and reducing the pH does not increase the solubility to a desirable extent. We hypothesized that adding a limited amount of a water miscible solvent in the active loading system could solubilize STS in the outer phase as well as improve its penetration through the lipid bilayer into the inner core. STS is dissolved freely in DMSO, which is miscible with water. We determined that 5 vol% DMSO is minimally required to dissolve STS in the outer phase of 100 nm preformed liposomes (100 mM acetate buffer, pH 5) at 1 mg/ml. When STS was incubated with the preformed liposomes containing an ammonium sulfate gradient in the presence of 5 vol% DMSO at 60°C, complete STS loading was reached within 5 min at a D/L of 0.31/1 (mol/mol). STS loading could also be achieved at room temperature, but required a longer time (15 min), suggesting the presence of DMSO might increase the membrane permeability of STS. On the other hand, in the absence of DMSO, <3% of the drug was loaded into the preformed liposomes, indicating that DMSO was required for efficiently loading of STS into the liposomes. We also compared the drug loading in the presence of 5-60 vol% DMSO at room temperature and discovered that even with 60 vol% DMSO in the system, complete STS loading was reached at a D/L of 0.31/1, suggesting the ammonium sulfate gradient could be maintained even in the presence of 60% DMSO at room temperature. However, if the system contained only 2 vol% DMSO which was not sufficient to dissolve STS, complete drug loading could not be achieved even after 1 h incubation at 60 °C, with significant precipitates in the final product. These results confirm the importance of completely dissolving STS by DMSO in the system for efficient drug loading. Mark et al. [81] proposed that DMSO could serve as an agent to increase

solubility of hydrophobic drugs to promote the drug loading. It is also hypothesized that the drug did not need to be completely solubilized in the outer phase, as when solubilized drug molecules are loaded inside the liposomes, the same amounts of molecules would be released from the insoluble aggregates until all the molecules were loaded. Indeed, ~95% of carfilzomib was actively loaded into the liposomes at a D/L of 0.12 (w/w) in the presence of 10 vol% DMSO, wherein the drug was not completely soluble and was in a suspension form in the beginning of the incubation. By the time when this thesis was being composed, this method was still not reported in any peer-reviewed journals but in a patent disclosure. There remain questions to be answered with this technology. First, can other solvents be used and can this method be applied to other drugs? Second, this method required frequent stir/vortex of the mixture to achieve good drug loading. This could be problematic in scale-up. Can an improved method be developed? Third, what is the role of DMSO in promoting drug loading? Forth, is complete solubilisation of drug really not necessary? Is there any advantage of complete solubilisation of drug?

The Bally lab previously reported that ethanol could facilitate DOX loading into liposomes containing a pH gradient [82]. However, the ethanol method could only be applied to cholesterol free liposomes, and the loading was needed to be performed at 37 °C in the presence of a narrow range of ethanol content (10-15 vol%). In the final step, STS-Lipo were purified by gel filtration or extended dialysis against HBS. As revealed in the cryo-TEM image, STS formed spherical nano-aggregates in the aqueous core of liposomes, resulting in high drug retention during 37 °C incubation in buffer or 50% serum. This stable drug encapsulation also resulted in the prolonged storage stability at 4 °C with no significant size change or drug leakage detected during 6 months of storage (study ongoing). It is worth mentioning that Cryo-TEM examines the morphology of the liposomes on a fixed plane of a frozen liquid sample, which reveals the detailed structure of

the liposomes. However, this fixed plane could be at the edge or center of a liposome. Therefore, the variation in size in Cryo-TEM images does not result from the real size variation, but the images at the edge or center of the liposomes. The size variation of the liposomes was measured by dynamic light scattering and the PDIs were all below 0.1, suggesting uniform size distribution. Prior studies using liposomes to encapsulate STS and its derivative (UCN-01) encompass two drug loading methods: passive loading using the reverse evaporation (RE) method [61], and the active loading via a normal or reversed pH gradient [83, 84]. These methods provided low to moderate drug loading efficiency, with a D/L of 0.008 (mol/mol) for the RE method, 0.035 (mol/mol) for the normal pH gradient, and 0.09 (mol/mol) for the reversed pH gradient method. Moreover, the stability of the liposomes (DSPC/DOPE/cholesterol/DSPE-PEG_{2000}) prepared with the reverse pH gradient method was poor, leaking ~70% of STS when incubated with PBS or serum at 37 °C within 24 h, possibly due to the unstable drug loading and/or lipid formulation with low lipid transition temperature. This result may also suggest a compromised storage stability, which may diminish the potential of developing this formulation into a pharmaceutical product. On the contrary, SALT provided a stable liposomal formulation of STS with a high D/L of 0.36 (mol/mol). In addition to these attempts, developing an active loading method for water insoluble drugs has been an actively pursued topic of research. [83-89]. Zhigaltsev et al. [63] chemically conjugated a piperizine group to docetaxel to introduce a weak base functional group (tertiary amine) to improve the drug solubility at pH 5 (1.7 mg/mL) as well as enable the prodrug to form complex with the sulfate ions inside the liposomes. A D/L of 0.4 (w/w) was achieved with this method. Sur et al. [85] chemically modified the hydrophilic surface of cyclodextran with an alkyl amino group and employed this ionizable cyclodextran as a solubilizing agent in the active loading process. The ionizable cyclodextran solubilized a water insoluble compound by incorporating it inside the

hydrophobic chamber and carried the drug through the lipid bilayer into the aqueous core, where the cyclodextran was ionized by a low pH and trapped. Our method also involves inclusion of a solubilizing agent (i.e. DMSO) in the active loading system. As many water insoluble compounds are freely soluble in DMSO, it is anticipated that our method could be employed to actively load many other water insoluble compounds into liposomes for targeted drug delivery. This new loading technology, although derived from the existing techniques, offers more than incremental improvements, as it enables stable encapsulation and delivery of STS and possibly many other water insoluble drugs that otherwise cannot be formulated with the standard active loading method. Compared to the Zhigaltsev and Sur methods, our approach does not need chemical modification of a solubilizing agent for drug loading. Additionally, high amounts of STS (1 mg/mL) can be efficiently loaded into liposomes at room temperature. In order to evaluate the potential of STS-Lipo in STS delivery for cancer therapy, we compared the activity of DTX, free STS and STS-Lipo against resistant tumor cells *in vitro* and *in vivo*. Free STS and STS-Lipo exhibited comparable potency against EMT6/AR1 and PC-3-RES cells and were 2- to 360-fold more potent than DTX. The overall dose of STS-Lipo that could be safely administered to mice was 3 times higher than free STS. As a result, STS-Lipo exhibited significantly improved antitumor activity against the DTX-resistant EMT6/AR1 tumor in mice compared to free STS at their MTDs.

2.6 Conclusion

The standard active loading technique cannot formulate water insoluble drugs into liposomes. Insoluble drugs account for a large percentage of therapeutic agents and require advanced technologies for effective delivery. We have developed a new active loading method to encapsulate a water insoluble drug STS into liposomes at a D/L of 0.31/1 (mol/mol). STS was loaded into the liposomes via an ammonium sulfate gradient in the presence of a water miscible

solubilizing solvent, DMSO, forming a spherical drug aggregate inside the core of liposomes with improved drug retention upon 4 °C storage or 37 °C incubation with 50% serum. The complete drug loading could be achieved within 15 min at room temperature. Compared to free STS, STS-Lipo exhibited comparable *in vitro* cytotoxic potency, but STS-Lipo could be safely dosed 3 times higher. As a result, the *in vivo* efficacy of STS-Lipo against a resistant tumor model was significantly improved compared to free STS and DTX. This simple and efficient drug loading method may potentially transform STS into an effective therapeutic agent against resistant cancer.

Chapter 3: Systemic Study of Solvent-Assisted Active Loading of Gambogic Acid into Liposomes and its formulation optimization for Improved Delivery

3.1 Project Summary

In Chapter 2, SALT was developed to encapsulate a water insoluble weak base efficiently into the liposomal core in the presence of 5 vol% DMSO. In this study, we further examined the effect of various water miscible solvents in promoting active loading of other types of drugs into liposomes. To achieve complete drug loading, the amount of solvent required must result in complete drug solubilization and membrane permeability enhancement, but must be below the threshold that induces liposomal aggregation or causes bilayer disruption. Afterwards, we used the SALT to load gambogic acid (GA, an insoluble model drug that shows promising anticancer effect) into preformed liposomes, and then optimized the loading gradient and lipid composition to prepare a stable formulation (Lipo-GA) that displayed >95% drug retention after incubation with serum for 3 days. Lipo-GA contained a high drug-to-lipid ratio of 1/5 (w/w) with a mean particle size of ~75 nm. It also displayed a prolonged circulation half-life (1.5 h vs. 18.6 h) and enhanced antitumor activity in two syngeneic mice models compared to free GA. Particularly, complete tumor regression was observed in the EMT6 tumor model for 14 d with significant inhibition of multiple oncogenes including HIF-1α, VEGF, STAT3, BCL-2, and NF-κB.

3.2 Introduction

Doxil® was the first FDA approved liposomal formulation. Since then, a number of liposomal formulations, such as Marqibo® (vincristine liposome), Onivyde® (irinotecan liposome), and Vyxeos® (cytarabine and daunorubicin co-encapsulated liposome), have been approved for cancer treatment [90-93]. These liposomal products are prepared by active loading, for which the

solubilized amphiphilic drug can diffuse through the lipid membrane to form impermeable complexes with the counter ions inside the aqueous core of liposomes. This method provides high drug encapsulation efficiency, minimal drug loss (<5%) during manufacturing, and increased stability for storage and in blood circulation. However, this technology can only be used for amphipathic drugs that exhibit both good aqueous solubility and membrane permeability, such as doxorubicin. Poorly water soluble drugs are normally loaded into the lipid bilayer with limited capacity and poor drug retention, leading to burst drug release and little improvements in efficacy and safety [94, 95]. We have previously showed that a water insoluble weak base drug (staurosporine, STS) could be actively loaded into the liposomal aqueous core via an ammonium gradient in the presence of 5 vol% DMSO [96]. It was hypothesized that DMSO could solubilize STS in the loading mixture (STS and liposomes in buffer) and promote the drug permeation into the liposomal core for active loading. This drug loading method was named **S**olvent-assisted **A**ctive **L**oading **T**echnology (SALT). To the best of our knowledge, this was the first report disclosing a technology allowing active and complete loading of an insoluble compound into the inner aqueous core of liposomes at a high drug-to-lipid ratio (0.2, w/w). This liposomal STS (STS-Lipo) displayed prolonged pharmacokinetics (PK), enhanced safety, and increased efficacy against the tumor in mice compared to free STS (dissolved in Tween80/ethanol/saline). However, it remains unclear whether the SALT can be applied to loading of different types of drugs, whether various solvents can be used in this system, and what the roles of the solvents are in promoting the drug loading (solubilization vs. liposomal membrane permeability). These fundamental questions need to be systemically studied to better understand the SALT system, tailor the loading for each drug and develop a solid platform technology for active loading of insoluble drugs. To study the first question, we selected

gambogic acid (GA, weak acid, water solubility <5 μg/mL) as the model compound to test whether the SALT can be applied to loading of different types of drugs. We also took the advantage that GA is soluble in a variety of water miscible solvents to examine the range of solvents that can be used for liposomal drug loading. Finally, we examined the solvent effect on solubilization of GA, aggregation/disruption of liposomes, and GA loading efficiency. The results were compared and analyzed to delineate the solvent effect in promoting GA loading into liposomes, and the optimal range of solvent content in the loading mixture was identified for each solvent to achieve complete loading of GA.

GA, a natural product extracted from the Garcinia hanburryi tree, has been demonstrated to exhibit potent anticancer activity against a wide range of cancers both *in vitro* and *in vivo* [97-99]. GA inhibits cancer cells through multiple mechanisms, including cell cycle arrest, apoptosis, anti-angiogenesis, anti-metastasis, and anti-inflammation [100-105]. GA can also synergistically enhance efficacy of other chemotherapeutic agents [106-108]. However, the clinical application of GA has been limited by its poor water solubility (<5 μg/mL) and short half-life (< 4h) [109, 110]. Strategies, including PEG conjugation and passive encapsulation of GA into the hydrophobic compartment of nanoparticles, have been developed to increase the drug solubility, but the improvements in PK and efficacy were only minimal to moderate, probably due to *in vivo* instability of the formulations with burst drug release [111-115]. In general, liposomes have been utilized to increase drug solubility by loading insoluble drugs in the lipid bilayer. However, the bilayer loading is often unstable with limited capacity, leading to instability of the formulation and/or burst drug release in blood circulation. The SALT might offer a solution to this challenge by forming stable drug complexes in the liposomal core. To advance this technology, the second part of this study was focused on optimizing the loading gradient and lipid composition for

preparing stable Lipo-GA that retained the drug when incubated with serum. Finally, the optimal Lipo-GA was compared with free GA in terms of the hemolytic activity, PK, and antitumor efficacy to demonstrate the utility of the SALT.

3.3 Methods and Materials

3.3.1 Materials

GA was purchased from Guangzhou Boji Medical Biotechnological Co. (Tianhe District, Guangzhou, China). Phospholipids were obtained from Avanti Polar Lipids (Alabaster, AL). Sepharose CL-4B, and Sephadex G-50 were purchased from Fisher Scientific (Ottawa, ON, Canada). Human and sheep red blood cells (RBCs) for hemolysis test were purchased from Innovative Research (Novi, MI). DiIC18(5); 1,1′-dioctadecyl-3,3,3′,3′-tetramethylindodicarbocyanine (DiD) & SuperScript III reverse transcriptase were purchased from ThermoFisher Scientific (Mississauga, ON, Canada). Primers for RT-PCR were purchased from Integrated DNA Technologies (Toronto, Ontario, Canada). All other chemical reagents and organic solvents were of analytical grade and obtained from Sigma-Aldrich (Oakville, ON, Canada).

3.3.2 Cell maintenance

B16F10 murine melanoma and EMT6 murine breast cancer cells were purchased from Cedarlane (Burlington, ON, Canada), and cultured in DMEM media supplemented with 10% FBS in T75 flasks in an incubator maintained at 37 °C with 5% CO_2.

3.3.3 Instrumentation and experimental analysis

A Waters ACQUITY Ultra Performance Liquid Chromatography (UPLC) H-Class System equipped with a photodiode array (PDA) detector was used to determine the solubility of GA

and the concentrations of GA in liposomal formulations. GA solutions and Liposomal GA formulations were diluted with acidified methanol (3 vol% acetic acid) prior to sample injection. Two µL of the diluted sample was injected and then separated through a BEH-C18 column (2.1 × 50 mm) using a gradient mobile phase. The mobile phase consisted of solvent A: acetonitrile with 0.1 vol% formic acid and solvent B: MilliQ water with 0.1 vol% formic acid. The flow rate was 0.4 mL/min with the following gradient: 0 min: A/B (10/90), 1.8 min: A/B (85/15), 2.7 min: A/B (15/85), 4 min: A/B (10/90). The concentration of GA was determined by integrating the chromatographic peak area detected at a wavelength of 360 nm using the Empower 3.0 software. The mobile phase was sterile filtered. The U(H)PLC-MS/MS system used for measuring GA in biological samples was composed of an Agilent 1290 Infinity Binary Pump, a 1290 Infinity Sampler, a 1290 Infinity Thermostat, and a 1290 Infinity Thermostatted Column Compartment (Agilent, Mississauga, ON, Canada). The U(H)PLC system was connected to an AB Sciex QTrap® 5500 hybrid linear ion-trap triple quadrupole mass spectrometer equipped with a Turbo Spray source (AB Sciex, Concord, ON, Canada). The mass spectrometer was operated in negative ionization mode. Chromatographic analysis was conducted using a Waters Acquity UPLC BEH-C18, 1.7 µm 2.1 × 100 mm column, which was protected by a Waters Acquity UPLC BEH-C18 VanGuard guard column (1.7 µm, 2.1 × 5 mm) (Waters Corp., Milford, MA). The mobile phase consisted of Solvent A: water with 2.5 mM ammonium formate (AF), and solvent B: acetonitrile with 2.5 mM AF. The mobile phase initial conditions were solvent A (10 vol%) and solvent B (90 vol%), which was ramped to solvent A (5 vol%) by 1.3 min and held until 3.0 min followed by an equilibration with solvent A (10 vol%) and solvent B (90 vol%) for 2 min. The flow rate was 0.2 mL/min, and the injection volume was 15 µL with a total run time of 6.0 min. The mobile phase flow was

diverted to the waste before 1.4 min and after 4.1 min during the chromatographic run. GA was quantified using a daughter ion (*m/z* 628.17 → 583.1) and the internal standard (IS; ursolic acid, m/z 455.5), and GA concentration in biological samples was determined by comparing the results from the standard samples containing known concentrations of GA (dissolved in 12 mM arginine solution) or liposomal GA (Lipo-GA) (25-750 ng/mL). The chromatographic retention time for GA and the I.S. were 2.49 min and 2.41 min, respectively. Data were acquired using the Analyst 1.5.2. software.

3.3.4 Liposome preparation and drug loading

All liposomal formulations were composed of phospholipids (DSPC or DOPC), cholesterol, and DSPE-mPEG2K with various ratios, and were prepared with the thin film hydration method. Briefly, the lipid film was hydrated with one of the internal phases listed in **Table 3.1** and extruded through a series of polycarbonate filters with pore sizes ranging from 0.2 to 0.08 μm, using a Lipex Extruder (Transferra, Vancouver, BC, Canada) to obtain small uni-lamellar vesicles with a mean diameter between 70-120 nm. Basified copper acetate (250 mM) or copper sulfate (250 mM) was prepared by titrating the pH to 9.5 using 28-30 vol% ammonium hydroxide solution.

The temperature applied during the extrusion depended on the phase transition temperature of the phospholipid component. DOPC liposomes were extruded at room temperature, whereas DSPC liposomes were extrude at 65 °C. Particle size and zeta potential were measured with a Zetasizer (Nano-ZS, Malvern Instruments, Malvern, UK). The external phase was exchanged by passing the liposomes through a Sephadex G-50 column pre-equilibrated with one of the external phases listed in **Table 3.1** containing 25 mM EDTA followed by another passage over a G-50 column pre-equilibrated with the EDTA free external phase. The liposomes containing a loading

gradient were then mixed with a drug in the presence of a miscible solvent (2-50 vol% for GA & 2-70 vol% for STS) selected from **Table 3.1** at room temperature for 30 min at a drug-to-total lipid ratio of 0.1 (w/w). Un-encapsulated drug and the miscible solvent were removed by dialysis or passage through a Sephadex G-50 column equilibrated with HEPES buffered saline (HBS, pH 7.5).

Table 3.1. Examples of trapping agents and miscible solvents for drug loading.

Gradient preparation for drug loading			**Drug loading**	**After loading**
Weak acid	**Internal phase** / **Trapping agent**	**External phase**	**Miscible solvent**	**External buffer**
Gambogic acid (GA, M.W. 628.76)	200 mM Calcium (II) formate 150 mM Magnesium (II) gluconate 250 mM Copper (II) acetate (pH 5.2) 250 mM Basified copper acetate (pH 9.5) 250 mM Basified copper sulfate (pH9.5)	50 mM Borate buffer (pH 8.5)	DMSO, DMF, EtOH, MeOH, acetonitrile, acetone, 1,4-dioxane, NMP	HEPES buffered saline (HBS, pH 7.5)
Weak base	**Trapping agent**	**External phase**	**Miscible solvent**	
Staurosporine (STS, M.W. 466.53)	300 mM Ammonium sulfate	100 mM Acetate buffer (pH 5.5)	DMSO, 1,4-dioxane	

3.3.5 Determination of the minimal amount of solvent required for complete solubilization of 1 mg/mL insoluble drugs

GA and STS were dissolved in 50 mM borate buffer (pH 8.5) and 100 mM acetate buffer (pH 5.5), respectively, at 1 mg/mL in the presence of 0-10 vol% of a solvent selected from **Table 3.1**. The solution/suspension was centrifuged at 14,000 rpm for 20 min, and the supernatant was analyzed for drug concentration by the UPLC-UV method described in **Method 3.2.3**.

3.3.6 Solvent impact on liposome integrity

Preformed liposomes composed of DSPC/Chol (55/45, molar ratio) were incubated in HBS containing 2-75 vol% of a solvent selected from **Table 3.1** at 10 mg total lipid/mL for 30 min at room temperature. The liposome integrity was analyzed by measuring the size and the polydispersity index (PDI) with a Zetasizer particle analyzer.

3.3.7 Solvent impact on drug loading

Preformed liposomes (DSPC/Chol, 55/45 mol%) containing either the Mg^{2+} gradient (150 mM magnesium gluconate) or ammonium gradient (300 mM ammonium sulfate) were mixed with either GA or STS, respectively, at 1 mg drug/mL with a drug-to-lipid ratio of 0.1 (w/w) in the presence of 0-60 vol% of a miscible solvent selected from the list in **Table 3. 1**. The mixture was incubated for 30 min, followed by purification using a Sephadex G-50 spin column pre-equilibrated with HBS. The loading efficiency was determined by the following equation, where the drug concentration was measured by the UPLC-UV method and the DSPC concentration was measured by the Stewart assay [116]

$$\text{Loading efficiency (\%)} = \frac{[\text{Drug}]_{\text{purified}} / [\text{DSPC}]_{\text{purified}}}{[\text{Drug}]_{\text{initial}} / [\text{DSPC}]_{\text{initial}}} \times 100\%$$

3.3.8 *In vitro* drug retention analysis

Various liposomal GA formulations labeled with DID (1% mol) were mixed with heat-deactivated FBS (1:1 v:v) at 800 µg GA /mL, and incubated at 37 °C over a period of 48 h. At selected time points, 300 µL of the mixture was collected, and passed through a Sepharose CL-4B column pre-equilibrated with HBS to remove released GA, and 150 µL of the liposomal

fraction was collected. The percentage of drug retention was calculated by the formula shown below, where [GA] was determined by the UPLC method, and [DID] was estimated by absorbance at 650 nm by a microplate reader.

3.3.9 Cryo-transmission electron microscopy (Cryo-TEM) analysis

Cryo-TEM imaging was performed using a modification to previously described methods [117, 118]. Liposomes were concentrated to ~15-25 mg/mL total lipid and vitrified using a Mark IV Vitrobot (FEI, Hillsboro, OR). Frozen grids were stored under liquid nitrogen until imaged. Grids were further prepared to support AutoLoader function on a FEI Titan Krios fitted with the Falcon III direct electron detector (FEI, Hillsboro, OR). Images were obtained at 47,000x magnification and a nominal under focus of 1-2um. All imaging was performed at the Life Sciences Institute (UBC, Vancouver, BC).

3.3.10 Hemolysis test

Free GA formulation was prepared as reported previously [111] by dissolving 2 mg GA in 1 mL of 12 mM arginine solution. GA formulations were then diluted with PBS and mixed with red blood cells (human or sheep, final 1.5 vol%) at a concentration of 40 µg GA/mL, representing the estimated C_0 for the *in vivo* study. The sample was incubated for 1 h at 37 °C, followed by centrifugation at 2,500 rpm for 10 min. The absorbance (OD) of the supernatant at 545 nm was determined by a microplate reader. TritonX-100 (2.5 vol%) was used as a positive control. The percentage of hemolysis was calculated as follows:

$$Hemolysis\ (\%) = \frac{OD_{sample} - OD_{blank\ control}}{OD_{positive\ control} - OD_{blank\ control}} \times 100$$

3.3.11 Animal models

Female BALB/c and C57/BL6 mice (18–20 g) were purchased from The Jackson Laboratory (Bar Harbor, ME). All the *in vivo* studies were conducted in accordance with the established experimental protocols approved by the Animal Care Committee of the University of British Columbia (Vancouver, BC, Canada). BALB/c and C57BL6 mice were implanted s.c. with EMT6 and B16F10 (2×10^5 cells in 50 µL media) into the shaved right lateral flank, respectively. One to two weeks later, mice were randomly divided into 4 groups when tumor size reached 70-110 mm^3. Each group was comprised of 5-6 mice for PK and antitumor efficacy studies described below.

3.3.12 Pharmacokinetic study

The EMT-6 tumor-bearing mice were i.v. injected with free GA or Lipo-GA at 10 mg GA/kg, and plasma was collected at different time points. Drug extraction from plasma was performed by modifying the previous method [119]. One hundred µL of plasma was mixed with 200 µL MeCN containing IS (20 ng/mL), 2 µL 3 M HCl, and 100 µL 2M ammonium sulfate. The mixture was then vortex for 2 min and centrifuged at 9,500 rpm for 6 min. Fifteen µL of the top phase was analyzed using the U(H)PLC-MS/MS method described above. PK parameters were obtained by analyzing the plasma profile with Phoenix WinNonlin® software (Princeton, NJ) using the non-compartmental model.

3.3.13 *In vivo* antitumor activity

Free GA (4 mg GA /kg) and Lipo-GA (4 or 20 mg GA/kg) were given intravenously when the tumor size reached 70-110 mm^3. In the control group, the mice were i.v. treated with 100 mg lipids/kg of empty liposomes (lipid dose equivalent to that of Lipo-GA at 20 mg GA/kg). The therapeutic efficacy was assessed by monitoring tumor size and body weight every day. The

tumor size was measured by a LCD digital caliper, and calculated as (tumor length) × (tumor width)^2 × 0.52. The tumor size and body weight of mice were monitored daily until the control group reached the end point (~1500 mm^3). In EMT6 tumor model, 3 mice from each group were euthanized 3 d post-administration to obtain tumor tissue for Real Time-Polymerase Chain Reaction (RT-PCR) analysis of selected genes. At the experimental endpoint for the EMT6 tumor model, mice were euthanized for tumor harvest. Tumors were incubated in 10 vol% formalin in PBS at room temperature for 2 days followed by paraffin-embed section and H&E or immunohistological staining for Ki67, CD31, and NF-κB p65. Image analysis was conducted with the ImageScope software using Positive Pixel Count algorithm. Image analysis output was positive pixel counts divided by the area analyzed. All data was normalized against the control.

3.3.14 RT-PCR

Total RNA from tumor was extracted with the Qiagen RNeasy Plus Mini Kit according to the manufacturer's instruction. Complementary DNA (cDNA) was reverse-transcribed using the First-Strand Synthesis System (Invitrogen). cDNA was amplified with specific primers (**Table 3.2**) using a Fast SYBR™ Green Master Mix (ThermoFisher Scientific) and a StepOnePlus™ RT-PCR System (Applied Biosystems). 18s rRNA was used as the endogenous control. the comparative CT Method (△△Ct) was used to calculate the relative fold difference of each gene expression.

Table 3.2 Primer sequences used for RT-PCR.

Gene	Primer	Sequence
Bcl-2	Forward primer	5'-GCTACCGTCGTGACTTCGC-3'
	Reverse primer	5'-TCCCAGCCTCCGTTATCC-3'
HIF-1α	Forward primer	5'-CCTTCTGATGGAAGCACTAGAC-3'
	Reverse primer	5'-CTGCCTTGTATGGGAGCATTA-3'
VEGF-A	Forward primer	5'-CGGGAGACAATGGGATGAAA-3'
	Reverse primer	5'-GGGAGAGAGAGATTGGAAACAC-3'
STAT3	Forward primer	5'-TCTCCACTTGTCTACCTCTACC-3'
	Reverse primer	5'-TCACCCACACTCACTCATTTC-3'
18S rRNA	Forward primer	5'-CGTCGTAGTTCCGACCATAAA-3'
	Reverse primer	5'-CGGAATCGAGAAAGAGCTATCA-3'

3.3.15 Statistical Analysis

Significant differences were determined by the Student's t test using GraphPad Prism 6.0 (La Jolla, CA). Difference between two groups with a p value< 0.05 was considered statistically significant. All data are express as mean± standard deviation.

3.4 Results and Discussion

3.4.1 Solvent effect on drug solubility, liposome integrity and drug loading

We have demonstrated that by including 5 vol% DMSO in the mixture of staurosporine (STS, solubility in water <2 μg/mL) and liposomes containing an ammonium sulfate gradient, STS could be actively loaded and stably encapsulated inside the liposomal core at a high drug-to-lipid ratio of 0.2 (w/w) in Chapter 2. It was observed that 5 vol% DMSO completely

solubilized STS and facilitated permeation of STS molecules through the lipid bilayer to form complexes inside the aqueous core, evidenced by Cryo-TEM images. In this chapter, we performed systemic studies on the SALT, aiming to answer three questions. First, can the SALT be applied to other types of drugs in addition to weak base compounds? Second, are other water miscible solvents compatible with the SALT system? Third, how can solvents promote drug loading?

We strategically selected GA as the model drug to perform the study as this weak acid drug belongs to a different class of compounds and is soluble (> 20 mg/mL) in a wide range of water miscible solvents (**Table 3.1**). We hypothesized that a water miscible solvent can help dissolve GA in the exterior phase and increase the membrane permeability, thereby promoting GA molecules to penetrate the lipid bilayer at room temperature and then form complexes with the metal ion to get trapped inside the liposomes. However, since the solvent could dissolve the lipids, if the solvent concentration exceeds a limit, the liposomal membrane may become too leaky to retain the loading gradient. It was also hypothesized that the concentration limit for each solvent for disrupting the bilayer would be different. To confirm the hypotheses, we first determined the minimal amount of solvent required to completely dissolve 1 mg/mL of GA in borate buffer, and then studied the solvent tolerability of the DSPC/Chol liposomes against different solvents at a range of concentrations by monitoring the particle size change. A total of 8 solvents were tested, and it was found that 2 vol% of solvent was needed for complete solubilization of GA in borate buffer at 1 mg/mL, except for dioxane, 5 vol% was required (**Figure 3.1**). In the solvent tolerability test (**Table 3.2**), DMSO, DMF, and MeOH did not cause liposomal particle size change up to a concentration of 50 vol%. However, for DMSO and DMF at 50 vol%, the mixture turned blurry, possibly due to precipitation of the salts.

EtOH, MeCN, acetone and dioxane did not aggregate liposomes up to a concentration of 20 vol%. The liposomes only tolerated NMP up to 5-10 vol%, but at 10 vol% the mixture turned blurry, again possibly due to insolubility of the salts. Measuring the particle size is a robust method to estimate the tolerability of the liposomal bilayer against different concentrations of solvents. However, it is understood that disruption of the liposomal loading gradient could occur at a lower solvent concentration (than the result from the solvent tolerability data), and the increase of membrane permeability could begin at an even lower solvent content. Nevertheless, the solvent tolerability data provide quick information of the upper limit for a solvent to be used in the SALT.

The fluorescent dye leakage assay is a standard method to measure liposomal membrane permeability [120, 121]. However, when a miscible organic solvent was present in the system, it was very challenging to study membrane leakage using this method. In fact, this assay was first employed, but the data were not conclusive as the fluorescence intensity of the released dye was affected by the organic solvent. Additionally, both solvent type and solvent amount in the system displayed significant impact on the fluorescence measurement, making the data difficult to interpret and conclude. Thus, we measured the loading efficiency to reflect the solvent effect on the membrane permeability, shown to be robust.

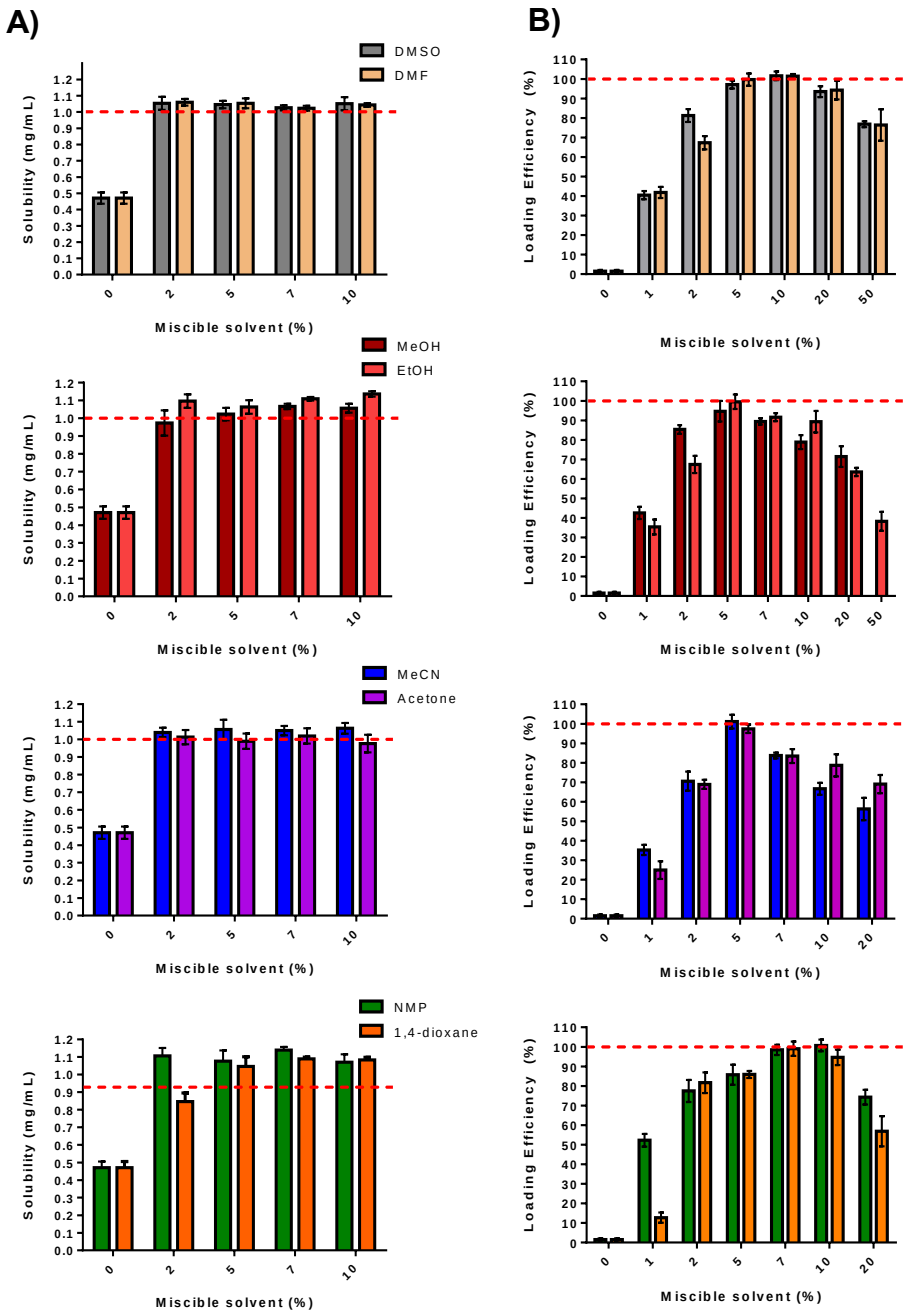

Figure 3.1. Solubility of GA in borate buffer in the presence of different amounts of miscible solvents (A), and the loading efficiency of GA in DSPC/Chol liposomes containing a magnesium gluconate gradient (150 mM). Data = mean ± SD (n = 3)

Miscible solvent	% of miscible solvent	5	10	20	50	70
Dimethyl sulfoxide (DMSO)	Size (nm)	112.5	112.1	109.4	108.7*	aggregation
	PDI	0.054	0.045	0.052	0.056	
Dimethylformamide (DMF)	Size (nm)	112.4	112.9	112.4	112.6*	aggregation
	PDI	0.061	0.043	0.039	0.062	
Methanol (MeOH)	Size (nm)	113.1	112.9	113.6	113.5	aggregation
	PDI	0.047	0.069	0.043	0.051	
Ethanol (EtOH)	Size (nm)	113.3	112.7	112.8	aggregation	aggregation
	PDI	0.048	0.033	0.043		
Acetonitrile (MeCN)	Size (nm)	112.9	112.3	113.1	aggregation	aggregation
	PDI	0.044	0.053	0.049		
Acetone	Size (nm)	113.4	113.9	113.2	aggregation	aggregation
	PDI	0.058	0.045	0.031		
N-Methyl-2-pyrrolidone (NMP)	Size (nm)	113.7	116.6*	300.7*	aggregation	aggregation
	PDI	0.098	0.193	0.358		
1,4 dioxane	Size (nm)	112.6	112.3	112.5	aggregation	aggregation
	PDI	0.045	0.05	0.06		

Table 3.2. The membrane integrity test of DSPC/Chol liposomes in the presence of different amounts of miscible solvent at 10 mg total lipid/mL. * indicates blurry

Liposomal loading of GA was performed in the presence of a range of solvents at various solvent concentrations, and the results are summarized in **Table 3.3**. It is established that complete GA loading could be achieved with all the tested solvents, and the optimal solvent concentration must exceed the minimal solvent content for complete drug solubilization. However, such solvent concentration cannot surpass the optimal threshold beyond which the solvent leads to liposomal aggregation. Similar results were also obtained with a weak base drug, STS as shown in **Table 3.3**. Nevertheless, the optimal range of concentration for the same solvent was different for different drugs (GA vs. STS). This may be attributed to the different ability of the liposomes for retaining different loading gradients. We then further demonstrated that this method could be used to load a variety of other drugs into liposomes, including artesunate, prednisolone hemisuccinate, and quercetin (**Table 3.4**). Our results indicate that: first, the SALT can be applied to a wide range of compounds; second, a variety of water miscible solvents are compatible with the SALT and can be used to facilitate drug loading; third, to achieve complete drug loading, the solvent concentration needs to slightly exceed that for complete drug solubilization, suggesting that the solvent acts both on solubilizing the drug as well as increasing the membrane permeability for effective drug permeation at room temperature.

Table 3.3 Summary of the solvent effect on drug solubility, liposomal aggregation and drug loading. DSPC/Chol liposomes (55/45, mol%) with a loading gradient were used. Drug loading for 1 mg/mL of GA or STS was performed at a D/L of 1/10, w/w) for 30 min at room temperature. The loading gradients for GA and STS were 150 mM magnesium gluconate and 300 mM ammonium sulfate, respectively. * high drug loading = loading efficiency >90%. Data = mean ± SD (n = 3). N.D. = not determined

Gambogic acid												
Miscible solvent	Minimal % of solvent for Complete solubilization	Optimal range to maintain high drug loading (%)*	Minimal % of solvent to cause size change	Loading efficiency (%)								
				% of miscible solvent	0	1	2	5	7	10	20	50
DMSO	2	5-20	70		1.55±0.57	41.36±2.12	81.26±3.30	97.11±2.02	N.D.	101.1±2.24	93.51±2.78	76.83±1.52
DMF	2	5-20	70		1.55±0.57	41.86±2.86	67.31±3.36	99.64±3.18	N.D.	101.42±1.16	94.31±4.76	76.38±8.04
MeOH	2	5-10	70		1.55±0.57	35.41±3.82	67.43±4.39	99.53±3.70	91.66±2.08	89.35±5.50	63.56±2.09	38.27±4.87
EtOH	2	5-7	50		1.55±0.57	42.57±3.12	85.37±2.49	94.67±5.24	89.44±1.61	78.91±3.58	71.47±5.31	N.D.
MeCN	2	5	50		1.55±0.57	35.26±2.61	70.57±4.91	101.12±3.51	83.70±1.45	66.65±3.08	56.30±5.70	N.D.
Acetone	2	5	50		1.55±0.57	24.95±4.51	67.54±3.35	97.40±2.15	83.47±3.61	78.69±5.69	69.11±4.68	N.D.
NMP	2	7-10	20		1.55±0.57	52.28±3.26	68.92±2.36	85.74±5.16	98.46±2.62	100.73±3.02	74.29±3.78	N.D.
14-dioxane	5	7-10	50		1.55±0.57	12.73±2.64	81.68±5.26	85.91±1.81	99.04±3.67	94.63±3.94	56.91±7.72	N.D.
Staurosporine												
Miscible solvent	Minimal % of solvent for Complete solubilization	Optimal range to maintain high drug loading (%)*	Minimal % of solvent to cause size change	Loading efficiency (%)								
				% of miscible solvent	0	2	5	7	20	60	70	
DMSO	2	5-60	70		2.31±1.28	87.52±2.12	103.15±4.17	103.31±4.55	100.45±0.92	97.21±2.41	81.8±0.42	
14-dioxane	2	5-20	70		2.31±1.28	37.61±3.53	87.21±3.76	99.65±5.15	101.55±3.66	88.11±1.41	73.15±4.37	

Table 3.4 Solvent-assisted active loading technology (SALT) can be applied to various drugs with poor water solubility. Drug loading for each drug candidate was performed with a fixed drug to lipid ratio (1/10, w/w) for 30 min.

Drug	Type	M.W.	Structure	Water Solubility (μg/mL)	Trapping agent	Miscible solvent (%)	Loading efficiency (%)	Size (nm)	PDI
Artesunate	weak acid	384.42	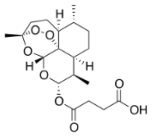	<500	Zinc acetate	5 (DMSO)	90.62	95.7	0.087
Prednisolone hemisuccinate	weak acid	460.52	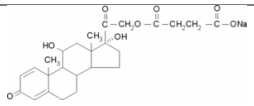	<500	Magnesium gluconate	5 (DMSO)	92.71	104.1	0.045
Quercetin	polyphenol	302.23	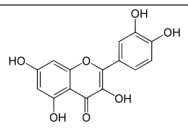	<500	Copper sulfate	9-12 (DMF)	82.12	105.2	0.153

3.4.2 Formulation optimization

The next aim of this study was to optimize the liposomal formulation for enhanced therapy of cancer to demonstrate the utility of SALT. We first compared GA loading efficiency of the DSPC/Chol/DSPE-mPEG2K liposomes with different loading gradients, including magnesium gluconate, calcium formate, copper acetate (pH 5.2), and basified copper acetate (pH 9.5). As depicted in **Figure 3.2A**, liposomes with all loading gradients achieved complete drug loading in the presence of 5 vol% DMSO at a drug-to-total lipid of 1/5 w/w. We then measured the drug retention in the liposomes composed of various loading gradients in the presence of 50% serum. Burst drug leakage was found in all the liposomal formulations (>60% in 2.5 h, **Figure 3.2B**); however, among these, the basified copper acetate gradient retained the drug the most. The data indicate that Cu^{2+} exhibited the highest activity forming stable complexes with GA among these different metal ions. Increasing the pH in the copper acetate loading gradient further increased the GA retention, and this could be due to that at the basic pH, GA was effectively ionized inside the liposomes and became less membrane permeable to leak out. We then employed the basified copper acetate as the loading gradient and altered the lipid composition to prepare different liposomal formulations and compared their drug retention in 50% serum. As shown in **Figure 3.2C**, decreasing the content of Chol in PEGylated DSPC liposomes improved GA retention from 40% to 68% (45 to 0 mol% of Chol) in the first 2.5 h. However, there was no significant improvement in drug retention 12 h post incubation (>70% drug leakage for all formulations). Reducing the Chol content in the lipid composition has been shown to improve retention for hydrophobic drugs, such as idarubicin [122]. It was speculated that hydrophobic drugs would exhibit decreased interaction with low-Chol liposomal membrane, resulting in decreased drug leakage.

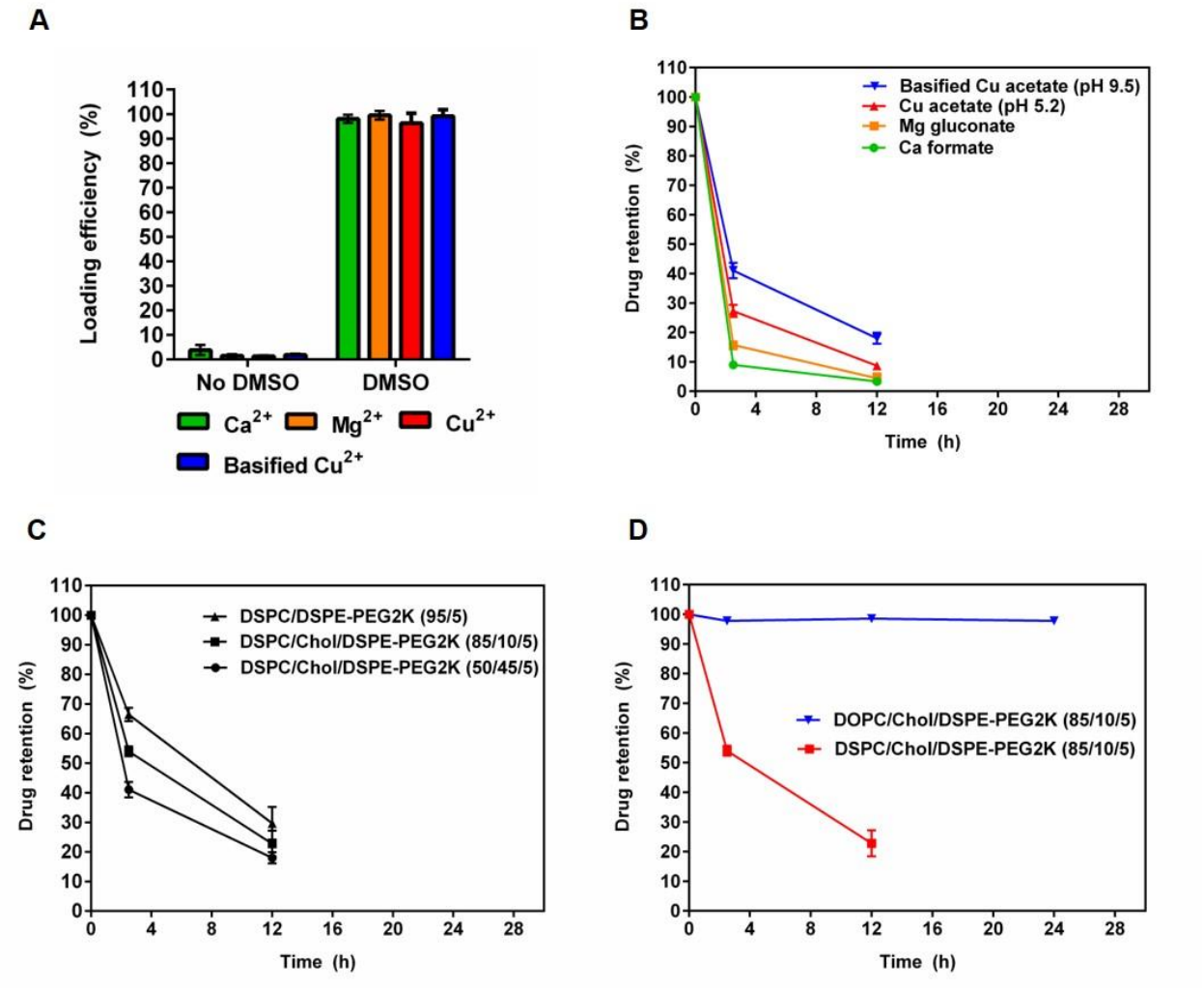

Figure 3.2 Optimization of liposomal formulations for GA. (A) GA loading into liposomes composed of DSPC/Chol/DSPE-mPEG2K (50/45/5, mol%) containing various trapping agents in the absence or presence of 5 vol% DMSO. (B) GA retention in liposomes containing different loading gradients when incubated in 50% FBS at 37 °C. (C) GA retention in liposomes containing various amounts of Chol when incubated in 50% FBS at 37 °C. (D) GA retention in liposomes composed of either DOPC or DSPC when incubated in 50% FBS at 37 °C

We then compared formulations prepared with either DOPC, an unsaturated phospholipid, or DSPC, a saturated phospholipid. As depicted in **Figure 3.2D**, the DOPC formulation (DOPC/Chol/DSPE-mPEG2K, 85/10/5, mol%) retained >95% drug after 24 h incubation in 50% FBS without significant size change (**Figure 3.3**), while its DSPC counterpart showed ~80% drug leakage within 12 h. This result was somewhat surprising as liposomes composed

of a saturated lipid with an increased transition temperature have been shown to retain doxorubicin better compared to an unsaturated lipid [123].

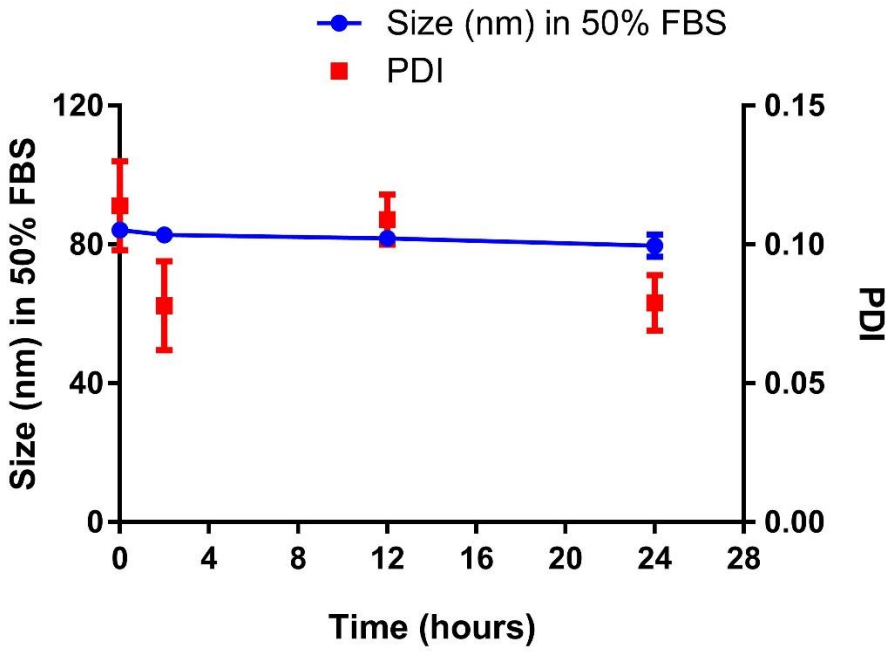

Figure 3.3 The stability of Lipo-GA in 50% FBS at 37 °C. Liposomal mixture after incubation was purified by a Sepharose CL-4B column to obtain liposomal fraction for size measurement. Data = mean ± SD (n = 3).

The reason that the DOPC formulation offered enhanced GA retention relative to the DSPC formulation remains unclear. However, it has been discovered that DOPC could form more flexible liposomes to trap hydrophobic molecules more efficiently relative to saturated lipids [124]. It is worth mentioning that our data also showed that the SALT could be applied for a variety of liposomal formulations for active drug loading, including non-PEGylated liposomes (DSPC/Chol), high and low Chol content liposomes, DSPC liposomes, and DOPC liposomes. The physical characteristics of the optimized Lipo-GA were summarized in **Table 3.5**, and the residual DMSO in the final formulation was <0.55 ppm. The formulation was used for the following studies in comparison with free GA. We also examined the morphology of Lipo-GA

using Cryo-TEM imaging. As shown in **Figure 3.4**, Lipo-GA displayed bilamellar conformation with an electron-dense structure inside the liposomal core. These two features of structure have been shown with other liposomal drug formulations with a copper gradient [125, 126], suggesting copper ions formed complexes with GA and contributed to the lipid bilayer rearrangement as well as enhanced drug retention.

Table 3.5 Characterization of Lipo-GA. Data = mean ± SD (n = 3).

	Lipid composition	Drug/lipid (w/w)	Size (nm)	PDI	Loading Efficiency (%)	DMSO (ppm)
Lipo-GA	DOPC/Chol/DSPE-mPEG2K (85/10/5, mol%)	1/5	74.81±0.69	0.081±0.04	99.21±1.31	<0.55

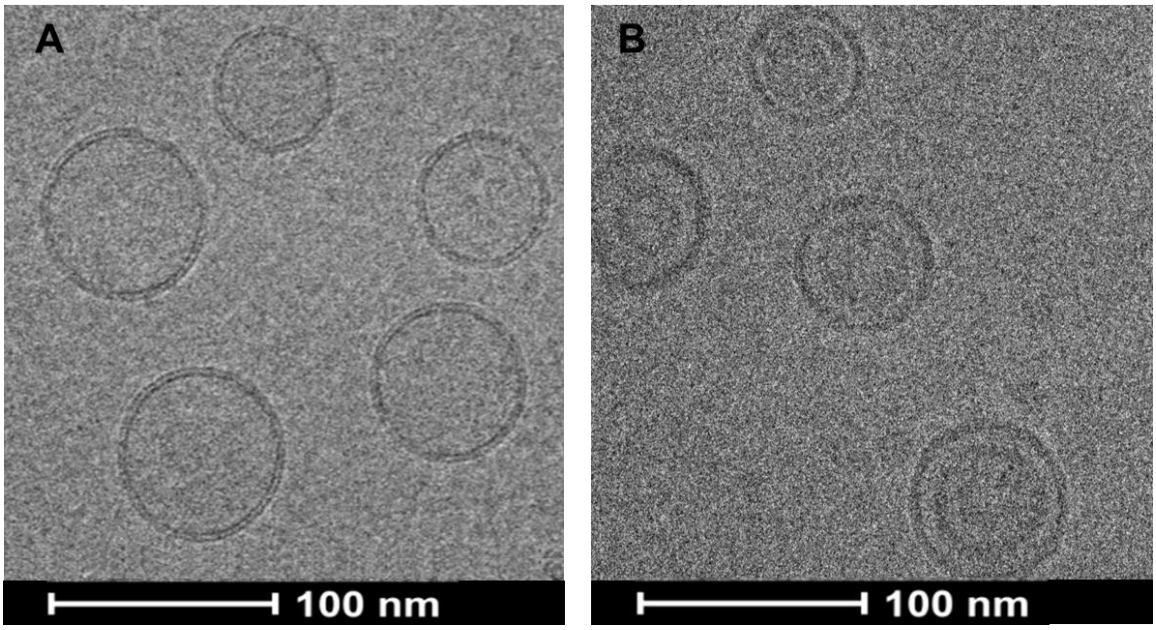

Figure 3.4 Cryo-TEM images of empty liposomes (DOPC/Chol/DSPE-PEG2K, 85/10/5 by mol%) (A) and Lipo-GA (B).

3.4.3 Hemolysis test

GA has been shown to induce apoptosis in erythrocytes, which could induce significant toxicity *in vivo* [127]. We hypothesized that in the Lipo-GA formulation, as the drug is loaded inside the liposomes with no burst release in the medium, the hemolytic toxicity would be reduced. In **Figure 3.5**, complete hemolysis of human and sheep RBCs was observed 1 h post incubation with free GA (40 μg GA /mL + 44 μg arginine/mL), whereas Lipo-GA (40 or 200 μg GA/mL) only resulted in mild hemolysis (<7%), which was comparable with negative controls including the arginine solution (44 μg arginine/mL) and empty liposomes (1 mg total lipid/mL). The tested concentrations were based on the estimated C_0 after an i.v. dose of free GA at 4 mg/kg and Lipo-GA at 4 mg/kg or 20 mg/kg. The data suggest Lipo-GA displayed little acute hemolytic toxicity, while free GA could induce significant hematological toxicity, such as anemia.

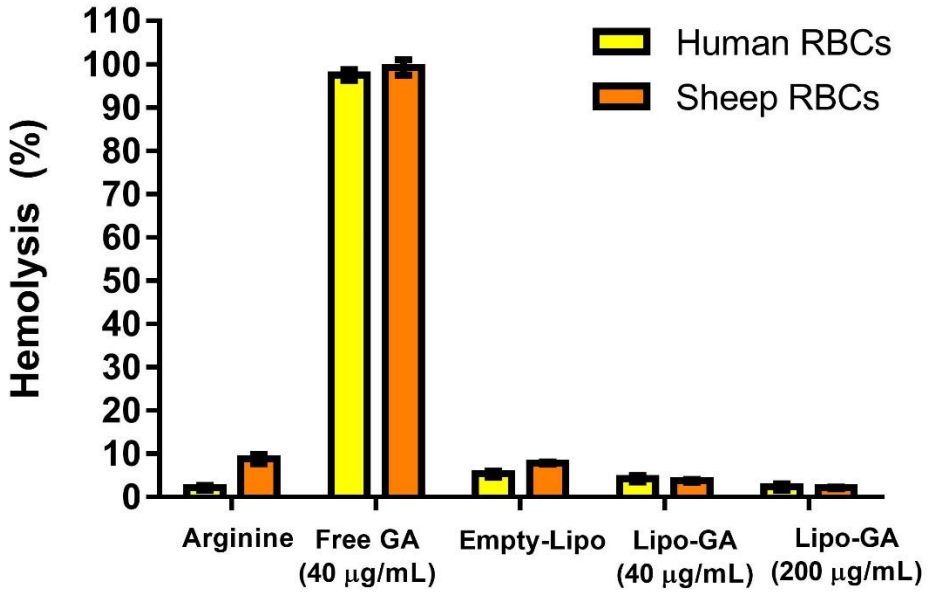

Figure 3.5 *In vitro* hemolysis test. Data = mean ± SD (n=3).

3.4.4 Pharmacokinetic study

Since Lipo-GA exhibited no burst release when incubated with serum, it was anticipated that Lipo-GA would displayed prolonged PK relative to free GA. Free GA and Lipo-GA were i.v. injected into BALB/c mice. Plasma was collected at selected time points and analyzed for GA using LC-MS/MS. The plasma profiles of free GA and Lipo-GA in mice were shown in **Figure 3.6**. Free GA was rapidly eliminated from the plasma and the concentration was below the detection limit 6 h post injection (<60 ng/mL). Lipo-GA, on the other hand, displayed an increased plasma concentration at any given time compared to free GA with a reduced rate of elimination. The plasma concentration of Lipo-GA at 48 h post injection was still above 100 ng/mL. PK parameters were obtained by fitting the plasma profile with the non-compartmental model and are presented in **Table 3.6**. The half-life of Lipo-GA was significantly extended in comparison with free GA with an 18-fold increase (1.33 h vs 18.62 h). Lipo-GA also exhibited 20-fold higher mean residence time, 7.5-fold higher area under the curve ($AUC_{0-\infty}$), and 10-fold decreased clearance, confirming its prolonged circulation relative to free GA.

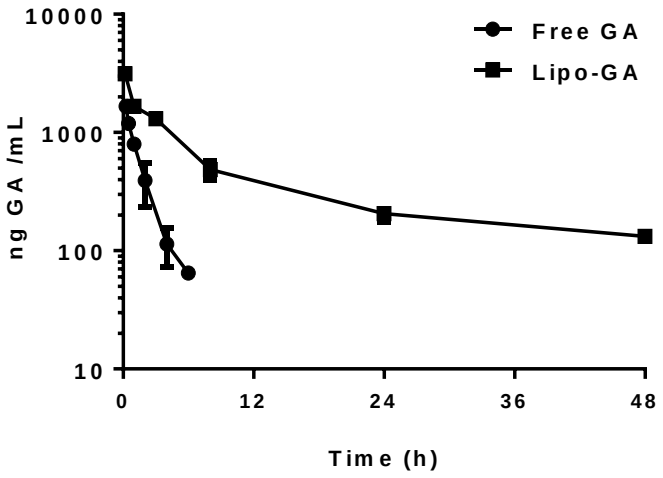

Figure 3.6 Pharmacokinetic profiles of free GA and Lipo-GA in plasma. Data= mean ± SD (n = 4).

Table 3.6 Non-compartmental PK analysis of plasma profiles of free GA and Lipo-GA. C_{max}: maximum plasma concentration. T½: half-life. $AUC_{0-\infty}$: area under the curve. Cl: clearance. Vd: volume of distribution. MRT: mean residence time.

	Free GA	Lipo-GA
C_{max} (µg/mL)	1.66±0.02	3.14±0.25
$AUC_{0-\infty}$ (µg/mL)	2.63±0.24	19.6±1.92
T½ (h)	1.33±0.28	18.62±3.98
MRT (h)	1.59±0.16	21.42±1.32
Cl (mL/h/kg)	72.91±7.05	8.72±0.98
Vz (mL)	140.04±26.06	231.19±34.53

3.4.5 Antitumor efficacy

The *in vitro* cytoxicity of Lipo-GA was comparable to free GA in both EMT6 and B16F10 cells with an IC50 of 0.2-1.2 µM upon 3 days of incubation (**Figure 3.7**).

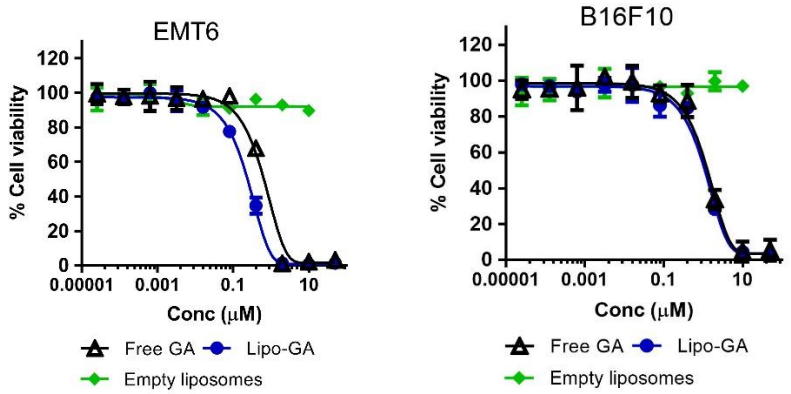

IC50 (µM)	free GA	Lipo-GA
EMT6	0.63±0.08	0.25±0.12
B16F10	1.24±0.28	1.09±0.23

Figure 3.7 Cell viability studies of free GA and Lipo-GA against EMT6 (top left) and B16F10 (top right) cancer cells. The IC_{50} value for each formulation against various cell lines is shown in the table (bottom). Data= mean ± SD (n = 4).

To evaluate the antitumor activity of Lipo-GA compared to free GA, mice with s.c. tumor (~100 mm^3) were randomly divided into 4 groups, and treated with control (empty liposome), free GA (4 mg GA/kg), or Lipo-GA (4 or 20 mg GA/kg) via tail vein injection (one dose). The dose was selected based on the previous report showing that 4 mg/kg of free GA was a non-toxic therapeutic dose that induced significant antitumor efficacy against a panel of human xenograft tumor models in mice [111, 128, 129].

In this study, we compared the one dose efficacy of free GA and Lipo-GA in murine syngeneic tumor models. In B16F10 melanoma model, free GA (4 mg GA/kg) did not show any significant antitumor effect relative to the negative control, whereas Lipo-GA at 4 mg GA/kg and 20 mg GA/kg significantly inhibited tumor growth by 47.5% ($p<0.001$) and 77.1% ($p<0.001$), respectively, on Day 7 (**Figure 3.8A**). The high-dose Lipo-GA (20 mg/kg) was significantly more efficacious than the low dose formulation (4 mg/kg). Similar results were obtained in the EMT6 breast tumor model, one dose treatment of Lipo-GA at 4 mg GA/kg and 20 mg GA/kg inhibited the tumor growth by 65.9% and 97%, respectively, while free GA at 4 mg/kg exhibited little efficacy (**Figure 3.8B**). It is worth mentioning that the high dose Lipo-GA (20 mg/kg) induced significant tumor regression with only one dose and the tumor size stayed completely inhibited for at least 12 days, followed by a slow rebound of the tumors. Preliminary safety of GA therapies was monitored by measuring the mice body weight. As shown in the lower panel of **Figure 3.8,** no significant weight loss was observed in both tumor models after all treatments except for free GA and the high dose Lipo-GA in the BALB/c model. The body weight loss in the Lipo-GA group was mild (<5%) and was only significant on Day 2 and 3, while free GA caused moderate weight loss (5-10%) during a period of time from Day 2-10. The data in **Figure 3.8** indicate that Lipo-GA was a safer and more efficacious formulation compared to free GA.

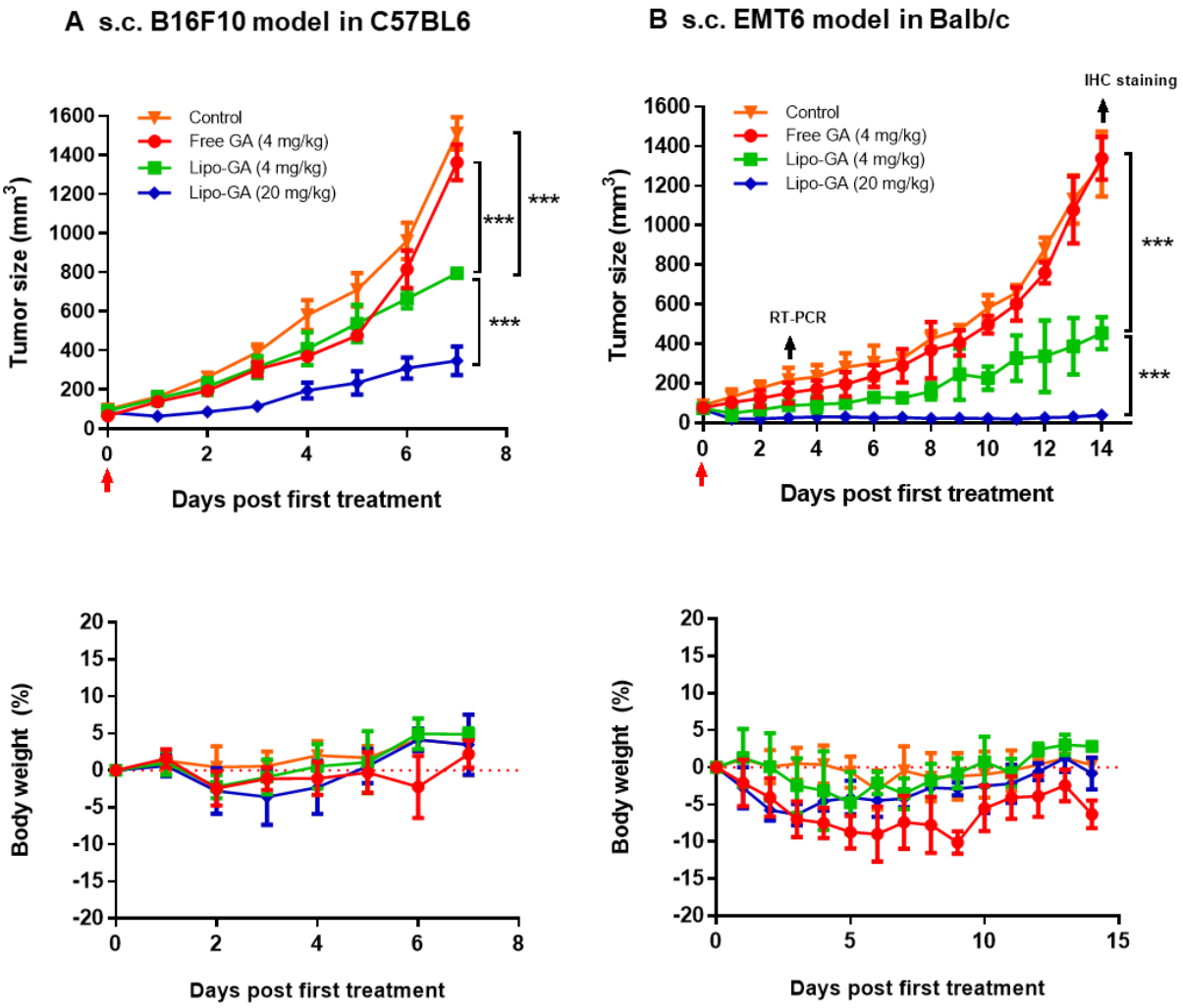

Figure 3.8 Antitumor efficacy and safety of free GA and Lipo-GA in B16F10 (A) and EMT-6 (B) tumor models. Upper panel: tumor size; lower panel: body weight change during therapy. Data = mean ± SD (n=5-6).

In recent studies, GA has been shown *in vitro* as an effective inhibitor against STAT3 and NF-κB, thereby downregulating the expression of a series of downstream genes related to angiogenesis, cell proliferation, and apoptosis, including Bcl-2, HIF-1α, and VEGF [130, 131]. In our study with the EMT6 tumor model, 3 days after the treatment, tumors were collected for analysis of these oncogenes by RT-PCR. As shown in **Figure 3.9**, free GA (4 mg/kg) only

mildly reduced the mRNA level of Bcl-2 and VEGF-A by 10% relative to the negative control. At the matched dose (4 mg GA/kg), Lipo-GA reduced the mRNA level of Bcl-2 by 40%, HIF-1α by 36%, VEGF-A by 15%, and Stat3 by 38%. The effects were significantly stronger with Lipo-GA compared to free GA in all the analyzed genes except VEGF-A. Increasing the Lipo-GA dose to 20 mg/kg further increased the activity in inhibiting these oncogenes by reducing the mRNA level of Bcl-2 by 75%, HIF-1α by 70%, VEGF-A by 55%, and Stat3 by 60%. The data confirmed that Lipo-GA exhibited increased biological activity compared to free GA, and the effect was dose dependent.

Two weeks after various treatments, the EMT6 tumors were collected and analyzed for expression of Ki67, CD31, and NF-κB p65. The H&E staining (**Figure 3.10A**) clearly showed significant difference in morphology among the tumors after different therapies. The high-dose Lipo-GA group displayed the most significantly altered tumor structure, indicating the highest antitumor efficacy. Ki67 is a proliferative marker and was highly expressed in the control tumor (65% positive, **Figure 3.10B**). While free GA (4 mg/kg) showed no significant effect in reducing Ki67, Lipo-GA (4 mg/kg and 20 mg/kg) down-regulated Ki67 in the tumors to only 38% and 20%, respectively. Overexpression of CD31 is commonly seen in rapidly growing tumors with active angiogenesis [132]. As shown in **Figure 3.10A&C**, free GA (4 mg/kg) did not exhibit significant anti-angiogenesis effect, whereas Lipo-GA at 4 mg/kg and 20 mg/kg reduced CD31 expression in the tumors by 50% and 75%, respectively, in comparison with the control. RelA, a subunit in the NF-kB complexes, is exposed when the complexes are activated and translocated into the nucleus. RelA can be recognized by the NF-kB p65 antibody to identify the active form of NF-kB. As shown in **Figure 3.10A&D**, free GA (4 mg/kg) displayed no activity in inhibiting NF-kB in the tumor, while Lipo-GA (4 mg/kg and 20 mg/kg) reduced the active form of NF-kB

by 40-50% compared to the negative control. However, in this case, there was no dose effect of Lipo-GA in inhibiting NF-kB. These IHC results were consistent with the tumor growth inhibition data. The increased antitumor activity of a single dose Lipo-GA relative to free GA could be mainly due to its increased half-life and systemic exposure (AUC), so that the effect of Lipo-GA could be enhanced and prolonged (up to 2 weeks in the EMT6 model). Additionally, since the hemolytic toxicity is reduced by the liposomal formulation, Lipo-GA could be safely given at a higher dose, leading to further enhanced antitumor efficacy.

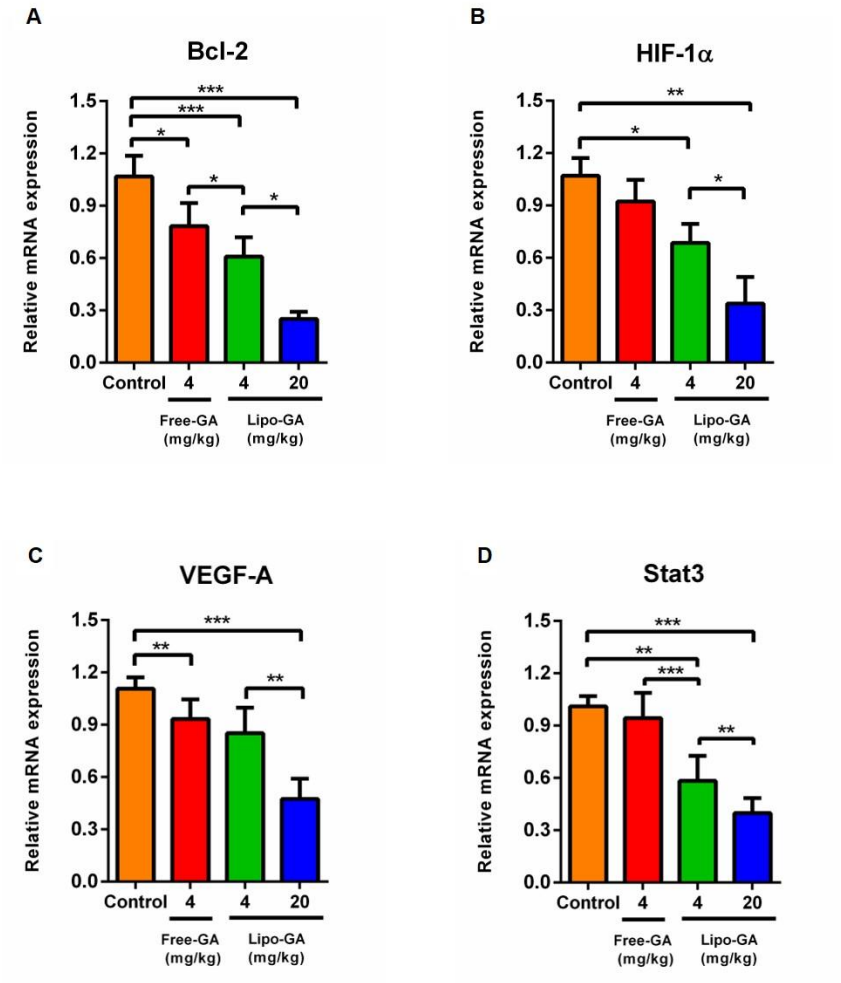

Figure 3.9 Relative mRNA expression of genes 3 d post-treatment of various formulations in EMT6 tumor model. (A) BCl-2, (B) HIF-1α, (C) VEGF-A, and (D) Stat3. Data represent mean ± SD (n = 3) (*P ≤ 0.05, **p<0.01, ***p<0.001)

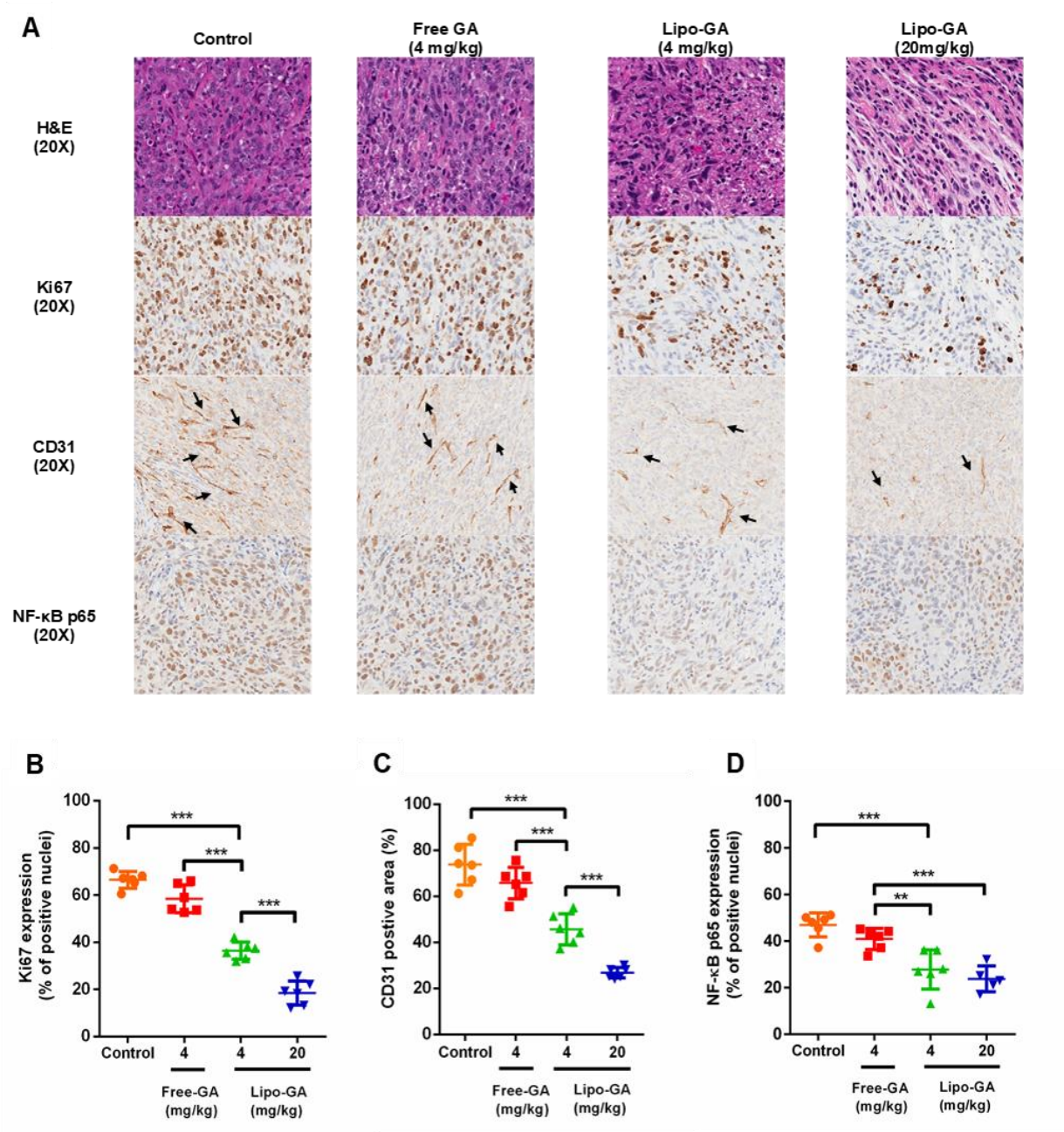

Figure 3.10 Histological analysis of EMT6 tumor 14 days post-treatment with various GA formulations. Representative images of immunohistologically stained tumor sections (A). Quantitative results of Ki67 (B), CD31 (C) and NF-kB p65 (D) expression in the tumors. Data represent mean ± SD (n = 6 images randomly selected from 5 tumors per group) (**p<0.01, ***p<0.001).

3.5 Discussion

Active loading of hydrophobic drugs into liposomes has been challenging [83-89]. Three such approaches have been developed recently [96, 133]. The first strategy is prodrug-based approach. Docetaxel was first chemically modified with an ionizable piperazine group via esterification, which increased the drug solubility at pH 5 and allowed the prodrug to permeate into the aqueous core, become ionized and form complexes with sulfate ions at a high drug-to-lipid ratio (0.4, w/w). However, this method required chemical modification of the drug. The second approach involved using a chemically modified cyclodextrin with an ionizable alkyl amino group as a solubilizer and a membrane shuttle for an insoluble drug. The drug could be incorporated inside the modified cyclodextrin, which could cross the lipid bilayer and became ionized and locked inside the low pH liposomal core. The highest drug-to-lipid ratio achieved with this method was 0.1 (w/w). However, this method required a long process of preparation (55 °C, 36-48 h) [85]. The final product would also contain the modified cyclodextrin with an unknown safety profile. Very recently, including a solvent during the loading process has been shown to promote active loading of poorly water soluble drugs into liposomes [82, 96, 133]. Previous work from the Bally lab showed that 10-15% (v/v) ethanol could be used as a permeability enhancer to increase loading efficiency of anthracyclines (e.g. doxorubicin, idarubicin, and so on) in Chol-free liposomes (DSPC/DSPE-mPEG2K, 95/5, mol%) [134]. Complete drug loading could be achieved at a temperature (40 °C) lower than the phase transition temperature of the major lipid (DSPC, 55 °C). However, heating was still required with the Bally method. Additionally, it was not demonstrated whether this method could be applied for Chol-containing liposomes for active loading, and the optimal EtOH concentration was not identified. The Szoka group recently demonstrated that 2-10% (v/v) DMSO could facilitate high drug encapsulation (>90%) of a

poorly water soluble drug (carfilzomib; logP 3.77) at a drug-to-lipid ratio of 0.12 (w/w). Under their specific conditions, carfilzomib was not completely soluble in the loading mixture [133]. With this method, while high drug encapsulation could be achieved at room temperature for liposomes composed of a low transition temperature lipid (POPC, Tc: -2 °C), heating (65 °C) was required for those prepared with a high phase transition temperature lipid (DSPC, Tc: 55 °C). On the contrary, in the SALT system, a sufficient amount of solvent was included in the loading mixture to completely dissolve the drug and promote its loading into the liposomes composed of DSPC/Chol at room temperature at a drug-to-lipid ratio of > 0.1 (w/w). The solvent could be efficiently removed from the final product by dialysis (< 0.55 ppm upon 2 h dialysis) or tangential flow filtration [135]. The resulting liposomal drug exhibited superior stability and improved PK relative to the free drug. This platform is simple and highly flexible, working for a wide range of compounds and water miscible solvents. The loading can be completed in 30 min at room temperature, which is highly favorable for heat-sensitive drugs and large-scale manufacturing with no need of a delicate heating system to ensure homogenous heating. With this technology, the drug-to-lipid ratio that could be reached (0.1 to 0.2, w/w) was 50 times higher than that achieved by the passive loading method [61, 136]. In this study, we also examined the optimal range of solvents for compete drug loading at room temperature. The data showed that just complete solubilization of the compound was not enough, and a slightly extra amount of the solvent was needed, possibly to increase the membrane permeability to facilitate drug permeation through the lipid bilayer into the liposomal core at room temperature. The upper limit of the optimal amount of solvent must be below that for inducing bilayer instability, which resulted in the loss of the loading gradient. This working model is proposed and summarized in **Figure 3.11**. The model suggests that the solvent used in the SALT is both a drug solubilizer and

a membrane permeability enhancer. In the standard active loading method, heating is often used to increase the bilayer permeability. Indeed, when heating is applied in the SALT system, a less amount of solvent would be needed for complete loading, but in the meantime, the upper limit of the solvent was also decreased (data not shown). The data are consistent with the reports from the Bally lab and the Szoka team, supporting that the solvent used in SALT increased the bilayer permeability.

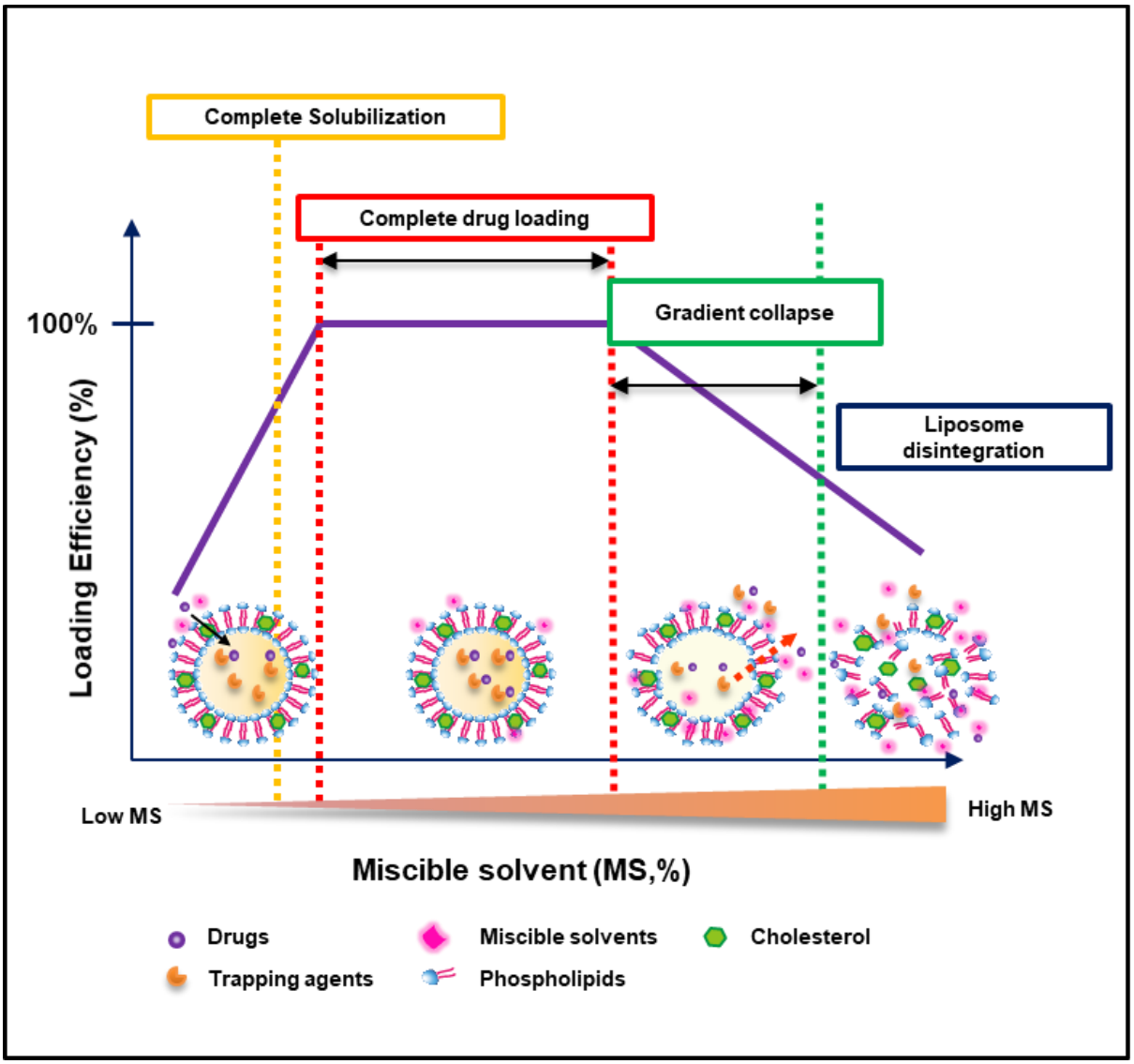

Figure 3.11 Proposed solvent effect on drug loading in the SALT system.

GA has shown significant antitumor efficacy in many studies [131, 137-140]. However, its clinical application is limited due to its poor solubility (< 5 μg/mL) and rapid drug clearance (half-life < 4 h in rat) [109, 110]. Various nanoparticle delivery systems have been utilized to incorporate GA in the hydrophobic compartment to increase the solubility [111, 114, 115, 141, 142]. However, the stability of these GA-loaded nano-formulations was poor even in serum-free media (> 40% release in 72 h). As the drug release was rapid, the circulation half-life was only marginally increased by < 2-fold at best [114], and the improvement in efficacy for these delivery systems relative to free GA was only minimal.

To develop a stable liposomal formulation for GA, our strategy was to employ the SALT to effectively encapsulate GA, and optimize the loading gradient and lipid composition to stably retain the drug. The optimal loading gradient and lipid composition were found to be basified copper acetate and DOPC/Chol/DSPE-mPEG2K (85/10/5, mol%), respectively. The proposed active loading mechanism for this formulation is depicted in **Figure 3.12**. The miscible solvent dissolves GA into individual molecules and facilitates permeation of the uncharged form of GA into the liposomal core, where the basic pH (9.5) promotes de-protonation of GA to lock this ionized form inside the liposomes. Additionally, Cu^{2+} ions in the liposomal core form complexes with GA molecules, preventing it from leaking out. This formulation retained almost 100% of GA when incubated with 50% serum at 37 °C for 24 h, a prerequisite for prolonged PK. The ammonia (permeability coefficient $P=6.6\cdot10^{-4}$ cm/s) and acetic acid (P=0.13 cm/s) dissociated from basified copper acetate then diffuse out of the liposomes [35, 143]. This equilibrated mechanism is anticipated to drive active and efficient loading of GA and maintain the stability. Indeed, in our attempts of using other salts of copper as the loading gradient, the liposomal drug retention was inferior to the basified copper acetate, including 100 mM copper gluconate/220

mM triethanolamine (TEA, pH 7.4), 250 mM basified copper sulfate (pH 9.5), and 250 mM copper sulfate (pH 4.0), shown in **Figure 3.13,** suggesting the stability of liposomal GA may be primarily attributed to both the counterions and the inside pH [144]. To the best of our knowledge, this metal ion gradient has never been used before for loading drugs, and the combination of the basified copper loading and DOPC formulation yielded a stable liposomal formulation for GA, which displayed prolonged PK relative to free GA. In fact, this was also the first reported liposomal formulation for GA prepared by active loading that displayed extended blood circulation, to the best of our knowledge.

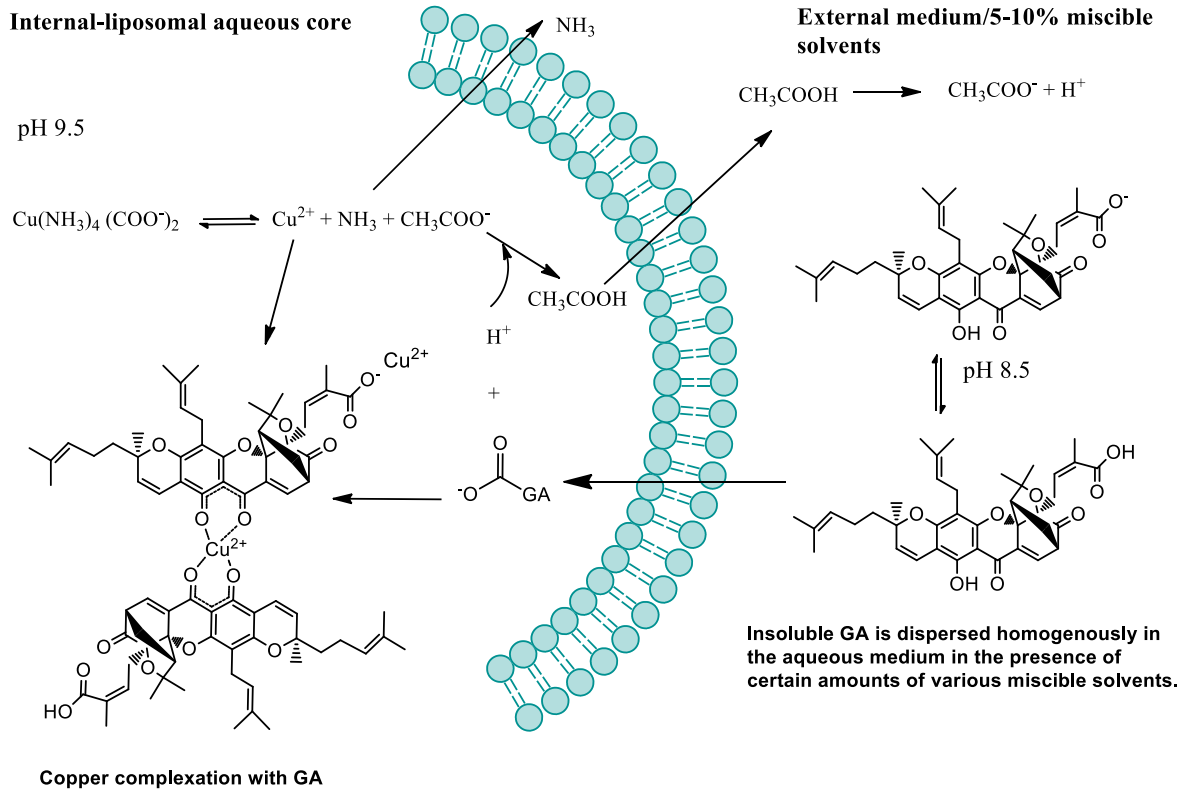

Figure 3.12 Proposed mechanism of GA loading using basified copper acetate.

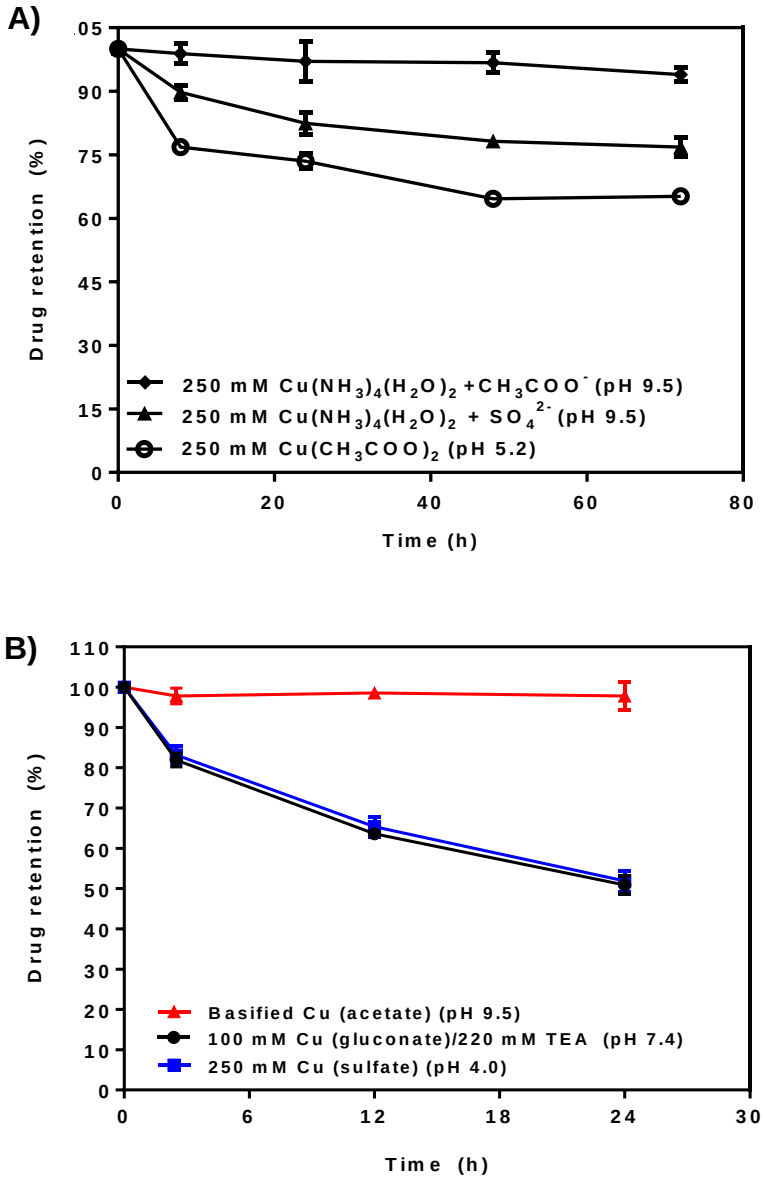

Figure 3.13 Drug retention of liposomal formulations prepared with different loading gradients. (A) Liposomes: DSPC/Chol/DSPE-mPEG2K (50/45/5, mol%). Release conditions: 37 °C in HBS buffer; (B) Liposomes: DOPC/Chol/DSPE-mPEG2K (85/10/5, mol%). Release conditions: 37 °C in 50% FBS. Data = mean ± SD (n = 3).

As a result, this Lipo-GA formulation displayed increased antitumor activity after only one single i.v. dose in two aggressive syngeneic tumor models in mice. This formulation also demonstrated unique antitumor mechanism by simultaneously inhibiting multiple oncogenes,

including NF-kB, Bcl-2, Stat3, HIF-1α, and VEGF, leading to significant anti-proliferation and anti-angiogenesis in the treated tumor with significant tumor regression. It is worth mentioning that there are still no effective and safe drugs approved for deactivating many of those targets that Lipo-GA effectively inhibited, including NF-kB, Bcl-2, Stat3, and HIF-1α. Therefore, the potential of Lipo-GA in augmenting the current cancer therapy is very significant.

3.6 Conclusion

Through a comprehensive study, our data support that the SALT is a flexible platform for developing effective and stable liposomal formulations for a wide range of poorly water soluble drugs. Our study also delineated the roles of the solvents used in the SALT system, including dissolving the compound and increasing the membrane permeation at room temperature. We then further utilized the SALT, and optimized the loading gradient as well as liposomal composition, to develop a stable liposomal formulation for GA. Compared to free GA, Lipo-GA displayed reduced hemolytic toxicity, prolonged PK, and enhanced efficacy against multiple tumor models by simultaneously inhibiting multiple oncogenes.

Chapter 4: Development of a Rapidly Dissolvable Oral Pediatric Formulation for Mefloquine Using Liposomes

4.1 Project Summary

Mefloquine (Mef), a poorly soluble and highly bitter drug, has been used for malaria prophylaxis and treatment. The dosage form for Mef is mostly available as adult tablets, and thus children under the age of 5 suffer from poor medication adherence. We have developed a stable, rapidly dissolvable, and palatable pediatric formulation for Mef using liposomes composed of 1,2-distearoyl-sn-glycero-3-phosphocholine (DSPC) and cholesterol with a mean diameter of ~110 nm. Mef was actively loaded into the liposomes via an ammonium sulfate gradient using the solvent-assisted loading technology (SALT) developed in our lab. Complete loading of Mef inside the liposomal core was achieved at a high drug-to-lipid ratio (D/L) of 0.1-0.2 (w/w), and the final drug content in the formulation was ~8 mg/ml, well above the solubility of Mef (<0.6 mg/ml in simulated fluids). The strong bitterness of Mef was masked by the liposomal encapsulation as measured by an electronic tongue. Incubating the Mef-liposomes (Mef-Lipo) in the simulated gastric fluid (pH 1.2) and the simulated intestinal fluid containing 3 mM sodium taucholate (pH 6.8) induced changes in liposome size and the polydispersity, resulting in drug release (~40% in 2 h). However, no drug release from the Mef-Lipo was measured in the bile salt-free intestinal fluid or simulated saliva (0% in 3 h). These data suggest that drug release from the Mef-Lipo was mediated by a low pH and the presence of a surfactant. Pancreatic lipase did not degrade DSPC in the Mef-Lipo after 8 h of incubation nor induce Mef release from the liposomes, indicating that lipid digestion played a minor role for drug release from the Mef-Lipo. In order to improve long-term room temperature storage, the Mef-Lipo was lyophilized to obtain a solid formulation, which was completely dissolvable in water in 10 s and displayed similar *in vitro* profiles of release as the liquid form. The lyophilized Mef-Lipo was stable at room

temperature for >3 months. In mice, orally delivered liquid and lyophilized Mef-Lipo displayed comparable absorption with bioavailability (BA) of 81-86%, while the absorption of the standard Mef suspension was significantly lower with BA of 70% and 20% decreased maximal plasma concentration and area under the curve. Our data suggest that the Mef-Lipo was a stable, palatable and bioavailable formulation that might be suitable for pediatric use.

4.2 Introduction

Malaria is the most prevalent parasitic disease in the world and more than 200 million cases occurred globally in 2015, leading to 438,000 deaths. The majority of these cases and deaths took place in Sub-Saharan Africa [145]. Young children under five years of age are the most severely affected sub-population, accounting for approximately 70% of global malaria deaths [146]. Particularly in Sub-Saharan Africa, the mortality rate is up to 95%, equivalent to 292,000 young children whose lives were taken by malaria in a single year. Although a number of antimalarial drugs and combined therapies have been developed over the past 40 years [147], the mortality rate in young children is still high, primarily caused by the lack of a suitable pediatric formulation for easy swallowing and accurate dosing [148]. Among the available antimalarial drugs, mefloquine (Mef) is a first-line antimalarial drug, and is frequently used alone or in combination with other drugs such as artesunate for prophylaxis or treatment in children [149]. Mef is poorly water soluble, strongly bitter and mostly available in the adult tablet form. For pediatric use, an adult tablet must be divided to obtain the desirable dose for children, grinded into a powder form and administrated with a large amount of food or milk. However, this process leads to dose loss, resulting in under-dosing. In addition, children often spit out this medication because of its unpleasant taste. These issues have led to inaccurate dosing, therapy failure, drug resistance development [150], and unexpected adverse

reactions if contaminations occur during the extemporaneous preparation. A few micro-emulsion formulations for Mef have been developed to improve drug solubility and bioavailability (BA) [151, 152]. However, the palatability of these formulations hasn't been studied yet and the use of large amounts of surfactants may raise a safety concern for pediatric use. Surfactants such as polysorbate 20 and 80 have been shown to cause liver and kidney failure in newborns and infants. Therefore, excipients used for developing pediatric formulations must be extra safe. Currently, there is only one palatable pediatric formulation containing Mef, called Artequin™ pediatric (50 mg artesunate + 125 mg mefloquine), prepared as pellets, available for children with a body weight of 10-20 kg. However, the pellet size of Artequin is still too bulky for newborns and infants to swallow.

Children prefer flavored liquid formulations, which also make weight-based dosing easier (i.e., using a syringe or measuring cup to deliver a precise volume). However, developing a stable liquid formulation for Mef is challenging because of its poor water solubility. Liquids also suffer from poor stability and require preservatives and storage under refrigeration, which is often not available in developing countries. In addition, preservatives cause safety concerns in young children. For examples, parabens that are commonly included in liquid formulations disrupt endocrine.

The National Institutes of Health's Best Pharmaceuticals for Children Act (BPCA) has recently identified developing pediatric formulations as one of the unmet priorities for children welfare, and Mef is in the priority drug list [153]. The BPCA emphasizes four aspects when designing an effective pediatric formulation, including safe excipients, palatability, stability, and orally dissolvable (also named oro-dispersible or rapidly dissolvable). The World Health Organization (WHO) also recommends oro-dispersible as the optimum formulation for

children's oral medicines [154]. First, oro-dispersible medicine can be rapidly dissolvable in the oral cavity for small children to swallow. Second, it can be prepared as an oral liquid for precise dosage and dose titration for children at different developmental stages. Third, it can be stored in the solid form with improved stability at room temperature and does not require preservatives. Technologies for taste masking and improving drug dissolution/solubility are critically needed for developing oro-dispersible formulations.

We hypothesized that liposomes would be a platform technology for developing a rapidly dissolvable and flexible solid pediatric formulation based on the following reasons: (a) Liposomes are composed of naturally occurring and safe excipients such as phospholipids and cholesterol; (b) Once a drug is stably encapsulated inside liposomes and is not in direct contact with the taste buds, the taste of the drug will be masked; (c) Liposomes can disperse poorly soluble drugs in small particles (~100 nm), leading to increased drug solubility/dissolution and oral absorption; (d) Liposomes can be lyophilized to produce a stable and rapidly dissolvable solid formulation. The remaining challenge is how to stably encapsulate poorly soluble Mef into liposomes with high efficiency. The standard passive encapsulation method allows loading of poorly soluble drugs into the liposomal bilayer, but the loading capacity is low and the stability of the resulting product is often poor. To resolve this challenge, we developed a solvent-assisted active loading technology (SALT, **Figure 4.1**) that could encapsulate poorly soluble Mef into the aqueous core of liposomes to improve the loading efficiency and the stability.

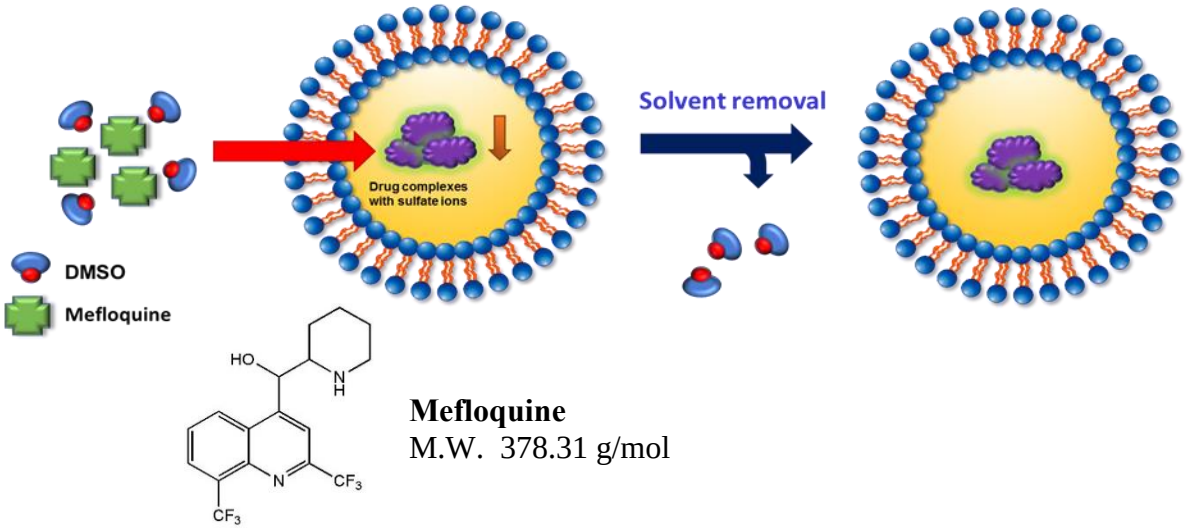

Figure 4.1 Illustration of solvent-assisted remote loading technology (SALT).

We then examined the release profile and oral absorption of the liquid and lyophilized forms of Mef-liposomes compared to Mef suspension. Their palatability was also compared using an innovative electronic tongue (E-tongue) technology [155]. To the best of our knowledge, this is the first report of using liposomes to resolve technology challenges in taste masking and solubility improvement to develop a flexible solid pediatric formulation.

4.3 Materials and Methods

4.3.1 Materials

Mefloquine·HCl was purchased from Toronto Research Chemical (Toronto, Ontario, Canada). Pancreatin from porcine pancreas (8 × U.S.P.) was obtained from Sigma-Aldrich (St. Louis, MO). 1,2-Distearoy-sn-glycero-3-phosphatidylcholine (DSPC) was purchased from Avanti Polar Lipids (Alabaster, AL). Concentrated solutions (HCl, NaCl and monosodium L-glutamate (MSG)) for conditioning, calibration and diagnostics of the E-tongue sensor array were purchased from Alpha MOS (Toulouse, France). All other chemicals were obtained from

Sigma-Aldrich. All the organic solvents were HPLC (high performance liquid chromatography) grade.

4.3.2 Simulated fluids

Simulated saliva (SS, pH 6.5) was prepared by titrating 10 mM phosphate buffered saline (PBS, pH 7.4) with 1.0 M phosphoric acid [156]. Simulated gastric fluid (SGF, pH 1.2) and simulated intestinal fluid (SIF, pH 6.8) were purchased from Sigma-Aldrich. In some experiments, a bile salt (3 mM sodium taucholate) and a lipase (10 mg/mL pancreatin) were supplemented to the SIF to prepare SIFst and SIFpl [157], respectively**.**

4.3.3 Drug analysis for formulation development and characterization

Mefloquine (Mef) content was quantified by a Waters ACQUITY Ultra Performance Liquid Chromatography (UPLC) H-Class System. The sample was separated through a BEH-C18 column (2.1×50 mm) using a gradient mobile phase. The mobile phase was composed of solvent A: methanol + 0.1% formic acid and solvent B: MilliQ water + 0.1% formic acid. The flow rate was 0.5 mL/min with the following gradient: 0 min: A/B (10/90), 1.8 min: A/B (85/15), 2.7 min: A/B (15/85), 4 min: A/B (10/90). Mef was quantified by a photodiode array (PDA) detector at a wavelength of 283 nm and the concentration of Mef was determined by integrating the peak area and compared with a standard curve of Mef.

4.3.4 Solubility study

Solubility of Mef in different fluids was determined by the shake-flask method [158]. Approximately 8 mg of Mef was added into 1 ml of various fluids, including SS, SGF, SIF and SIF_{st}. The suspension was incubated at 37 °C in a shaking incubator (Innova® 44) at 150 rpm for 24 h, followed by filtration with a 0.22 µm syringe filter (PVDF, 33 mm Millex-GV) to remove

insoluble solids. The filtrate was diluted with methanol and analyzed by the UPLC to determine the solubility.

4.3.5 Liposome preparation

A lipid mixture (DSPC/Cholesterol: 55/45, molar ratio; total lipid = 200 mg) was dissolved in ethanol and dried with rotary evaporator to form a thin film. The thin film was hydrated with 2 mL of 300 mM ammonium sulfate at 60 °C and then extruded through a series of polycarbonate membranes by the Lipex Extruder (Transferra, Burnaby, BC, Canada) to prepare small unilamellar vesicles (SUVs) with a size of ~100 nm. The liposomes were then dialyzed against 10% sucrose to establish an ammonium sulfate gradient for active loading. The DSPC concentration in preformed liposomes was measured by the Stewart assay [116]. Mef was dissolved in DMSO to prepare a stock solution (80 mg/ml), and 300 µL of the stock solution was mixed with 750- 2,400 µL of the preformed liposomes, followed by the addition of 10% sucrose solution to maintain the total volume as 3 mL containing 10% DMSO. The drug-to-lipid ratio (D/L) in the mixture was dependent on the amount that liposomes were included, and a range of D/L (w/w) between 0.1 and 0.4 was tested. The mixture was incubated at room temperature for 35 min. Un-encapsulated drugs and DMSO were removed by dialysis (Slide-A-Lyzer™ Dialysis Cassette, 10kDa MWCO) against 10 % sucrose for 24 h to obtain mefloquine encapsulated liposomes (Mef-Lipo). The drug was quantitatively analyzed using the UPLC assay as described previously. The Stewart assay was used to determine DSPC concentration in liposomes. The drug loading efficiency was determined by comparing the D/L of purified liposomes (after dialysis) to that of unpurified/initial liposomes (before dialysis):

$$Loading\ efficiency\ (\%) = \frac{[D]_{purified} / [DSPC]_{purified}}{[D]_{initial} / [DSPC]_{initial}} \times 100\%$$

where [D] represents Mef concentration, and [DSPC] represents DSPC concentration. Particle size and zeta potential of the Mef-Lipo were measured by a particle analyzer (Zetasizer Nano-ZS, Malvern Instruments Ltd, Malvern, UK). Morphology of the Mef-Lipo was imaged by cryo-transmission electron microscopy as described previously [96].

4.3.6 Residual DMSO analysis

Residual DMSO content in liposomes was measured by UPLC-MS. At selected time points during the final stage of dialysis, 5 µL of the liposomes was diluted with 1-2 mL methanol, and 2 µL of which was injected to the UPLC. The sample was separated by a BEH-C18 column (2.1×50 mm) with a gradient mobile phase (solvent A: MilliQ water containing 0.1% formic acid; solvent B: methanol containing 0.1% formic acid): 0-0.5 min: A/B (95/5); 0.2 mL/min, 5-10 min: A/B (5/95); 0.5 mL/min. DMSO was quantified by a QDa Mass (MS) Spectrometry detector. The LC/MS Single Ion Recording (SIR) chromatograms was utilized to determine residual DMSO under the following conditions: SIR: 78.93 $[M+H]^+$; cone voltage 15 V.

4.3.7 Bitterness masking measurement

Bitterness masking of the formulations was determined using the Astree® electronic tongue (E-tongue, Alpha MOS, Toulouse, France) equipped with a liquid autosampler (LS48). The sensor array set (Set #2) was composed of seven sensors (ZZ, AB, BA, BB, CA, DA, JE) and an Ag/AgCl reference electrode. The Astree® starting procedure (conditioning, calibration and diagnostics of sensors) was conducted using 0.01M HCl, NaCl and MSG as described previously [159]. The taste fingerprint of 10% sucrose (placebo), infant Tylenol®, Mef suspension (in 0.4% Tween80/0.2% methylcellulose/saline), and the Mef-Lipo were obtained using a six-looped autosampler method with the following parameters: delay = 0 sec; acquisition time = 120 sec; stirring rate = 1, acquisition period = 1 and rinsing time of 40 secs. The analysis was conducted

at room temperature, and Milli-Q filtered water was used as a rinsing solution between samples to prevent carrier over effects. Data analysis was conducted using the Astree® Alpha Soft (version 12) chemometrics software using triplicate determinations with relative standard deviation (RSD) < 15%.

4.3.8 Lyophilization of Mef-Lipo

Mef-Lipo (350 µl, 2 mg Mef/ml) was lyophilized using the REVO Research & Development Freeze Dryer (Milrock Technology, Kingston, NY). Two formulation parameters were analyzed including the D/L (0.1 or 0.2 w/w) and the exterior phase of the liposomes (10% sucrose or 20 mM phosphate buffered 10% sucrose, pH 7.4). Briefly, liposomes were loaded into the tray (pre-equilibrated at 0 °C) of the freeze dryer and frozen to -35 °C at the freezing rate of 1 °C/min and the tray temperature was maintained at -35 °C for 6 h. The pressure in the chamber of the freeze dryer was then reduced to 50 mTorr for 1 h, and the tray temperature was increased to -20 °C at a rate of 0.5 °C/min and remained for 7 h. The tray temperature was then increased to -10 °C and held for another 18 h. Finally, the tray temperature was increased to 4 °C and maintained for 2 h, and then increased to room temperature for 3 h, followed by release of the vacuum. Each vial of liposomes was filled with nitrogen gas and sealed with stopper and kept at room temperature. Lyophilization process of mefloquine encapsulated liposomes is summarized in **Figure 4.2**. Residual moisture content in the lyophilized Mef-Lipo was determined by a Q50 thermal gravimetric analyzer (TGA Q50) as reported previously [160].

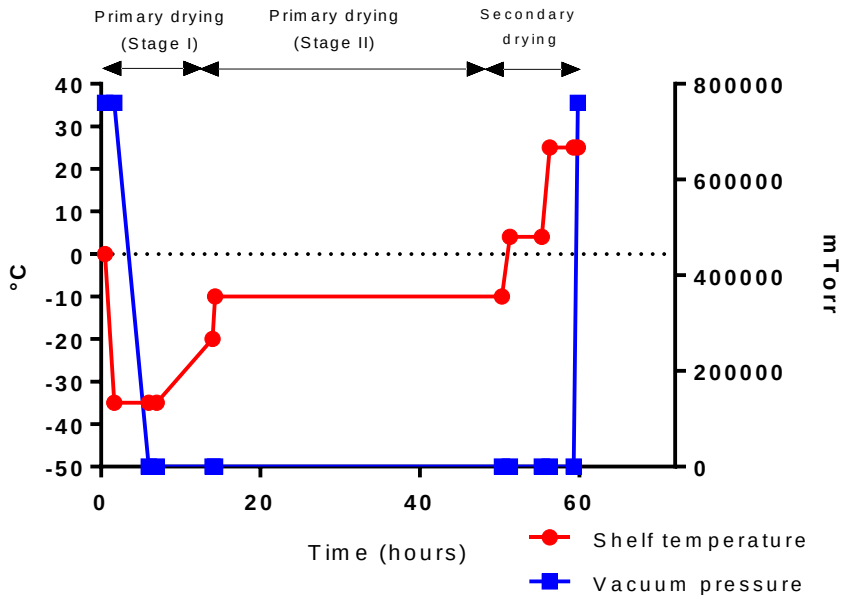

Figure 4.2 Lyophilization process to obtain the lyophilized Mef-Lipo.

4.3.9 *In vitro* drug release

The *in vitro* release study of Mef from different formulations in various simulated fluids was carried using the dialysis method. Formulations included Mef suspension (2 mg/mL) in 0.4% Tween80/0.2% methylcellulose/saline [161], and Mef-Lipo (liquid or lyophilized form, 2 mg/mL) containing a D/L of 0.1 or 0.2. Release media included SGF, SIF, SIF_{st}, SIF_{pl}, and SS. The Mef formulation (1 mL) was added into a dialysis tubing (Spectra/Por ® 2 Standard RC Dry Dialysis Tubing, 12-14 kDa MWCO, Rancho Dominguez, CA) and dialyzed against 16 mL of the release medium to simulate the *in vivo* conditions in children under the age of 5 (**Table 4.1**). The dialysis system was incubated at 37 °C and stirred at 150 rpm. At selected time points, 500 µL of the release medium was collected for UPLC analysis. Fresh release medium was immediately supplemented back to the system to maintain the total volume. The change of

average size and polydispersity of Mef-Lipo incubated in different release media was monitored by a particle analyzer (Zetasizer Nano-ZS, Malvern Instruments Ltd, Malvern, UK).

Table 4.1 Estimated mefloquine concentration in stomach after weight-dependent dosing based on the FDA medication guide: 5 to 10 kg: 31.25 mg, and 9 to 19 kg: 62.5 mg (1/4 tablet).

Source:
1. http://www.who.int/childgrowth/standards/en/

2. http://reference.medscape.com/drug/mefloquine-342689

Year	Mean body weight (kg)	Dose (mg)	Stomach Capacity (mL)	Assume 80% full in stomach (mL)	Estimated [Mef] in stomach right after oral ingestion (mg/mL)
0.5	7.9	31.25	200	160	0.20
1	9.6	31.25	390	312	0.1
2	12.2	62.5	500	400	0.16
3	14.3	62.5	520	416	0.15
4	16.3	62.5	560	448	0.14
5	18.3	62.5	650	520	0.12

4.3.10 PK study

Female BALB/c mice (6–8 weeks old) purchased from the Jackson Laboratory (Bar Harbor, ME) were used to conduct the PK study. All animal studies were performed in the Modified Barrier Facility (MBF) in the University British Columbia (Vancouver, BC, Canada) with approved protocols in compliance with the guidelines established by the Canadian Council on Animal Care. Female mice were fasted for 6 h prior to drug treatment and 5 mice were used in each group. Mef-Lipo (lyophilized or liquid) or Mef suspension was administered by oral gavage, and Mef solution was injected via the tail vein. The lyophilized Mef-Lipo was reconstituted with de-ionized water before oral administration. After administration at 40 mg/kg, ~250 μL of blood

was collected from saphenous vein at selected time points (for oral formulations: 1, 2, 4, 8, 24, and 72 h; for i.v. formulation: 0.5, 6, 24, and 72 h). Blood was centrifuged at 11,000 rpm for 7 mins to isolate plasma. Plasma (100 µL) was mixed with 250 µL methanol and centrifuged at 7,000 rpm at 10 °C for 10 min. Ten µL of the supernatant was diluted with 0.1-0.3 mL methanol, and 50 µL of the diluted sample was mixed with 50 µL of methanol containing 12.5 ng/mL mirtazapine as an internal standard (IS). The sample was injected to the UHPLC-MS/MS system for drug analysis. The UHPLC/MS/MS system was composed of a Waters ACQUITY BEH™ C18 column, an Agilent 1290 Infinity Binary Pump, a 1290 Infinity Sampler, a 1290 Infinity Thermostat, and a 1290 Infinity Thermostatted Column Compartment (Agilent, Mississauga, ON, Canada) connected to an AB Sciex QTrap® 5500 hybrid linear ion-trap triple quadrupole mass spectrometer equipped with a Turbo Spray source (AB Sciex, Concord, ON, Canada). The sample was separated by the C18 column under a gradient mobile phase consisting of solvent A (MilliQ water with 0.1 % formic acid) and solvent B (methanol with 0.1 % formic acid) at a flow rate of 0.2 mL/min with the designed gradient program (0 min: A/B (50/50), 2 min: A/B (5/95),4 min: A/B (5/95),4.1 min: A/B (50/50), 6 min: A/B (50/50)). Detection of Mef and the IS were monitored in ES+ mode using a daughter ion (m/z= 361.3 for Mef and m/z= 195 for IS). All data was acquired using the Analyst 1.5.2 software on a Microsoft Windows XP Professional operating platform. PK parameters for the analyzed formulations including T_{max}, C_{max}, and AUC (area under the curve), were obtained using Phoenix WinNonlin® software (Princeton, NJ). The bioavailability of the Mef formulations was calculated based on the following equation.

B.A. (Bioavailability, %) = $\frac{AUC_{p.o.} \cdot Dose_{i.v.}}{AUC_{i.v.} \cdot Dose_{p.o.}} \cdot 100\%$

4.3.11 Stability study

The liquid and lyophilized forms of Mef-Lipo were stored at 4 °C and room temperature, respectively. At selected time points, 100 µL of the liquid liposomes was collected directly, whereas the lyophilized Mef-Lipo was reconstituted with Milli-Q water first. Stability of the samples was examined by measuring the size, the size polydispersity and the encapsulation efficiency as describe above.

4.3.12 Statistical analysis

All data are expressed as mean ± SD. Statistical analysis was conducted with Student *t* test for two-group comparison or one-way ANOVA for more than two group comparison using GraphPad Prism 6.0 (La Jolla, CA). A difference between two groups with a P value< 0.05 was considered to be statistically significant.

4.4 Results & Discussion

4.4.1 Solubility in various simulated fluids

The solubility of Mef is low in various simulated fluids at 37 °C, ranging between 0.35 and 0.57 mg/mL (**Table 4.2**). For this class of drugs, if the solubility/dissolution can be increased by formulation, the oral absorption will be improved [162]. For example, PEGylated liposomes was used to incorporate insoluble paclitaxel in the lipid bilayer to increase the oral BA in rats [163] and the BA of all-trans-retinoic acid (ATRA) formulated inside solid lipid nanoparticles (SLNs) was increased by 4- to 5-fold compared to ATRA [164].

Table 4.2 Solubility of Mef at 37 °C in simulated fluids. Data = Mean±S.D. (n=3).

Medium	pH	Solubility (mg/mL)
Simulated gastric fluid	1.2	0.573±0.021
Simulated intestinal fluid	6.8	0.377±0.015
Simulated intestinal fluid (3 mM sodium taucholate)	6.8	0.388±0.039
Simulated saliva	6.5	0.347±0.041

4.4.2 Development of mefloquine encapsulated liposomes

As described in the introduction, liposomes exhibit significant potential as a child-friendly oral delivery system for poorly soluble and highly bitter drugs. However, liposomes have not been actively studied for oral delivery of drugs. For orally available drugs, they often exhibit good lipid membrane permeability, and therefore, the retention of this type of drugs within liposomes is poor, leading to compromised stability and palatability. For hydrophobic and poorly water soluble drugs, they tend to be incorporated into the lipid bilayer through hydrophobic interactions. However, the capacity of a lipid bilayer is limited and the encapsulation is often not stable. To resolve this technical challenge, we have developed the solvent-assisted active loading technology (SALT) that involves the inclusion of a small amount of organic solvent (i.e. DMSO) in the loading system to avoid drug precipitation and facilitate its permeation through the lipid bilayer for active loading [96]. Complete loading of staurosporine, a weak base drug with solubility < 1 μg/ml, into liposomes containing an ammonium sulfate gradient was achieved at a D/L of 1/5 (w/w) in the presence of 5% DMSO. Without DMSO, no drug could be actively

loaded. Mef contains an ionizable secondary amine group with a logP of 3.9, suggesting if Mef could be solubilized in the exterior phase of a liposome, the drug would efficiently permeate into the liposomal core to form complexes with sulfate ions.

We first tested Mef loading into DSPC/cholesterol liposomes via an ammonium sulfate gradient in the presence of 10 vol% DMSO at room temperature. As shown in **Figure 4.3A**, complete loading was achieved at a D/L of 0.1-0.2 (w/w), and the final drug concentration was ~8 mg/mL, while the drug solubility was only ~0.5 mg/mL. When performed at a D/L of 0.4, the loading efficiency declined to 70%. We selected DSPC and cholesterol as the components of the liposomes, as they are both extremely safe materials. DSPC has a transition temperature at 55 °C, which would improve the thermo-stability of the liposomes when stored at room temperature. Cholesterol has been shown to improve stability of liposomes and reduce premature drug leakage [165]. Free of DMSO in the final Mef-Lipo (total lipid concentration: 80 mg/mL) was confirmed after 1 h of dialysis (**Figure 4.3B**). Compared to the empty liposomes (**Figure 4.3C**), the Cryo-TEM image of the Mef-Lipo indicated that a Mef crystal was formed and located randomly within the liposomal aqueous core (**Figure 4.3D**).

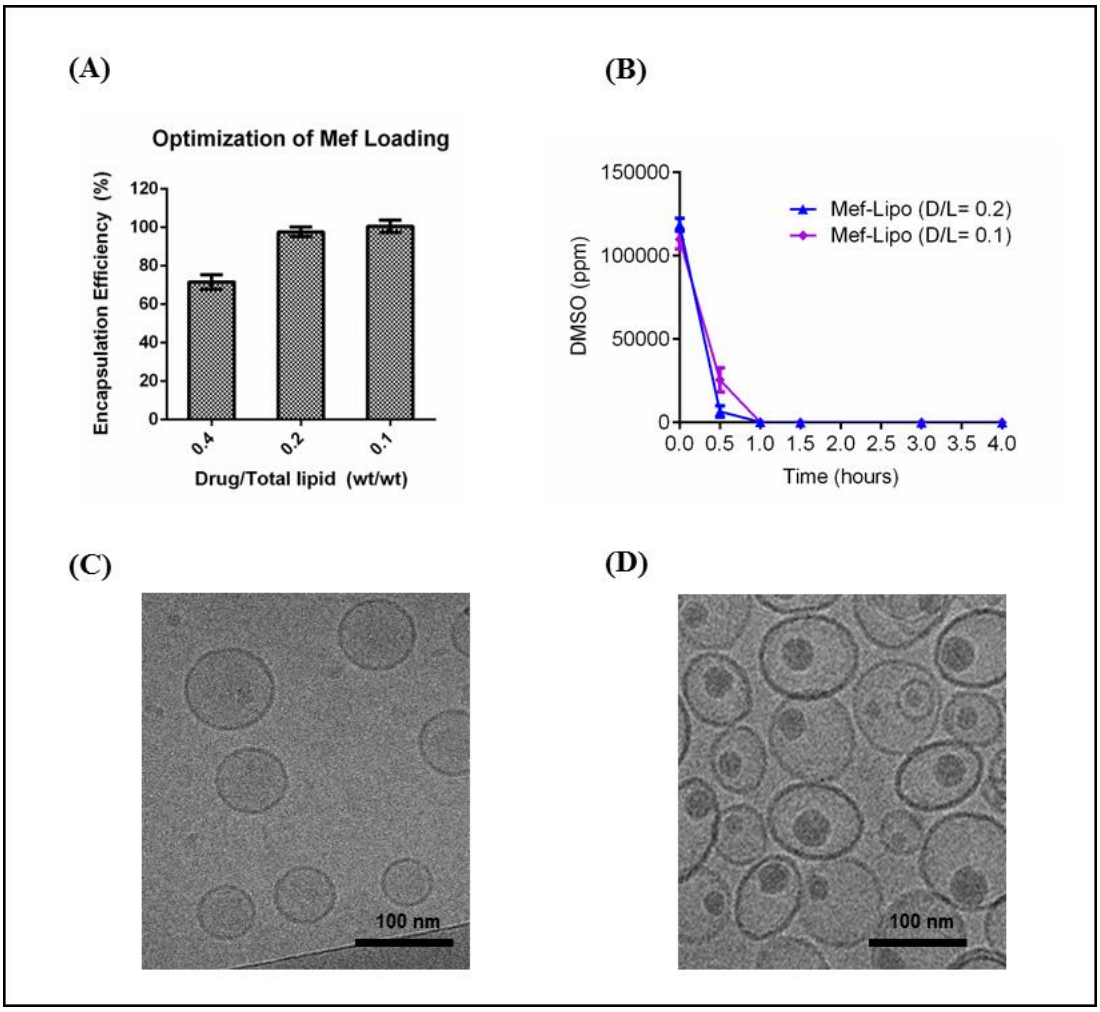

Figure 4.3 Preparation and characterization of the Mef-Lipo formulations. (A) Loading optimization of the Mef-Lipo formulations. (B) Residual DMSO content in the Mef-Lipo during the final dialysis step. Mean±S.D. (n=3). (C) Cryo-TEM image of drug-free liposomes composed of DSPC/Chol (55/45, mol%). (D) Cryo-TEM image of the Mef-Lipo (D/L=0.1).

The Mef-Lipo prepared with different D/L ratios was characterized and shown in **Table 4.3**. These two formulations are comparable in size and size polydispersity index (PDI), while the zeta potential of the high D/L (0.2) formulation was more positive compared to empty liposomes and Mef-Lipo with a D/L of 0.1. In the high D/L (0.2) formulation, some positively charged Mef might be loaded in the bilayer, increasing the zeta potential from -28 mV to -13 mV.

Table 4.3 Physical properties of the liquid Mef-Lipo with different D/L ratios (0.1 and 0.2). Data = Mean ± S.D. (n=3).

	Size (nm)	PDI	Zeta Potential (mV)	Loading Efficiency (%)	D/L (w/w)	DMSO (ppm)	[Mef] (mg/mL)
Empty liposomes	107.2±2.1	0.041±0.055	-2.7±3.6	-	-	-	-
Mef-Lipo (D/L=0.1)	110.7±0.7	0.065±0.033	-27.8±3.1	99.97±1.23	0.1	<0.55	7.93±0.17
Mef-Lipo (D/L=0.2)	109.2±1.1	0.056±0.026	-12.8±1.7	101.12±1.43	0.2	<0.55	8.03±0.14

Detection limit for DMSO using the QDa detector = 0.55 ppm. PDI = polydispersity index.

A few analytical methods have been developed to determine the residual content of DMSO in pharmaceutical products [166-168]. However, these methods might not be suitable for determining DMSO content in liposomal products due to the interference of UV absorbance from other components such as sucrose, cholesterol and phospholipids. The method we developed to quantify DMSO utilized a high sensitivity QDa mass spectrometry detector to isolate the DMSO signal from other interferences. This sensitive method provided a robust tool to characterize the Mef-Lipo, and the linear range for DMSO detection was 0.55-550 ppm with an R^2 of 0.9999 (**Figure 4.4**). This analytical method could also be used to determine other non-volatile and water-miscible solvents such as dimethylformamide and N-Methyl-2-pyrrolidone in liposomal products. The residual DMSO content in the Mef-Lipo was under the detection limit 0.55 ppm, well below the accepted criteria for class III solvents (5000 ppm) based on International Conference on Harmonisation (ICH) Q3C guideline [169].

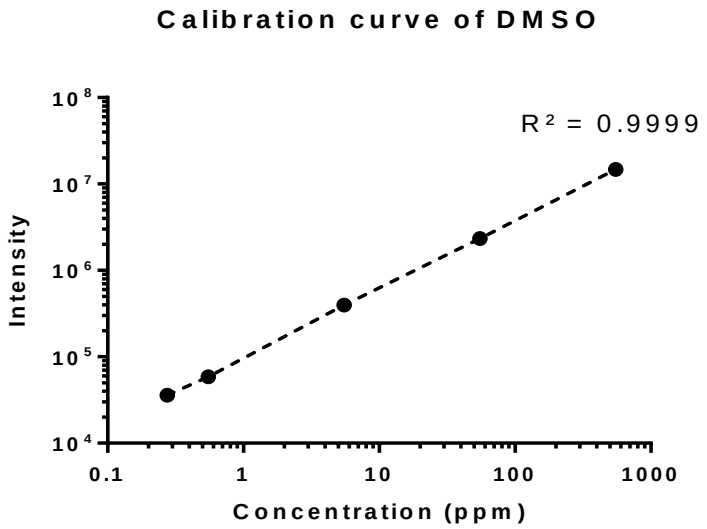

Figure 4.4 A standard calibration curve of DMSO established by the LC-MS method described in section 4.3.6. The linear range for DMSO detection was between 0.55 and 550 ppm.

4.4.3 *In vitro* drug release in simulated fluids

Drug release profiles from the Mef suspension and Mef-Lipo with D/L of 0.1 and 0.2 were compared in SGF, SIF, SIF supplemented with a bile salt (3 mM sodium taucholate) or a lipase (10 mg/mL pancreatic lipase) and SS, using the dialysis method. The experimental conditions for drug release in SGF mimicked that in children (0-5 years old) right after they ingest the FDA recommended dose as outlined in **Table 4.1**. The dialysis method was employed to determine the drug release profiles in various simulated fluids. In this model, the drug must be released from the formulation, and then diffuse through the dialysis membrane to the acceptor site to be measured. Therefore, the release kinetics measured by this method is often slower than in the real conditions [170]. Additionally, due to drug binding with the dialysis membrane, the cumulative drug release measured by this method often does not reach 100%. Nevertheless, the dialysis method offers a robust means to separate released and bound drug, and has been frequently used to compare drug release kinetics of various drug formulations in different release

media [171]. As shown in **Figure 4.5A**, all three formulations displayed near zero order release kinetics for the first 2 h when incubated with the SGF (pH 1.2), and the release rates for the Mef suspension, Mef-Lipo (D/L=0.2, w/w) and Mef-Lipo (D/L=0.1, w/w) were 30%/h, 25%/h and 20%/h, respectively. The drug release rate decreased significantly after 3 h possibly probably due to the reduced drug concentration gradient between the donor and acceptor compartments [172]. Drug release from the Mef suspension in SGF was significantly faster than that from the Mef-Lipo formulations for the first 3 h. This could be due to that the Mef suspension already contained free Mef (~0.6 mg/mL = the solubility of Mef) that would readily diffuse to the acceptor compartment. No significant difference in drug release between the two liquid Mef-Lipo formulations was measured in the first 2 h, while the high D/L formulation exhibited increased drug release after 2 h compared to the low D/L formulation. For a single liposomal vehicle (fixed amount of lipid), the high D/L formulation contained a 2-fold higher amount of drug within the liposome compared to the low D/L formulation. This resulted in higher drug concentration gradient between the release medium and the liposomal compartment in the high D/L formulation, leading to faster drug release compared to the low D/L formulation. However, this increased drug release from the high D/L formulation was only observed after 2 h, and this phenomenon could be explained by that the drug diffusion from the donor to the acceptor site was the rate limiting step for the first 2 h. The drug release rate from the Mef suspension in the plain SIF was similar compared to that in the SGF (40-50%/h in the first 1 h) (Figure 2B). There was no drug release from both Mef-Lipo formulations in the plain SIF. The results from **Figures 4.5A&B** suggest that pH might be an important factor triggering drug release from the Mef-Lipo. We then examined what components in the intestine would induce drug release from the Mef-Lipo. We first investigated the effect of pancreatic lipase alone that digests phospholipids, and as

shown in **Figure 4.5C**, pancreatic lipase in this study did not induce any drug release from the liposomes. Our unpublished data showed that DSPC formulated within the high-cholesterol liposomes was not degraded by the pancreatic lipase during the incubation. On the other hand, sodium taucholate, a form of bile salts present in the intestine was shown to effectively enhance drug release from the liposomes at a rate of 30%/h during 0.5-2 h (**Figure 4.5D**). In the presence of a bile salt, there was no difference in drug release from the high and low D/L liposomal formulations. Sodium taucholate is a surfactant and can induce disruption of liposomal membrane, resulting in drug release. Released Mef would cause strongly bitter taste when in contact with the taste buds in the mouth, and therefore, it is of importance to have a formulation that does not release Mef in the saliva. As shown in **Figure 4.5E**, Mef suspension displayed a linear drug release profile in SS at ~18%/h for the first 3 h, while no drug release could be measured from the two Mef-Lipo formulations, suggesting the drug could be stably retained within the liposomes in the oral cavity to avoid the unpleasant taste.

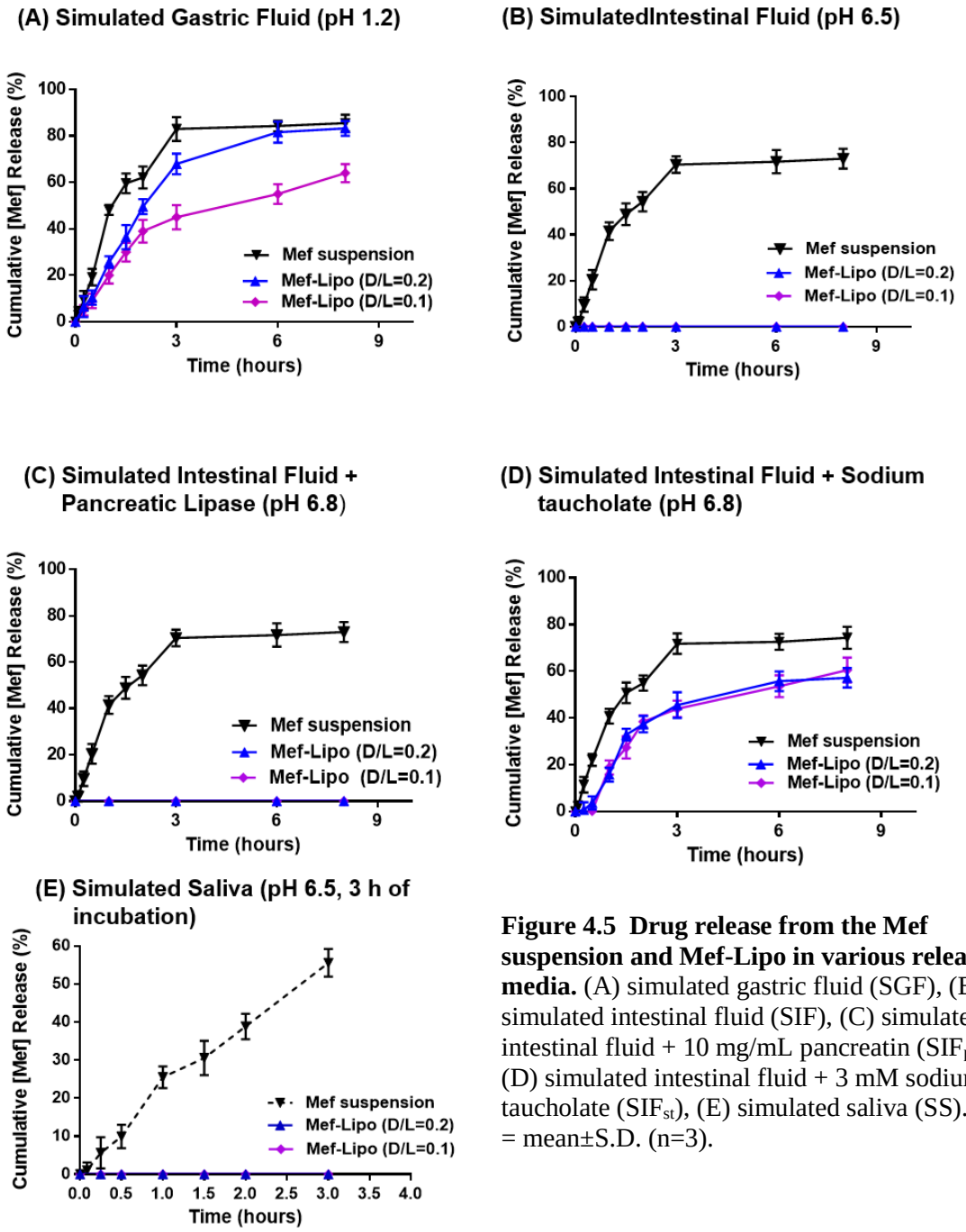

Figure 4.5 Drug release from the Mef suspension and Mef-Lipo in various release media. (A) simulated gastric fluid (SGF), (B) simulated intestinal fluid (SIF), (C) simulated intestinal fluid + 10 mg/mL pancreatin (SIF_{pl}), (D) simulated intestinal fluid + 3 mM sodium taucholate (SIF_{st}), (E) simulated saliva (SS). Data = mean±S.D. (n=3).

To further examine the mechanism of drug release from the Mef-Lipo in SGF and SIF_{st}, the formulation was incubated with the simulated fluids and the particle size and PDI were monitored. As shown in **Figure 4.6**, the particle size and PDI of the Mef-Lipo remained stable

during the incubation at 37 °C for 8 h in the plain SIF (pH 6.8). In SGF (pH 1.2), there was a slight increase of the size (from 114.5 to 141.6 nm) and PDI (from 0.069 to 0.111) after 2 h of incubation. After 8 h of incubation in the SGF, the size and PDI of the Mef-Lipo were increased to 197.8 nm and 0.278, respectively. In the presence of sodium taucholate, the size and PDI of the Mef-Lipo changed rapidly within 0.5 h: the size was increased from 133.0 nm to 396.2 nm, and the PDI was increased from 0.205 to 0.527. The change of size and PDI of the Mef-Lipo corresponded with the drug release, suggesting in these conditions (low pH or bile salt) the liposomal membrane integrity was compromised, resulting in drug release.

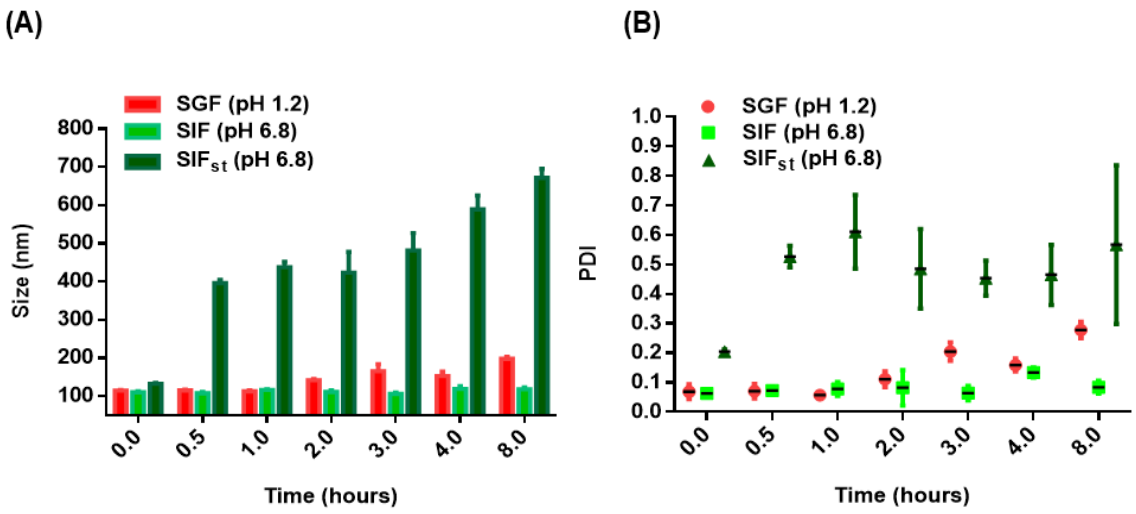

Figure 4.6 Change in particle size (A) and polydispersity index (PDI) of the Mef-Lipo (D/L=0.1) after incubated in simulated gastric fluid (SGF, red), simulated intestinal fluid (SIF, fluorescent green), and simulated intestinal fluid containing 3 mM sodium taucholate (SIF_{st}, dark green) at 37 °C. Data = mean±S.D. (n=3)

In the SGF (pH 1.2), the phosphate group (pKa ~2) of DSPC would be protonated, resulting in imbalance between the hydrophobicity and hydrophilicity of DSPC and consequently instability of the lipid bilayer. There was another possibility that at such a low pH, phospholipids might be

hydrolyzed, leading to disruption of the lipid bilayer. However, a thin layer chromatography study did not show significant degradation of DSPC after 8 h incubation in the SGF (**Figure 4.7)**.

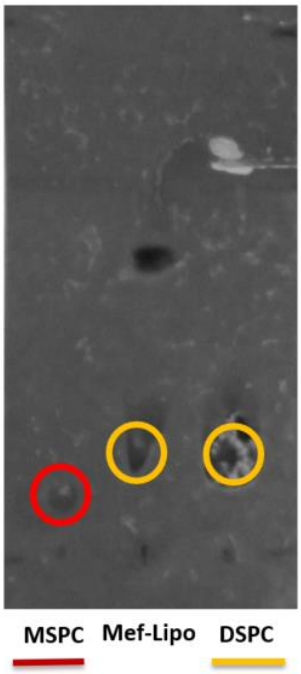

Figure 4.7 Thin layer chromatography (TLC) analysis. Pure MSPC, lipids extracted from Mef-Lipo after 8 h incubation in simulated gastric fluid (SGF), and pure DSPC. The Mef-Lipo was incubated in SGF for 8 h, and 100 µl of the mixture (~10 mg lipid/ml) was mixed with 100 µl of chloroform and 150 µl of methanol to create a homogeneous phase. Three hundred µl of water was then added to separate the mixture into two phases and the bottom layer was analyzed by TLC. The TLC plate was developed with chloroform/methanol/acetic acid/water 40:20:3:1, and then imaged with iodoplatinate. No significant degradation of DSPC from the Mef-Lipo was detected.

4.4.4 Stability of liquid Mef-Lipo

To evaluate the D/L effect on long-term storage, the stability of the liquid Mef-Lipo with different D/L ratios (0.1 and 0.2) was studied. As shown in **Table 4.4**, ~15% drug leakage was found with the high D/L Mef-Lipo, and the size and PDI increased over time from 109 nm to 117 nm and from 0.056 to 0.155. In contrast, no significant changes in drug encapsulation, size and PDI were observed in the low D/L formulation. The total drug concentration (released + encapsulated) in the formulations remained the same as the original during the stability test.

Table 4.4 Stability of the liquid Mef-Lipo during storage at 4 °C. Data = Mean±S.D. (n=3)

Formulation	Month	Size (nm)	PDI	% drug encapsulated	% total drug content compared to original
Mef-Lipo (D/L=0.1)	0	110.7±0.7	0.065±0.033	99.97±1.23	-
	1st	110.8±0.6	0.061±0.021	99.32±2.12	99.74±0.63
	2nd	111.1±0.3	0.072±0.047	99.21±0.93	100.12±1.26
	3rd	111.3±0.8	0.087±0.067	99.86±1.95	100.51±0.79
Mef-Lipo (D/L=0.2)	0	109.2±1.1	0.056±0.026	101.12±1.43	-
	1st	113.2±0.9	0.093±0.112	99.21±3.43	99.75±0.45
	2nd	114.9±2.3	0.123±0.087	90.2±2.56	100.21±0.92
	3rd	117.1±1.4	0.155±0.108	86.92±1.42	100.01±0.33

Therefore, the Mef-Lipo with D/L of 0.1 was selected for the e-tongue and PK studies. The decreased stability of the high D/L formulation could be due to that some drug was loaded in the bilayer instead of the core as suggested by the zeta potential data (**Table 4.3**). These results support the importance of loading poorly soluble Mef inside the liposomal core to improve the stability as well as the utility of the SALT to fabricate such stable formulation.

4.4.5 Bitterness masking

Taste panel is often employed in food industry to evaluate foods and wines. However, due to issues of ethics and personal bias, the e-tongue technology has gained increased attention as an alternative to evaluate taste. The Astree® e-tongue was used in this study to qualitatively assess the bitterness of the liquid Mef-Lipo in comparison with other controls such as 10% sucrose, Infant Tylenol®, and the Mef suspension. This e-tongue is a potentiometric device whose data acquisition is based upon the potential difference between each individual coated sensor and the Ag/AgCl reference electrode. Operating on the Chemical Sensitive Field Effect Transistor

(ChemFETs) technology [159], the sensors interact with the molecular and ionic environment of the samples and generate a corresponding taste pattern for each sample. In this study, the e-tongue was first calibrated using known standards to quantify bitterness in samples, and the taste fingerprint of the placebo (10% sucrose) was compared to Mef-Lipo, Infant Tylenol® and Mef suspension to ascertain which of these three formulations has a similar profile to 10% sucrose. **Figure 4.8** shows the bitterness profiles of various formulations: a high positive bitterness score indicates the formulation is strongly bitter, while a negative score suggests the formulation would taste sweet, and pure water would produce a score of 0. As shown in **Figure 4.8**, the taste profile of the Mef-Lipo was similar to its external phase 10% sucrose, while the Mef suspension showed strong bitterness as indicated by the response of the bitterness sensor.

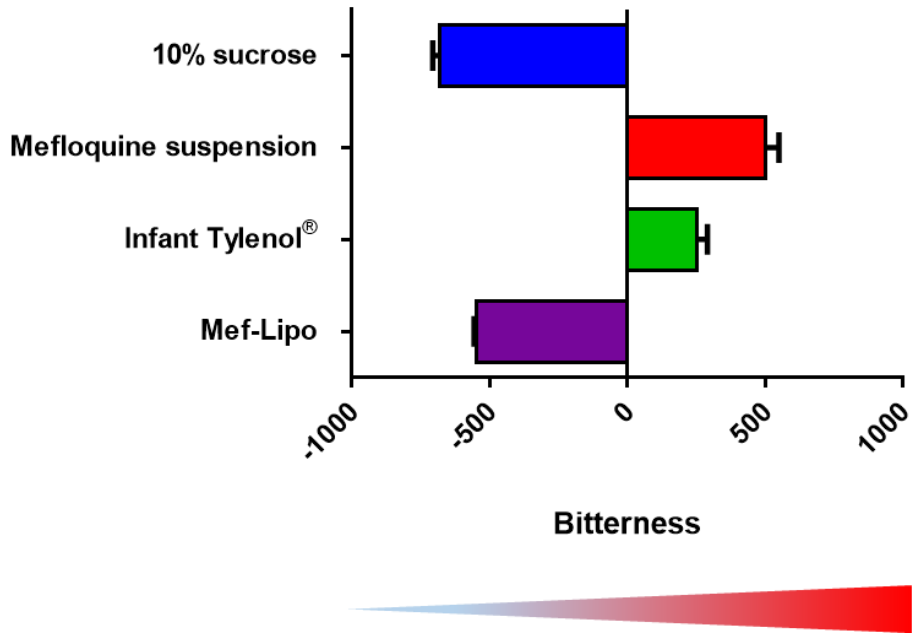

Figure 4.8 Quantification of bitterness of various drug formulations using E-tongue. Data = mean±S.D. (n=3)

The Infant Tylenol® formulation was used as an indicator of a pediatric formulation with an acceptable taste. The data suggest that the Mef-Lipo would exhibit a favorable taste by children, and that the taste of Mef could be masked by drug encapsulation into the liposomal core. In fact, by the E-tongue measurement, the Mef-Lipo tasted similarly as 10% sucrose because the exterior phase of the liposomes was 10% sucrose.

4.4.6 Preparation of rapidly dissolvable Mef-Lipo

Liquid formulations are usually unstable and require antimicrobial preservatives to prevent microbiological contamination upon storage. To improve the stability of Mef-Lipo without adding preservatives that may cause safety concerns in young children, we developed a flexible solid formulation from the liquid Mef-Lipo (D/L=0.1, w/w) by lyophilization. Lyophilization is a common approach to extend the long-term storage of liposomal products and has been widely used [124]. To maintain the liposomal integrity during the freeze-drying process, a lyoprotectant is required. Sucrose was included in the Mef-Lipo system because of its excellent lyoprotecting effect and has been widely applied in the development of water-free liposomal formulations [173-175]. In addition, sucrose is relatively inexpensive compared to other lyoprotectants (eg. trehalose), and can be used as a sweetener for pediatric patients with lactose intolerance [176] (70-90% of the population in Africa). In our study, the tray lyophilizer with programming functions was used to lyophilize the Mef-Lipo to better control the freeze-drying processes and minimize the variation between batches. After lyophilization, the size and PDI of the Mef-Lipo with 300 mM sucrose were significantly increased from 110 nm to 200 nm and from 0.06 to 0.3, respectively (**Table 4**), and ~28% of the drug content leaked out from the liposomes. In this reconstituted formulation, the released Mef concentration was ~0.56 mg/mL, which is the solubility of Mef, resulting in similar bitterness as the Mef suspension measured by E-tongue

(data not shown). These data confirm the necessity of retaining Mef in liposomes for complete taste masking. As the bitterness measured by E-tongue is proportional to the Mef concentration, our unpublished data suggest that a formulation with < 15% drug leakage would result in similar bitterness as the Infant Tylenol formulation, which is clinically acceptable by children. These results also suggest that the high D/L Mef-Lipo would cause significant bitterness after 3 months of storage at 4 °C, and thus would no longer be suitable for use in young children.

In order to minimize drug leakage during lyophilization, we included 20 mM phosphate in 300 mM sucrose to buffer the exterior phase at pH 7.4. Wolkers et al. [177] showed that phosphate may increase the glass temperature (T_g) of the liposomes via the formation of a strong hydrogen bond network with sucrose to further strength the integrity of liposomes. With this new external phase, the size of the Mef-Lipo after lyophlization was slightly increased from 110 nm to 130 nm with a narrow PDI (<0.1), but without any significant drug leakage (**Table 4.5**).

Table 4.5 Characterization of the lyophilized Mef-Lipo formulations after reconstitution. Data = Mean±S.D. (n=3)

Formulations	D/L (w/w)	Size (nm)	PDI	% drug encapsulated
Reference **Liquid Mef-Lipo**	0.1	110.7±0.7	0.065±0.033	99.97±1.23
Conditions 1 **Lyophilization with an exterior phase = 10% sucrose**	0.1	199.6±9.8	0.326±0.151	73.51±4.46
Conditions 2 **Lyophilization with an exterior phase = 20 mM phosphate buffered 10% sucrose, pH 7.4**	0.1	130.7±0.5	0.084±0.051	99.63±2.35

The lyophilized Mef-Lipo in the presence of phosphate salts showed good stability upon storage at room temperature, and no significant drug release was determined in 3 months (**Table 4.6**). The lyophilized Mef-Lipo could be rapidly dissolved with water in 10 s (**Figure 4.9**), suggesting this lyophilized powder form of Mef-Lipo would be orally dispersible and suitable for pediatric use.

Liquid Mef-Lipo	
Size	110.1
PDI	0.056
[Mef]	8-10 (mg/mL)

Lyophilized Mef-Lipo	
Size	130.3
PDI	0.084
Mef Encapsulation (%)	99.1±1.2 (%)

Figure 4.9 Rapid dissolution of lyophilized Mef-Lipo.

Table 4.6 Stability study of the lyophilized Mef-Lipo (20 mM phosphate buffered 10% sucrose) at room temperature. Data = Mean±S.D. (n=3)

Formulation	Month	Size (nm)	PDI	% drug encapsulated	% total drug content compared to original
Lyophilized Mef-Lipo (D/L=0.1)	0	130.5±1.2	0.089±0.013	99.31±2.12	-
	1st	132.1±1.4	0.094±0.022	99.01±0.89	98.51±1.11
	2nd	133.2±0.9	0.135±0.031	98.43±3.12	100.91±0.98
	3rd	138.4±3.2	0.131±0.044	96.03±1.78	99.01±0.65

4.4.7 *In vitro* drug release of the liquid and lyophilized forms of Mef-Lipo

The lyophilized Mef-Lipo (20 mM phosphate buffered 10% sucrose as the exterior phase) exhibited comparable physical features in PDI, zeta potential, encapsulation efficiency and DMSO residual content (**Table 4.7**) as the liquid Mef-Lipo.

Table 4.7 Summary of the Mef-Lipo formulations in liquid/lyophilized form. Data = Mean±S.D. (n=3)

	Size (nm)	PDI	Zeta potential (mV)	% drug encapsulated	D/L (w/w)	DMSO (ppm)	Water content (%)
Liquid Mef-Lipo	110.7±0.7	0.065±0.033	-27±3.1	100.2±2.6	0.1	<0.55	-
Lyophilized Mef-Lipo	130.5±1.2	0.089±0.013	-23.1±2.5	99.1±1.5	0.1	<0.55	2.59%

We also compared their *in vitro* release profiles in simulated fluids, and as shown in **Figure 4.10**, the two forms of Mef-Lipo exhibited similar drug release profiles in SGF, SIF, SIF_{st} and SS.

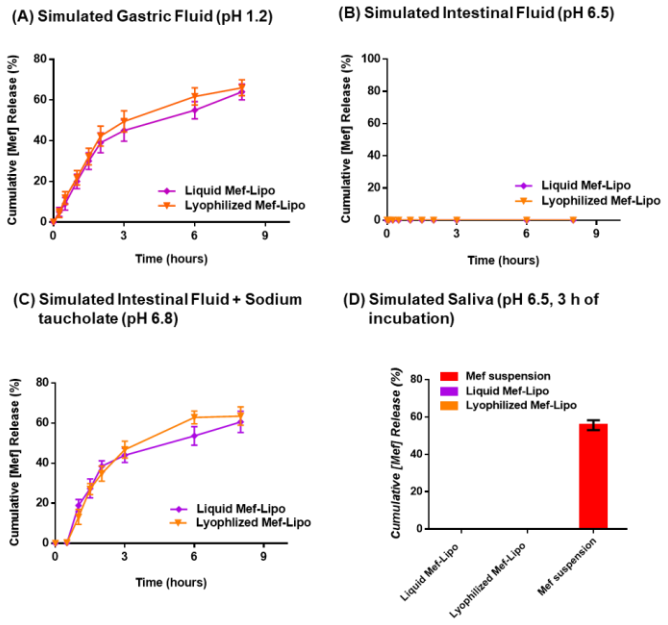

Figure 4.10 Drug release profiles of the liquid and lyophilized Mef-Lipo formulations in (A) simulated gastric fluid, (B) simulated intestinal fluid, (C) simulated intestinal fluid + 3 mM sodium taucholate, and (D) simulated saliva. Data = mean±S.D. (n=3)

4.4.8 Pharmacokinetic (PK) and bioavailability (BA) analysis

To examine whether the Mef-Lipo could be absorbed in vivo, we compared their PK and BA with Mef suspension in BALB/c mice. Liquid Mef-Lipo, reconstituted Mef-Lipo from the lyophilized form or Mef suspension was orally delivered to mice, and plasma was isolated from mice at different timepoints to measure Mef concentration. The plasma profiles of Mef over 72 h after a single dose of various formulations, shown in **Figure 4.11,** are compared with that of a single i.v. dose of Mef solution (dissolved in 300 mM sucrose in the presence of 10% ethanol). As shown in **Figure 4.11**, the plasma profiles of liquid and lyophilized Mef-Lipo were overlapping, while that of Mef suspension appeared to be lower, especially at the T_{max} 4 h. We further analyzed the PK parameters of absorption for these formulations (**Table 4.8**).

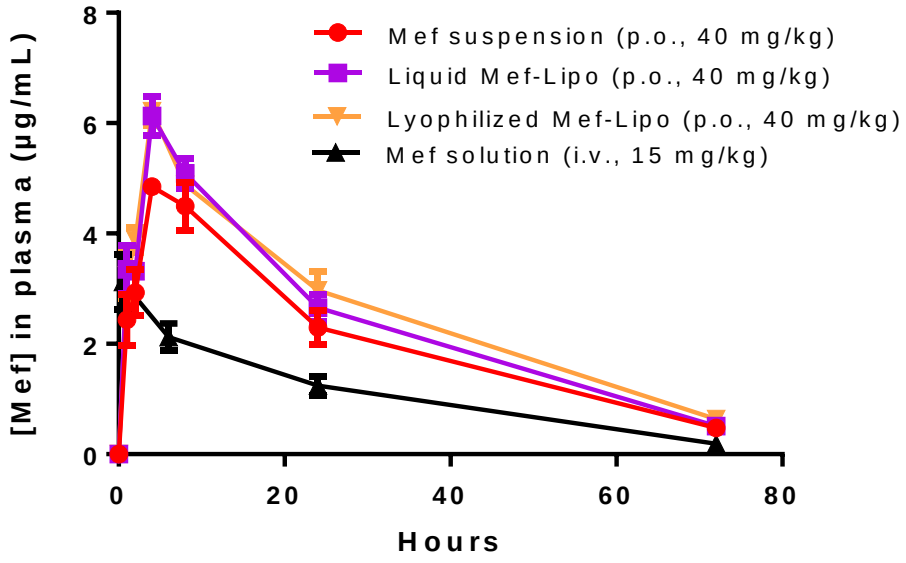

Figure 4.11. Pharmacokinetics of the Mef solution, the Mef suspension, and Mef-Lipo formulations after oral administration to BALB/c mice. Data = mean ± S.D. (n=5)

Table 4.8 Pharmacokinetic parameters of Mef suspension, liquid Mef-Lipo, and Lyophilized Mef-Lipo. Data = mean ± SD, n=5

	Mef dose (mg/kg)	C_{max} (μg/mL)	T_{max} (h)	$AUC_{(0-72h)}$ (μg*h/mL)	$t_{1/2}$ (h)	Bioavailability (%)
Mef solution	15 (i.v.)	3.12±0.49	0.5	80.63±9.58	18.56±1.89	100
Mef suspension	40 (p.o.)	4.86±0.11	4.0	151.21±10.96	19.44±2.15	70.32±5.09
Liquid Mef-Lipo	40 (p.o.)	6.13±0.35*	4.0	174.95±5.72*	20.15±1.01	81.36±2.67*
Lyophilized Mef-Lipo	40 (p.o.)	6.21±0.26*	4.0	185.71±10.20*	21.83±1.81	86.37±4.74*

C_{max}: maximal concentration in plasma; T_{max}: time of the maximal plasma drug concentration; AUC: area under the curve; $t_{1/2}$: half-life. Statistical comparison was performed with Mef suspension, liquid Mef-Lipo and lyophilized Mef-Lipo. * indicates $p<0.05$ compared to Mef suspension.

The data confirmed that the liquid and lyophilized Mef-Lipo were comparable formulations with similar C_{max}, T_{max}, AUC and BA (81-86%). Mef suspension, however, displayed ~20% decreased C_{max}, AUC and BA compared to the liposomal formulation. There was no difference in $t_{1/2}$ among these three formulations, suggesting the formulations did not alter the metabolism or elimination of the drug, and the difference in BA was due to the absorption.

Liposomes and nanoparticles have been shown to improve absorption of poorly soluble drugs through various mechanisms, including increased drug solubility/dissolution [178, 179], reduced drug degradation in gastrointestinal tract by encapsulation [180], and additional absorption pathways such as direct uptake by enteric cells and M cells [181]. As Mef-Lipo did not show increased drug dissolution in our *in vitro* tests, the improved oral absorption of Mef-Lipo compared to Mef suspension could be due to the latter two reasons. More studies need to be performed to draw solid conclusions. In our study, liposomes were used to disperse Mef in nano-sized particles, significantly increasing the "solubilized" drug concentration to 8 mg/mL, well above its solubility ~0.5 mg/mL. Although liposomes have been used to formulate poorly soluble drugs to increase their oral absorption [182, 183], to the best of our knowledge, this is the first report

demonstrating liposomal encapsulation of a drug could mask its taste and that liposomes is an alternative system for developing a rapidly dissolvable and palatable formulation that is child-friendly. Pediatric formulation development is an under pursued area, and this research is of importance and significance.

4.5 Conclusion

We have demonstrated that the poorly soluble antimalarial drug Mef could be actively loaded into the liposomal core using the SALT method we developed. By encapsulating Mef into the liposomes, the solubilized drug concentration was increased from ~0.5 mg/mL to 8 mg/mL and taste of the drug was masked. Mef was stably retained within the liposomes in the simulated saliva, but efficiently released in low pH and bile salt-containing environments, representing the conditions in the stomach and intestine, respectively. The liquid Mef-Lipo formulation was stable for >3 months upon storage at 4 °C. With 20 mM phosphate buffered 10% sucrose as a lyoprotectant, the Mef-Lipo could be lyophilized into a powder form that were stable for >3 months upon storage at room temperature and could be rapidly dissolved in water in 10 s. Two forms (liquid and lyophilized) of Mef-Lipo exhibited comparable oral absorption in mice with BA of 81-86%, and were superior to the standard Mef suspension that exhibited BA of 70%. Our data suggest that both liquid and lyophilized Mef-Lipo formulations were palatable, stable and bioavailable formulations suitable for the use in infants or young children.

Chapter 5: Summary and Future Directions

5.1 Original Contribution

Liposomal formulations with hydrophobic compounds incorporated in the lipid bilayer were developed by passive loading to increase drug solubility, but suffered from low drug loading efficiency/capacity, rapid drug release, and poor *in vitro/vivo* stability. Besides, hydrophobic drugs cannot be loaded by currently standard active loadings due to poor drug solubility, which hinder drug permeation through the lipid bilayer to accumulate in the aqueous core of liposomes, often leading to scant drug encapsulation. To overcome this limitation, we have developed the solvent-assisted active loading technology (SALT) that involves inclusion of a limited amount of water-miscible solvent in the loading mixture that contains preformed liposomes incorporated with a trapping agent and a hydrophobic drug. As shown in **Figure 5.1**, this technique promotes active loading of the hydrophobic drug efficiently into the aqueous core of liposomes to form drug aggregates/complexes with increased drug loading efficiency (> 80% drug encapsulation) and stability.

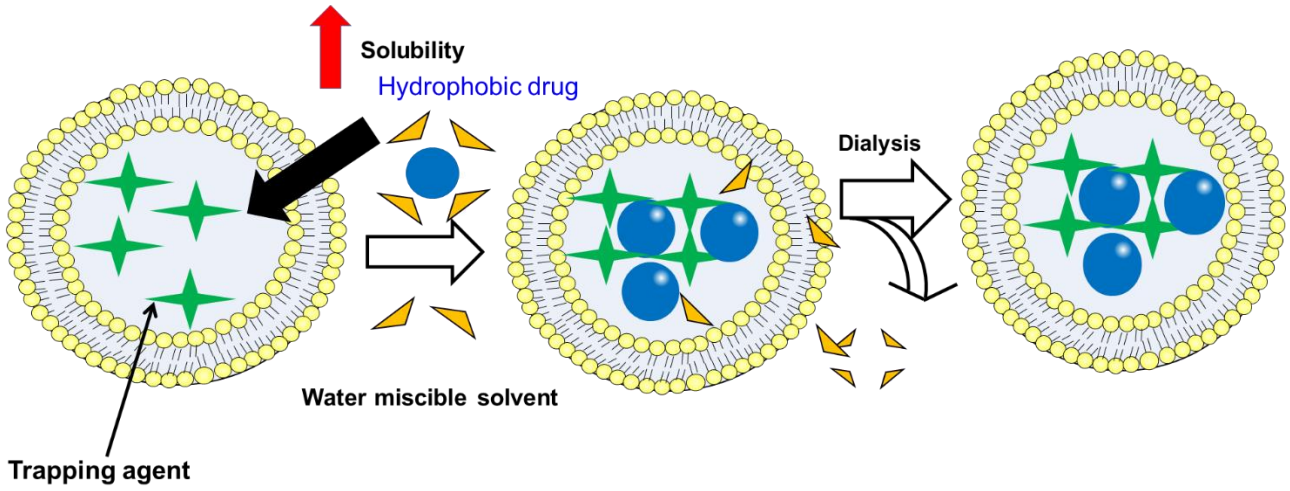

Figure 5. 1 The rationale of the SALT.

5.2 Summary & Future Directions

This thesis project focused on the development and optimization of the SALT and demonstration of the potential applications of this technology.

Chapter 2 described the proof-of-principle work showing that the SALT could be employed to actively encapsulate a model insoluble weak base drug, staurosporine (STS), into the aqueous core of liposomes via an ammonium sulfate gradient. This was the first study to reveal by cryo-TEM that a hydrophobic drug could be entrapped stably inside the core of liposomes. Complete encapsulation of STS into the preformed liposomes with a high transition temperature (> 55 °C) at a high D/L (0.2 w/w) could be achieved without heating when 5% of DMSO was added.

Chapter 3 studies further demonstrated that the SALT could be applied to load different types of compounds into liposomes, and a wide range of water-miscible organic solvents could be used to promote the drug loading. It was also shown that the solvent included in the SALT helped dissolve the compound in the exterior phase of liposomes as well as increased the membrane permeability to allow better penetration of the compound into the inner aqueous core for loading. To achieve maximal loading efficiency, the content of solvent must exceed the minimal requirement for complete solubilization of the compound but be within the limit that caused membrane instability. With a model insoluble weakly acidic drug, gambogic acid (GA), we also discovered that both the loading gradient and the liposomal formulation must be optimized to develop an optimal formulation that displayed improved drug retention within the liposomes in the presence of serum, prolonged pharmacokinetics (PK), reduced toxicity and enhanced antitumor efficacy. To the best of our knowledge, our liposomal formulation provided the first example of liposomal GA that was prepared using an active loading technology and displayed a prolonged half-life relative to the free drug.

In Chapter 4, we explored the utility of SALT to prepare a child-friendly oral formulation for mefloquine (Mef), a poorly water-soluble weak base drug. We were the first group to report bitterness masking was achieved by complete loading of Mef into liposomes, and the liposomal formulation could be lyophilized to prepare a rapidly dissolvable solid formulation that was stable at room temperature and suitable for pediatric use.

Overall, the work reported in this thesis supports that the SALT is a versatile and robust platform technology that can be utilized to prepare liposomal drug formulations to increase the drug solubility, drug retention, formulation stability, oral palatability, circulation half-life, and efficacy. Multiple examples were generated to demonstrate potential medical utilities of the SALT and the resulting liposomal formulations, including cancer therapy and oro-dispersible pediatric formulation. As a platform technology, it is believed that the SALT can be employed to prepare stable liposomal formulations for various drugs that cannot be effectively delivered using standard methods. For example, many natural products exhibit poor water-solubility and their delivery and efficacy may be improved if they can be stably formulated in liposomes using the SALT. GA is one example from this class of drugs and the robustness of the SALT was demonstrated in the studies reported in Chapter 3. Another example is resiquimod (R-848), which is a poorly soluble toll-like receptor agonist. When ingested orally, resiquimod induces non-specific immune response, and thus, cannot be used clinically [184]. Resiqumod was successfully formulated within liposomes using the SALT and shown to target tumors to boost tumor-specific immune response. As demonstrated in a preliminary study (**Figure 5.2**), the liposomal resiquimod (Lipo-Vac) regressed the EMT6 tumor completely after one single dose and the cured mouse exhibited specific EMT6 tumor immunity. These exciting results warrant further investigation of this formulation for cancer immunotherapy.

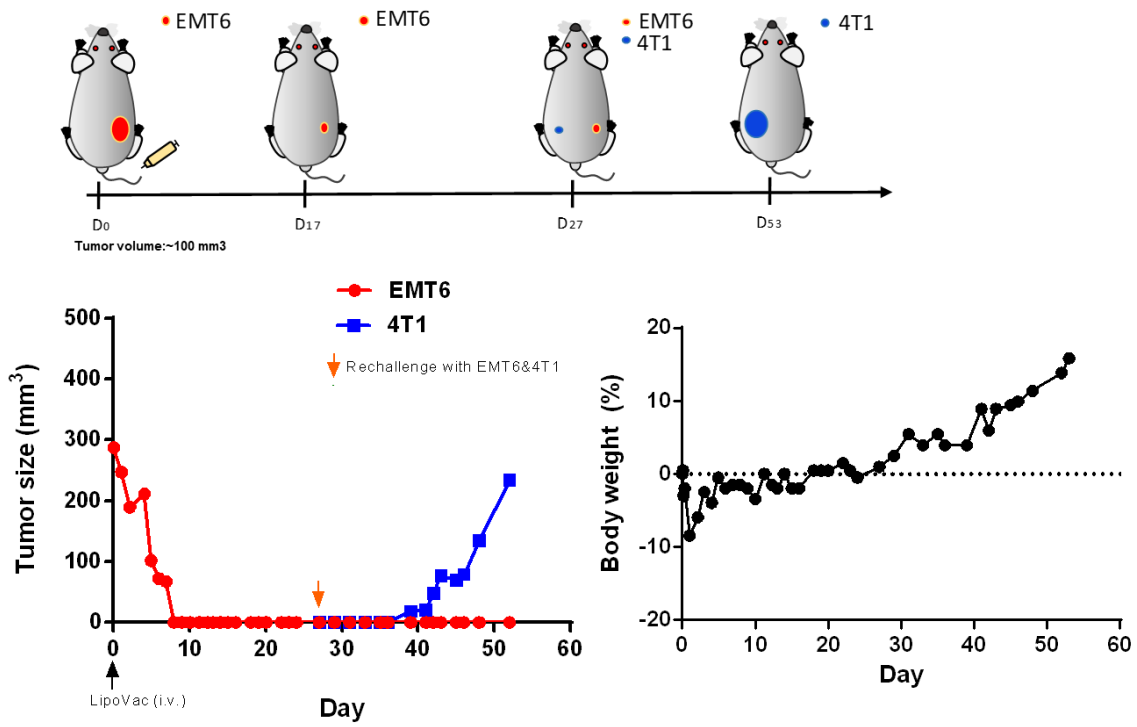

Figure 5. 2Anti-tumor efficacy of the liposomal resiquimod (Lipo-Vac) against EMT6 cancer model (n=2). EMT6 (mice breast cancer cells); 4T1 (mice breast cancer cells). The disappearance of EMT6 tumors treated with one dose of Lipo-Vac was observed between Day 10-20. The cured mice developed specific immunity against EMT6 tumor.

The SALT may also be used for reformulation of some liposomal products to improve the stability and enhance the therapeutic efficacy. For example, AmBisome® (liposomal amphotericin B) is manufactured using the passive loading method [185]. AmBisome exhibits improved safety but the efficacy was only comparable relative to the free drug. With the SALT, it is possible to stably load amphotericin B (a weak base drug) into liposomes that will display reduced drug leakage and prolonged PK, leading to further improved safety and efficacy. It is also worth reinvestigating liposomal products that failed clinical trials due to rapid drug release and limited improvements in PK. The SALT may be employed to enhance the performance of these drugs. In addition to therapeutic drugs, the SALT may be particularly useful for stably loading a hydrophobic imaging probe or a combination of a poorly soluble probe and a

hydrophobic drug into liposomes for imaging and theranostics (**Figure 5.3**), respectively. As reviewed earlier [186], one of the significant challenges in the theranostic field is the weak association between the imaging probe and the nanoparticles, leading to inaccurate report of drug delivery under imaging. The SALT may be employed to address this shortcoming.

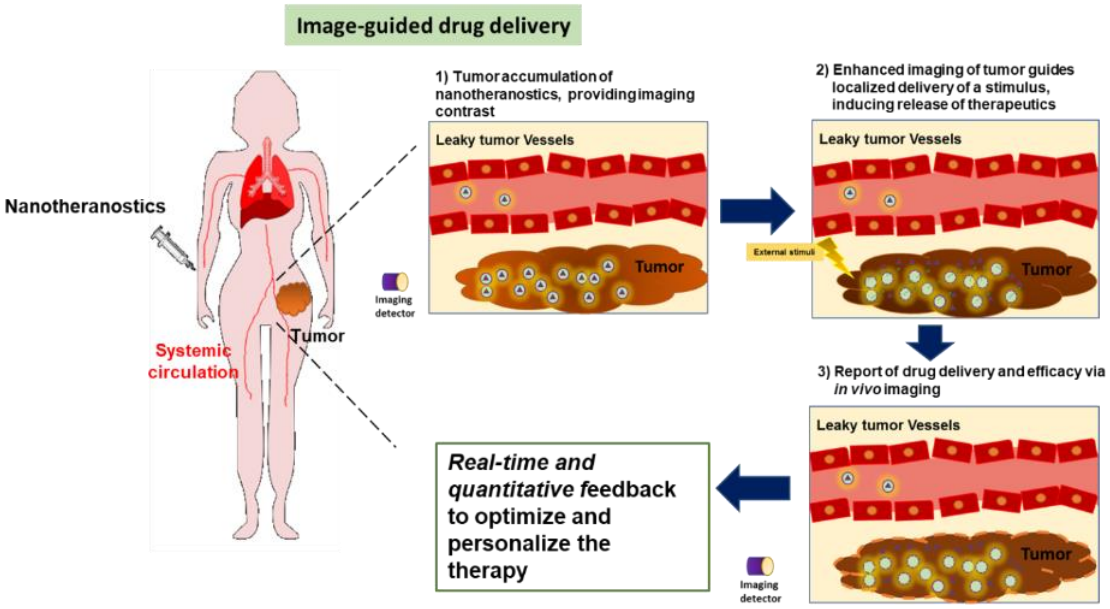

Figure 5. 3 Illustration of image-guided drug delivery enabled by nanotheranostics. 1) Preferential accumulation of liposomes in the tumor can be achieved by the EPR effect; 2) the drug release from the accumulated liposomes can be triggered by an external stimulus to release the cargo; 3) Real-time and quantitative feedback of drug delivery of nanotheranostics can be acquired noninvasively through a specific imaging modality that can be further exploited to optimize and personalize the therapy.

Although the SALT is a robust platform technology for liposomal drug loading, the properties of the resulting formulation is highly dependent on the loading gradient and lipid composition. As demonstrated in Chapter 4, loading gradient (metal ion, counter ion, pH) affected the loading efficiency and drug retention. It was also shown that different drugs required different loading gradients to achieve optimal drug encapsulation. Likewise, the lipid composition determined the drug retention within the liposomes in the presence of serum or the blood stream [39,164].

Therefore, different loading gradients and lipid formulations have to be developed and optimized for different drugs. The working principles are that a trapping agent must be included inside the aqueous core to form stable complexes with the drug and the lipid bilayer must retain its impermeability for the complexes. A trapping agent may be rationally selected based on the chemical structure of the drug and the functional groups, while the lipid formulation may need to be empirically optimized. The pH gradient is the method of choice when ionizable drugs are to be loaded, while the transition metal ions appear to interact with a wide range of functional groups for trapping compounds inside the liposomes. Nevertheless, the safety of using these transition metal ions in liposomal formulations needs to be tested. While versatile liposomal formulations can be developed using the commercially available lipids, it is being recognized that innovative lipids can be rationally designed and synthesized to prepare a more potent lipid formulation for drug targeting. More effort will be focused on developing new drug loading gradients and innovative lipids to expand the spectrum of the SALT and the liposomal drug delivery. As discussed above, the SALT is most suitable for poorly water-soluble but membrane permeable drugs. However, highly water-soluble but membrane impermeable drugs such as nucleic acids and peptides cannot be actively loaded using the SALT and a new method needs to be developed for targeting this emerging class of drugs. Again, this will involve the development of a new loading gradient, a lipid composition and more importantly, an innovative technique to increase the membrane permeability of these drugs.

Although the utility of the SALT has only been demonstrated with liposomes, other types of vesicular delivery systems with a bilayer membrane would be amenable to the SALT, like niosomes, exosomes, porphysomes, and polymersomes [187-189]. It would be of interest to expand the utility of SALT to other delivery systems and explore the applications to improve

current therapies for various diseases. The successful development of such lipid- or polymer-based platforms is expected to generate a novel class of therapeutics. A notable example is porphysomes, made of porphyrin conjugated phospholipids. Porphysomes can selectively accumulate in tumors and can be detected by various imaging modalities, such as fluorescence imaging, which help guide specific light irradiation to the tumors for enhanced photothermal therapy (PTT) or photodynamic therapy (PDT) [190, 191]. However, the drug loading and retention in porphysomes are yet to be optimized and the SALT might provide a ready solution to this challenge.

Bibliography

[1] C. Taniguchi, Y. Kawabata, K. Wada, S. Yamada, S. Onoue, Microenvironmental pH-modification to improve dissolution behavior and oral absorption for drugs with pH-dependent solubility, Expert Opinion on Drug Delivery 11(4) (2014) 505-516.
[2] Y. Huang, W.-G. Dai, Fundamental aspects of solid dispersion technology for poorly soluble drugs, Acta Pharmaceutica Sinica B 4(1) (2014) 18-25.
[3] T.R. Buggins, P.A. Dickinson, G. Taylor, The effects of pharmaceutical excipients on drug disposition, Advanced Drug Delivery Reviews 59(15) (2007) 1482-1503.
[4] M. Sharma, R. Sharma, D.K. Jain, Nanotechnology based approaches for enhancing oral bioavailability of poorly water soluble antihypertensive drugs, Scientifica 2016 (2016) 8525679.
[5] A. Mahmood, R.S. Muhammad, M. Asif, Hydrogel microparticles as an emerging tool in pharmaceutical field: A review, Advances in Polymer Technology 35(2) (2016) 121-128.
[6] J.L.H. Johnson, Y. He, S.H. Yalkowsky, Prediction of precipitation-induced phlebitis: A statistical validation of an in vitro model, Journal of Pharmaceutical Sciences 92(8) (2003) 1574-1581.
[7] G. Van den Mooter, The use of amorphous solid dispersions: A formulation strategy to overcome poor solubility and dissolution rate, Drug Discovery Today: Technologies 9(2) (2012) e79-e85.
[8] S. Gurunath, S. Pradeep Kumar, N.K. Basavaraj, P.A. Patil, Amorphous solid dispersion method for improving oral bioavailability of poorly water-soluble drugs, Journal of Pharmacy Research 6(4) (2013) 476-480.
[9] S. Baghel, H. Cathcart, N.J. O'Reilly, Polymeric amorphous solid dispersions: A review of amorphization, crystallization, stabilization, solid-state characterization, and aqueous solubilization of biopharmaceutical classification system class II drugs, Journal of Pharmaceutical Sciences 105(9) (2016) 2527-2544.
[10] K. Amin, R.-M. Dannenfelser, In vitro hemolysis: Guidance for the pharmaceutical scientist, Journal of Pharmaceutical Sciences 95(6) (2006) 1173-1176.
[11] H. Gelderblom, J. Verweij, K. Nooter, A. Sparreboom, Cremophor EL: the drawbacks and advantages of vehicle selection for drug formulation, European Journal of Cancer 37(13) (2001) 1590-1598.
[12] C.D. Scripture, W.D. Figg, A. Sparreboom, Paclitaxel chemotherapy: from empiricism to a mechanism-based formulation strategy, Therapeutics and Clinical Risk Management 1(2) (2005) 107-114.
[13] F.K. Engels, R.A.A. Mathot, J. Verweij, Alternative drug formulations of docetaxel: a review, Anti-Cancer Drugs 18(2) (2007) 95-103.
[14] S. Kalepu, V. Nekkanti, Insoluble drug delivery strategies: review of recent advances and business prospects, Acta Pharmaceutica Sinica B 5(5) (2015) 442-453.
[15] H. Chen, C. Khemtong, X. Yang, X. Chang, J. Gao, Nanonization strategies for poorly water-soluble drugs, Drug Discovery Today 16(7) (2011) 354-360.
[16] H. Wang, Q. Li, S. Reyes, J. Zhang, L. Xie, V. Melendez, M. Hickman, M.P. Kozar, Formulation and particle size reduction improve bioavailability of poorly water-soluble compounds with antimalarial activity, Malaria Research and Treatment 2013 (2013) 10.
[17] S. Emami, S. Azadmard-Damirchi, S.H. Peighambardoust, H. Valizadeh, J. Hesari, Liposomes as carrier vehicles for functional compounds in food sector, Journal of Experimental Nanoscience 11(9) (2016) 737-759.

[18] U. Bulbake, S. Doppalapudi, N. Kommineni, W. Khan, Liposomal formulations in clinical use: An updated review, Pharmaceutics 9(2) (2017) 12.
[19] B.S. Pattni, V.V. Chupin, V.P. Torchilin, New developments in liposomal drug delivery, Chemical Reviews 115(19) (2015) 10938-10966.
[20] M. Maeki, N. Kimura, Y. Sato, H. Harashima, M. Tokeshi, Advances in microfluidics for lipid nanoparticles and extracellular vesicles and applications in drug delivery systems, Advanced Drug Delivery Reviews (2018).
[21] N. Dimov, E. Kastner, M. Hussain, Y. Perrie, N. Szita, Formation and purification of tailored liposomes for drug delivery using a module-based micro continuous-flow system, Scientific Reports 7(1) (2017) 12045.
[22] M.L. Immordino, F. Dosio, L. Cattel, Stealth liposomes: review of the basic science, rationale, and clinical applications, existing and potential, International Journal of Nanomedicine 1(3) (2006) 297-315.
[23] J.J.F. Verhoef, T.J. Anchordoquy, Questioning the use of PEGylation for drug delivery, Drug delivery and translational research 3(6) (2013) 499-503.
[24] R. Li, K. Zheng, C. Yuan, Z. Chen, M. Huang, Be active or not: the relative contribution of active and passive tumor targeting of nanomaterials, Nanotheranostics 1(4) (2017) 346-357.
[25] C. Zylberberg, S. Matosevic, Pharmaceutical liposomal drug delivery: a review of new delivery systems and a look at the regulatory landscape, Drug Delivery 23(9) (2016) 3319-3329.
[26] H. Kim, Y. Kim, J. Lee, Liposomal formulations for enhanced lymphatic drug delivery, Asian Journal of Pharmaceutical Sciences 8(2) (2013) 96-103.
[27] P.R. Cullis, L.D. Mayer, M.B. Bally, T.D. Madden, M.J. Hope, Generating and loading of liposomal systems for drug-delivery applications, Advanced Drug Delivery Reviews 3(3) (1989) 267-282.
[28] J. Gubernator, Active methods of drug loading into liposomes: recent strategies for stable drug entrapment and increased in vivo activity, Expert Opinion on Drug Delivery 8(5) (2011) 565-580.
[29] Y. Zhao, J.P. May, I.-W. Chen, E. Undzys, S.-D. Li, A study of liposomal formulations to improve the delivery of aquated cisplatin to a multidrug resistant tumor, Pharmaceutical Research 32(10) (2015) 3261-3268.
[30] D. Zucker, D. Marcus, Y. Barenholz, A. Goldblum, Liposome drugs' loading efficiency: A working model based on loading conditions and drug's physicochemical properties, Journal of Controlled Release 139(1) (2009) 73-80.
[31] S.H. Hwang, Y. Maitani, X.R. Qi, K. Takayama, T. Nagai, Remote loading of diclofenac, insulin and fluorescein isothiocyanate labeled insulin into liposomes by pH and acetate gradient methods, International journal of pharmaceutics 179(1) (1999) 85-95.
[32] L.D. Mayer, M.B. Bally, P.R. Cullis, Uptake of adriamycin into large unilamellar vesicles in response to a pH gradient, Biochimica et biophysica acta 857(1) (1986) 123-6.
[33] Y. Avnir, R. Ulmansky, V. Wasserman, S. Even-Chen, M. Broyer, Y. Barenholz, Y. Naparstek, Amphipathic weak acid glucocorticoid prodrugs remote-loaded into sterically stabilized nanoliposomes evaluated in arthritic rats and in a Beagle dog: a novel approach to treating autoimmune arthritis, Arthritis Rheum 58(1) (2008) 119-29.
[34] A. Yuval, U. Rina, W. Veronica, E.C. Simcha, B. Maya, B. Yechezkel, N. Yaakov, Amphipathic weak acid glucocorticoid prodrugs remote-loaded into sterically stabilized nanoliposomes evaluated in arthritic rats and in a Beagle dog: A novel approach to treating autoimmune arthritis, Arthritis & Rheumatism 58(1) (2008) 119-129.

[35] S. Clerc, Y. Barenholz, Loading of amphipathic weak acids into liposomes in response to transmembrane calcium acetate gradients, Biochimica et Biophysica Acta (BBA) - Biomembranes 1240(2) (1995) 257-265.
[36] E. Ramsay, J. Alnajim, M. Anantha, A. Taggar, A. Thomas, K. Edwards, G. Karlsson, M. Webb, M. Bally, Transition metal-mediated liposomal encapsulation of irinotecan (CPT-11) stabilizes the drug in the therapeutically active lactone conformation, Pharmaceutical Research 23(12) (2006) 2799-2808.
[37] A.S. Taggar, J. Alnajim, M. Anantha, A. Thomas, M. Webb, E. Ramsay, M.B. Bally, Copper–topotecan complexation mediates drug accumulation into liposomes, Journal of Controlled Release 114(1) (2006) 78-88.
[38] G.N.C. Chiu, S.A. Abraham, L.M. Ickenstein, R. Ng, G. Karlsson, K. Edwards, E.K. Wasan, M.B. Bally, Encapsulation of doxorubicin into thermosensitive liposomes via complexation with the transition metal manganese, Journal of Controlled Release 104(2) (2005) 271-288.
[39] S.A. Abraham, C. McKenzie, D. Masin, R. Ng, T.O. Harasym, L.D. Mayer, M.B. Bally, In vitro and in vivo characterization of doxorubicin and vincristine coencapsulated within liposomes through use of transition metal ion complexation and pH gradient loading, Clinical Cancer Research 10(2) (2004) 728-738.
[40] J. Gubernator, Active methods of drug loading into liposomes: recent strategies for stable drug entrapment and increased in vivo activity, Expert opinion on drug delivery 8(5) (2011) 565-80.
[41] D.C. Drummond, C.O. Noble, Z. Guo, K. Hong, J.W. Park, D.B. Kirpotin, Development of a highly active nanoliposomal irinotecan using a novel intraliposomal stabilization strategy, Cancer research 66(6) (2006) 3271-7.
[42] T. Fujisawa, H. Miyai, K. Hironaka, T. Tsukamoto, K. Tahara, Y. Tozuka, M. Ito, H. Takeuchi, Liposomal diclofenac eye drop formulations targeting the retina: formulation stability improvement using surface modification of liposomes, International journal of pharmaceutics 436(1-2) (2012) 564-7.
[43] C. Li, C. Wang, H. Yang, X. Zhao, N. Wei, J. Cui, Liposomal topotecan formulation with a low polyethylene glycol grafting density: pharmacokinetics and antitumour activity, The Journal of pharmacy and pharmacology 64(3) (2012) 372-82.
[44] Y. Avnir, K. Turjeman, D. Tulchinsky, A. Sigal, P. Kizelsztein, D. Tzemach, A. Gabizon, Y. Barenholz, Fabrication principles and their contribution to the superior in vivo therapeutic efficacy of nano-liposomes remote loaded with glucocorticoids, PloS one 6(10) (2011) e25721.
[45] E. Ramsay, J. Alnajim, M. Anantha, A. Taggar, A. Thomas, K. Edwards, G. Karlsson, M. Webb, M. Bally, Transition metal-mediated liposomal encapsulation of irinotecan (CPT-11) stabilizes the drug in the therapeutically active lactone conformation, Pharmaceutical research 23(12) (2006) 2799-808.
[46] A.S. Taggar, J. Alnajim, M. Anantha, A. Thomas, M. Webb, E. Ramsay, M.B. Bally, Copper-topotecan complexation mediates drug accumulation into liposomes, Journal of controlled release : official journal of the Controlled Release Society 114(1) (2006) 78-88.
[47] E. See, W. Zhang, J. Liu, D. Svirskis, B.C. Baguley, J.P. Shaw, G. Wang, Z. Wu, Physicochemical characterization of asulacrine towards the development of an anticancer liposomal formulation via active drug loading: stability, solubility, lipophilicity and ionization, International journal of pharmaceutics 473(1-2) (2014) 528-35.

[48] P.B. Pisal, M.A. Joshi, M.N. Padamwar, S.S. Patil, V.B. Pokharkar, Probing influence of methodological variation on active loading of acetazolamide into nanoliposomes: biophysical, in vitro, ex vivo, in vivo and rheological investigation, International journal of pharmaceutics 461(1-2) (2014) 82-8.
[49] D. Lipka, J. Gubernator, N. Filipczak, S. Barnert, R. Suss, M. Legut, A. Kozubek, Vitamin C-driven epirubicin loading into liposomes, Int J Nanomedicine 8 (2013) 3573-85.
[50] J. Gubernator, G. Chwastek, M. Korycinska, M. Stasiuk, G. Grynkiewicz, F. Lewrick, R. Suss, A. Kozubek, The encapsulation of idarubicin within liposomes using the novel EDTA ion gradient method ensures improved drug retention in vitro and in vivo, Journal of controlled release : official journal of the Controlled Release Society 146(1) (2010) 68-75.
[51] A.C. Pinto, S. Angelo, J.N. Moreira, S. Simoes, Development, characterization and in vitro evaluation of single or co-loaded imatinib mesylate liposomal formulations, Journal of nanoscience and nanotechnology 12(3) (2012) 2891-900.
[52] Y. Yang, Y. Ma, S. Wang, A novel method to load topotecan into liposomes driven by a transmembrane NH(4)EDTA gradient, Eur J Pharm Biopharm 80(2) (2012) 332-9.
[53] J. Gubernator, D. Lipka, M. Korycinska, K. Kempinska, M. Milczarek, J. Wietrzyk, R. Hrynyk, S. Barnert, R. Suss, A. Kozubek, Efficient human breast cancer xenograft regression after a single treatment with a novel liposomal formulation of epirubicin prepared using the EDTA ion gradient method, PloS one 9(3) (2014) e91487.
[54] A. Gabizon, R. Catane, B. Uziely, B. Kaufman, T. Safra, R. Cohen, F. Martin, A. Huang, Y. Barenholz, Prolonged circulation time and enhanced accumulation in malignant exudates of doxorubicin encapsulated in polyethylene-glycol coated liposomes, Cancer research 54(4) (1994) 987-92.
[55] Y. Barenholz, Doxil(R)--the first FDA-approved nano-drug: lessons learned, Journal of controlled release : official journal of the Controlled Release Society 160(2) (2012) 117-34.
[56] D.C. Drummond, C.O. Noble, Z. Guo, M.E. Hayes, J.W. Park, C.J. Ou, Y.L. Tseng, K. Hong, D.B. Kirpotin, Improved pharmacokinetics and efficacy of a highly stable nanoliposomal vinorelbine, The Journal of pharmacology and experimental therapeutics 328(1) (2009) 321-30.
[57] H. Xing, K. Hwang, Y. Lu, Recent developments of liposomes as nanocarriers for theranostic applications, Theranostics 6(9) (2016) 1336-1352.
[58] M.S. Webb, N.L. Boman, D.J. Wiseman, D. Saxon, K. Sutton, K.F. Wong, P. Logan, M.J. Hope, Antibacterial efficacy against an in vivo salmonella typhimurium infection model and pharmacokinetics of a liposomal ciprofloxacin formulation, Antimicrobial Agents and Chemotherapy 42(1) (1998) 45-52.
[59] E. See, W. Zhang, J. Liu, D. Svirskis, B.C. Baguley, J.P. Shaw, G. Wang, Z. Wu, Physicochemical characterization of asulacrine towards the development of an anticancer liposomal formulation via active drug loading: Stability, solubility, lipophilicity and ionization, International journal of pharmaceutics 473(1–2) (2014) 528-535.
[60] R. Mukthavaram, P. Jiang, R. Saklecha, D. Simberg, I.S. Bharati, N. Nomura, Y. Chao, S. Pastorino, S.C. Pingle, V. Fogal, W. Wrasidlo, M. Makale, S. Kesari, High-efficiency liposomal encapsulation of a tyrosine kinase inhibitor leads to improved in vivo toxicity and tumor response profile, International Journal of Nanomedicine 8 (2013) 3991-4006.
[61] K. Tschaikowsky, Protein kinase C inhibitors suppress LPS-induced TNF production in alveolar macrophages and in whole blood: The role of encapsulation into liposomes, Biochimica et Biophysica Acta (BBA) - Molecular Cell Research 1222(1) (1994) 113-121.
[62] F.M. Samuel Zalipsky, Liposome formulations of boronic acid compounds, 2006.

[63] I.V. Zhigaltsev, G. Winters, M. Srinivasulu, J. Crawford, M. Wong, L. Amankwa, D. Waterhouse, D. Masin, M. Webb, N. Harasym, L. Heller, M.B. Bally, M.A. Ciufolini, P.R. Cullis, N. Maurer, Development of a weak-base docetaxel derivative that can be loaded into lipid nanoparticles, Journal of Controlled Release 144(3) (2010) 332-340.
[64] Y. Wang, S. Tu, A.N. Pinchuk, M.P. Xiong, Active drug encapsulation and release kinetics from hydrogel-in-liposome nanoparticles, Journal of Colloid and Interface Science 406(0) (2013) 247-255.
[65] W. Zhang, G. Wang, J. Falconer, B. Baguley, J. Shaw, J. Liu, H. Xu, E. See, J. Sun, J. Aa, Z. Wu, Strategies to maximize liposomal drug loading for a poorly water-soluble anticancer drug, Pharmaceutical Research 32(4) (2015) 1451-1461.
[66] S. Sur, A.C. Fries, K.W. Kinzler, S. Zhou, B. Vogelstein, Remote loading of preencapsulated drugs into stealth liposomes, Proceedings of the National Academy of Sciences 111(6) (2014) 2283-2288.
[67] K.-M. Debatin, D. Poncet, G. Kroemer, Chemotherapy: targeting the mitochondrial cell death pathway, Oncogene 21 (2002) 8786.
[68] X.D. Zhang, S.K. Gillespie, P. Hersey, Staurosporine induces apoptosis of melanoma by both caspase-dependent and -independent apoptotic pathways, Molecular Cancer Therapeutics 3(2) (2004) 187-197.
[69] G.K. Schwartz, S.M. Redwood, T. Ohnuma, J.F. Holland, M.J. Droller, B.C. Liu, Inhibition of invasion of invasive human bladder carcinoma cells by protein kinase C inhibitor staurosporine, Journal of the National Cancer Institute 82(22) (1990) 1753-6.
[70] S. Akinaga, K. Gomi, M. Morimoto, T. Tamaoki, M. Okabe, Antitumor activity of UCN-01, a selective inhibitor of protein kinase C, in murine and human tumor models, Cancer research 51(18) (1991) 4888-92.
[71] T. Li, S.D. Christensen, P.H. Frankel, K.A. Margolin, S.S. Agarwala, T. Luu, P.C. Mack, P.N. Lara, Jr., D.R. Gandara, A phase II study of cell cycle inhibitor UCN-01 in patients with metastatic melanoma: a California Cancer Consortium trial, Investigational new drugs 30(2) (2012) 741-8.
[72] T.M. Allen, P.R. Cullis, Liposomal drug delivery systems: from concept to clinical applications, Adv Drug Deliv Rev 65(1) (2013) 36-48.
[73] A. Roy, M. Murakami, M.J. Ernsting, B. Hoang, E. Undzys, S.D. Li, Carboxymethylcellulose-based and docetaxel-loaded nanoparticles circumvent P-glycoprotein-mediated multidrug resistance, Molecular pharmaceutics 11(8) (2014) 2592-9.
[74] K.J. Patel, I.F. Tannock, The influence of P-glycoprotein expression and its inhibitors on the distribution of doxorubicin in breast tumors, BMC cancer 9 (2009) 356.
[75] N.M. Belliveau, J. Huft, P.J. Lin, S. Chen, A.K. Leung, T.J. Leaver, A.W. Wild, J.B. Lee, R.J. Taylor, Y.K. Tam, C.L. Hansen, P.R. Cullis, Microfluidic synthesis of highly potent limit-size lipid nanoparticles for in vivo delivery of siRNA, Molecular therapy. Nucleic acids 1 (2012) e37.
[76] T. Tagami, M.J. Ernsting, S.D. Li, Efficient tumor regression by a single and low dose treatment with a novel and enhanced formulation of thermosensitive liposomal doxorubicin, Journal of controlled release : official journal of the Controlled Release Society 152(2) (2011) 303-9.
[77] M. de Smet, S. Langereis, S. van den Bosch, H. Grull, Temperature-sensitive liposomes for doxorubicin delivery under MRI guidance, Journal of controlled release : official journal of the Controlled Release Society 143(1) (2010) 120-7.

[78] T. Burkholder, C. Foltz, E. Karlsson, C.G. Linton, J.M. Smith, Health evaluation of experimental laboratory mice, Current protocols in mouse biology 2 (2012) 145-165.
[79] A. Roy, M.J. Ernsting, E. Undzys, S.-D. Li, A highly tumor-targeted nanoparticle of podophyllotoxin penetrated tumor core and regressed multidrug resistant tumors, Biomaterials 52 (2015) 335-346.
[80] D.R. Utkhede, C.P. Tilcock, Effect of lipid dose on the redistribution and blood pool clearance kinetics of Peg-modified Technetium-labeled lipid vesicles, Journal of Liposome Research 8(3) (1998) 381-390.
[81] J. Mark E. HayesCharles O. NobleFrancis C. Szoka, Remote loading of sparingly water-soluble drugs into liposomes, 2014.
[82] N. Dos Santos, K.A. Cox, C.A. McKenzie, F. van Baarda, R.C. Gallagher, G. Karlsson, K. Edwards, L.D. Mayer, C. Allen, M.B. Bally, pH gradient loading of anthracyclines into cholesterol-free liposomes: enhancing drug loading rates through use of ethanol, Biochimica et biophysica acta 1661(1) (2004) 47-60.
[83] M. Yamauchi, H. Kusano, M. Nakakura, Y. Kato, Reducing the impact of binding of UCN-01 to human alpha1-acid glycoprotein by encapsulation in liposomes, Biological & pharmaceutical bulletin 28(7) (2005) 1259-64.
[84] R. Mukthavaram, P. Jiang, R. Saklecha, D. Simberg, I.S. Bharati, N. Nomura, Y. Chao, S. Pastorino, S.C. Pingle, V. Fogal, W. Wrasidlo, M. Makale, S. Kesari, High-efficiency liposomal encapsulation of a tyrosine kinase inhibitor leads to improved in vivo toxicity and tumor response profile, International journal of nanomedicine 8 (2013) 3991-4006.
[85] S. Sur, A.C. Fries, K.W. Kinzler, S. Zhou, B. Vogelstein, Remote loading of preencapsulated drugs into stealth liposomes, Proceedings of the National Academy of Sciences of the United States of America 111(6) (2014) 2283-8.
[86] T. Shigehiro, T. Kasai, M. Murakami, S.C. Sekhar, Y. Tominaga, M. Okada, T. Kudoh, A. Mizutani, H. Murakami, D.S. Salomon, K. Mikuni, T. Mandai, H. Hamada, M. Seno, Efficient drug delivery of paclitaxel glycoside: a novel solubility gradient encapsulation into liposomes coupled with immunoliposomes preparation, PloS one 9(9) (2014) e107976.
[87] S. Modi, T.X. Xiang, B.D. Anderson, Enhanced active liposomal loading of a poorly soluble ionizable drug using supersaturated drug solutions, Journal of controlled release : official journal of the Controlled Release Society 162(2) (2012) 330-9.
[88] V. Joguparthi, T.X. Xiang, B.D. Anderson, Liposome transport of hydrophobic drugs: gel phase lipid bilayer permeability and partitioning of the lactone form of a hydrophobic camptothecin, DB-67, J Pharm Sci 97(1) (2008) 400-20.
[89] K. Park, Active liposomal loading of a poorly soluble ionizable drug, Journal of controlled release : official journal of the Controlled Release Society 162(2) (2012) 475.
[90] J.E. Lancet, J.E. Cortes, D.E. Hogge, M.S. Tallman, T.J. Kovacsovics, L.E. Damon, R. Komrokji, S.R. Solomon, J.E. Kolitz, M. Cooper, A.M. Yeager, A.C. Louie, E.J. Feldman, Phase 2 trial of CPX-351, a fixed 5:1 molar ratio of cytarabine/daunorubicin, vs cytarabine/daunorubicin in older adults with untreated AML, Blood 123(21) (2014) 3239-3246.
[91] E. Alphandéry, P. Grand-Dewyse, R. Lefèvre, C. Mandawala, M. Durand-Dubief, Cancer therapy using nanoformulated substances: scientific, regulatory and financial aspects, Expert Review of Anticancer Therapy 15(10) (2015) 1233-1255.
[92] C.M. Dawidczyk, C. Kim, J.H. Park, L.M. Russell, K.H. Lee, M.G. Pomper, P.C. Searson, State-of-the-art in design rules for drug delivery platforms: Lessons from FDA-approved

nanomedicines, Journal of controlled release : official journal of the Controlled Release Society 187 (2014) 133-144.
[93] F.N.U.A.u. Rahman, S. Ali, M.W. Saif, Update on the role of nanoliposomal irinotecan in the treatment of metastatic pancreatic cancer, Therapeutic Advances in Gastroenterology 10(7) (2017) 563-572.
[94] Q. Xu, Y. Tanaka, J.T. Czernuszka, Encapsulation and release of a hydrophobic drug from hydroxyapatite coated liposomes, Biomaterials 28(16) (2007) 2687-2694.
[95] P. Kan, C.-W. Tsao, A.-J. Wang, W.-C. Su, H.-F. Liang, A liposomal formulation able to incorporate a high content of paclitaxel and exert promising anticancer effect, Journal of Drug Delivery 2011 (2011).
[96] W.-L. Tang, W.C. Chen, A. Roy, E. Undzys, S.-D. Li, A simple and improved active loading method to efficiently encapsulate staurosporine into lipid-based nanoparticles for enhanced therapy of multidrug resistant cancer, Pharmaceutical Research 33(5) (2016) 1104-1114.
[97] Z.-Q. Wu, Q.-L. Guo, Q.-D. You, L. Zhao, H.-Y. Gu, Gambogic acid inhibits proliferation of human lung carcinoma SPC-A1 cells in vivo and in vitro and represses telomerase activity and telomerase reverse transcriptase mRNA expression in the cells, Biological and Pharmaceutical Bulletin 27(11) (2004) 1769-1774.
[98] X. Li, S. Liu, H. Huang, N. Liu, C. Zhao, S. Liao, C. Yang, Y. Liu, C. Zhao, S. Li, X. Lu, C. Liu, L. Guan, K. Zhao, X. Shi, W. Song, P. Zhou, X. Dong, H. Guo, G. Wen, C. Zhang, L. Jiang, N. Ma, B. Li, S. Wang, H. Tan, X. Wang, Q.P. Dou, J. Liu, Gambogic acid is a tissue-specific proteasome inhibitor in vitro and in vivo, Cell Reports 3(1) (2013) 211-22.
[99] M. Ishaq, M.A. Khan, K. Sharma, G. Sharma, R.K. Dutta, S. Majumdar, Gambogic acid induced oxidative stress dependent caspase activation regulates both apoptosis and autophagy by targeting various key molecules (NF-kappaB, Beclin-1, p62 and NBR1) in human bladder cancer cells, Biochimica et biophysica acta 1840(12) (2014) 3374-84.
[100] J. Yu, Q.-L. Guo, Q.-D. You, L. Zhao, H.-Y. Gu, Y. Yang, H.-w. Zhang, Z. Tan, X. Wang, Gambogic acid-induced G 2 /M phase cell-cycle arrest via disturbing CDK7-mediated phosphorylation of CDC2/p34 in human gastric carcinoma BGC-823 cells, Carcinogenesis 28(3) (2007) 632-638.
[101] T. Yi, Z. Yi, S.-G. Cho, J. Luo, M.K. Pandey, B.B. Aggarwal, M. Liu, Gambogic acid inhibits angiogenesis and prostate tumor growth by suppressing vascular endothelial growth factor receptor 2 signaling, Cancer research 68(6) (2008) 1843-1850.
[102] S. Prasad, M.K. Pandey, V.R. Yadav, B.B. Aggarwal, Gambogic acid inhibits STAT3 phosphorylation through activation of protein tyrosine phosphatase SHP-1: potential role in proliferation and apoptosis, Cancer prevention research (Philadelphia, Pa.) 4(7) (2011) 1084-1094.
[103] T. Yi, Z. Yi, S.-G. Cho, J. Luo, M.K. Pandey, B.B. Aggarwal, M. Liu, Gambogic acid inhibits angiogenesis and prostate tumor growth by suppressing VEGFR2 signaling, Cancer research 68(6) (2008) 1843-1850.
[104] V.B. Casc Rita, Raquel Helena, Neves-Costa, Ana Figueiredo, Nuno Gupta, Vineet Fonseca, Jo Eurico, Ferreira Moita Luis Potent anti-inflammatory and antiproliferative effects of gambogic acid in a rat model of antigen-induced arthritis, Mediators of Inflammation 2014 (2014) 7.

[105] M.-S. Park, N.-H. Kim, C.-W. Kang, C.-W. Oh, G.-D. Kim, Antimetastatic effects of gambogic acid are mediated via the actin cytoskeleton and NF-κB pathways in SK-HEP1 cells, Drug Development Research 76(3) (2015) 132-142.
[106] S. Wang, L. Wang, M. Chen, Y. Wang, Gambogic acid sensitizes resistant breast cancer cells to doxorubicin through inhibiting P-glycoprotein and suppressing survivin expression, Chemico-Biological Interactions 235(Supplement C) (2015) 76-84.
[107] C. Wang, W. Wang, C. Wang, Y. Tang, H. Tian, Combined therapy with EGFR TKI and gambogic acid for overcoming resistance in EGFR-T790M mutant lung cancer, Oncol Lett 10(4) (2015) 2063-2066.
[108] G. Xia, H. Wang, Z. Song, Q. Meng, X. Huang, X. Huang, Gambogic acid sensitizes gemcitabine efficacy in pancreatic cancer by reducing the expression of ribonucleotide reductase subunit-M2 (RRM2), Journal of Experimental & Clinical Cancer Research : CR 36 (2017) 107.
[109] K. Hao, X.-Q. Liu, G.-J. Wang, X.-P. Zhao, Pharmacokinetics, tissue distribution and excretion of gambogic acid in rats, European Journal of Drug Metabolism and Pharmacokinetics 32(2) (2007) 63-68.
[110] Z. Zheng, W. Ou, X. Zhang, Y. Li, Y. Li, UHPLC-MS method for determination of gambogic acid and application to bioavailability, pharmacokinetics, excretion and tissue distribution in rats, Biomedical Chromatography 29(10) (2015) 1581-1588.
[111] L. Cai, N. Qiu, M. Xiang, R. Tong, J. Yan, L. He, J. Shi, T. Chen, J. Wen, W. Wang, L. Chen, Improving aqueous solubility and antitumor effects by nanosized gambogic acid-mPEG(2000) micelles, International Journal of Nanomedicine 9 (2014) 243-255.
[112] R. Doddapaneni, K. Patel, I.H. Owaid, M. Singh, Tumor neo-vasculature targeted cationic PEGylated liposomes of gambogic acid for the treatment of triple negative breast cancer, Drug Delivery 23(4) (2016) 1232-1241.
[113] Z. Zhang, H. Qian, M. Yang, R. Li, J. Hu, L. Li, L. Yu, B. Liu, X. Qian, Gambogic acid-loaded biomimetic nanoparticles in colorectal cancer treatment, International Journal of Nanomedicine 12 (2017) 1593-1605.
[114] D. Yin, Y. Yang, H. Cai, F. Wang, D. Peng, L. He, Gambogic acid-loaded electrosprayed particles for site-specific treatment of hepatocellular carcinoma, Molecular pharmaceutics 11(11) (2014) 4107-4117.
[115] D. Zhang, Z. Zou, W. Ren, H. Qian, Q. Cheng, L. Ji, B. Liu, Q. Liu, Gambogic acid-loaded PEG–PCL nanoparticles act as an effective antitumor agent against gastric cancer, Pharmaceutical Development and Technology (2017) 1-8.
[116] J.C.M. Stewart, Colorimetric determination of phospholipids with ammonium ferrothiocyanate, Analytical Biochemistry 104(1) (1980) 10-14.
[117] A.K.K. Leung, Y.Y.C. Tam, S. Chen, I.M. Hafez, P.R. Cullis, Microfluidic mixing: a general method for encapsulating macromolecules in lipid nanoparticle systems, The Journal of Physical Chemistry B 119(28) (2015) 8698-8706.
[118] J.A. Kulkarni, Y.Y.C. Tam, S. Chen, Y.K. Tam, J. Zaifman, P.R. Cullis, S. Biswas, Rapid synthesis of lipid nanoparticles containing hydrophobic inorganic nanoparticles, Nanoscale 9(36) (2017) 13600-13609.
[119] T. Li, L. Zhang, L. Tong, Q. Liao, High-throughput salting-out-assisted homogeneous liquid–liquid extraction with acetonitrile for determination of baicalin in rat plasma with high-performance liquid chromatography, Biomedical Chromatography 28(5) (2014) 648-653.
[120] L. Clary, G. Verderone, C. Santaella, P. Vierling, Membrane permeability and stability of liposomes made from highly fluorinated double-chain phosphocholines derived from

diaminopropanol, serine or ethanolamine, Biochimica et Biophysica Acta (BBA) - Biomembranes 1328(1) (1997) 55-64.
[121] A.M. Firsov, E.A. Kotova, E.A. Korepanova, A.N. Osipov, Y.N. Antonenko, Peroxidative permeabilization of liposomes induced by cytochrome c/cardiolipin complex, Biochimica et Biophysica Acta (BBA) - Biomembranes 1848(3) (2015) 767-774.
[122] N. Dos Santos, L.D. Mayer, S.A. Abraham, R.C. Gallagher, K.A.K. Cox, P.G. Tardi, M.B. Bally, Improved retention of idarubicin after intravenous injection obtained for cholesterol-free liposomes, Biochimica et Biophysica Acta (BBA) - Biomembranes 1561(2) (2002) 188-201.
[123] G.J.R. Charrois, T.M. Allen, Drug release rate influences the pharmacokinetics, biodistribution, therapeutic activity, and toxicity of pegylated liposomal doxorubicin formulations in murine breast cancer, Biochimica et Biophysica Acta (BBA) - Biomembranes 1663(1–2) (2004) 167-177.
[124] H.-I. Chang, M.-K. Yeh, Clinical development of liposome-based drugs: formulation, characterization, and therapeutic efficacy, International Journal of Nanomedicine 7 (2012) 49-60.
[125] A. Kheirolomoom, L.M. Mahakian, C.-Y. Lai, H.A. Lindfors, J.W. Seo, E.E. Paoli, K.D. Watson, E.M. Haynam, E.S. Ingham, L. Xing, R.H. Cheng, A.D. Borowsky, R.D. Cardiff, K.W. Ferrara, Copper-doxorubicin as a nanoparticle cargo retains efficacy with minimal toxicity, Molecular pharmaceutics 7(6) (2010) 1948-1958.
[126] A. Dicko, S. Kwak, A.A. Frazier, L.D. Mayer, B.D. Liboiron, Biophysical characterization of a liposomal formulation of cytarabine and daunorubicin, International journal of pharmaceutics 391(1) (2010) 248-259.
[127] A. Lupescu, K. Jilani, C. Zelenak, M. Zbidah, N. Shaik, F. Lang, Induction of programmed erythrocyte death by gambogic acid, Cellular Physiology and Biochemistry 30(2) (2012) 428-438.
[128] Q. Guo, Q. Qi, Q. You, H. Gu, L. Zhao, Z. Wu, Toxicological studies of gambogic acid and its potential targets in experimental animals, Basic & Clinical Pharmacology & Toxicology 99(2) (2006) 178-184.
[129] X. Li, S. Liu, H. Huang, N. Liu, C. Zhao, S. Liao, C. Yang, Y. Liu, C. Zhao, S. Li, X. Lu, C. Liu, L. Guan, K. Zhao, X. Shi, W. Song, P. Zhou, X. Dong, H. Guo, G. Wen, C. Zhang, L. Jiang, N. Ma, B. Li, S. Wang, H. Tan, X. Wang, Q.P. Dou, J. Liu, Gambogic Acid Is a Tissue-Specific Proteasome Inhibitor In Vitro and In Vivo, Cell Reports 3(1) (2013) 211-222.
[130] S. Prasad, M.K. Pandey, V.R. Yadav, B.B. Aggarwal, Gambogic acid inhibits STAT3 phosphorylation through activation of protein tyrosine phosphatase SHP-1: potential role in proliferation and apoptosis, Cancer prevention research 4(7) (2011) 1084-1094.
[131] K. Zhao, S. Zhang, X. Song, Y. Yao, Y. Zhou, Q. You, Q. Guo, N. Lu, Gambogic acid suppresses cancer invasion and migration by inhibiting TGFbeta1-induced epithelial-to-mesenchymal transition, Oncotarget 8(16) (2017) 27120-27136.
[132] D. Wang, C.R. Stockard, L. Harkins, P. Lott, C. Salih, K. Yuan, D. Buchsbaum, A. Hashim, M. Zayzafoon, R. Hardy, O. Hameed, W. Grizzle, G.P. Siegal, Immunohistochemistry in the evaluation of neovascularization in tumor xenografts, Biotechnic & histochemistry : official publication of the Biological Stain Commission 83(0) (2008) 179-189.
[133] M.E. Hayes, C.O. Noble, F.C. Szoka, Remote loading of sparingly water-soluble drugs into liposomes, Google Patents, 2014.
[134] N. Dos Santos, K.A. Cox, C.A. McKenzie, F. van Baarda, R.C. Gallagher, G. Karlsson, K. Edwards, L.D. Mayer, C. Allen, M.B. Bally, pH gradient loading of anthracyclines into

cholesterol-free liposomes: enhancing drug loading rates through use of ethanol, Biochimica et Biophysica Acta (BBA) - Biomembranes 1661(1) (2004) 47-60.
[135] W.-L. Tang, W.-H. Tang, W.C. Chen, C. Diako, C.F. Ross, S.-D. Li, Development of a rapidly dissolvable oral pediatric formulation for mefloquine using liposomes, Molecular pharmaceutics 14(6) (2017) 1969-1979.
[136] M. Mahmud, A. Piwoni, N. Filiczak, M. Janicka, J. Gubernator, Long-circulating curcumin-loaded liposome formulations with high incorporation efficiency, stability and anticancer activity towards pancreatic adenocarcinoma cell lines in vitro, PloS one 11(12) (2016) e0167787.
[137] X. Shi, X. Lan, X. Chen, C. Zhao, X. Li, S. Liu, H. Huang, N. Liu, D. Zang, Y. Liao, P. Zhang, X. Wang, J. Liu, Gambogic acid induces apoptosis in diffuse large B-cell lymphoma cells via inducing proteasome inhibition, Sci Rep 5 (2015) 9694.
[138] Q. Qi, N. Lu, C. Li, J. Zhao, W. Liu, Q. You, Q. Guo, Involvement of RECK in gambogic acid induced anti-invasive effect in A549 human lung carcinoma cells, Mol Carcinog 54 Suppl 1 (2015) E13-25.
[139] L.H. Wang, J.Y. Yang, S.N. Yang, Y. Li, G.F. Ping, Y. Hou, W. Cui, Z.Z. Wang, W. Xiao, C.F. Wu, Suppression of NF-kappaB signaling and P-glycoprotein function by gambogic acid synergistically potentiates adriamycin -induced apoptosis in lung cancer, Curr Cancer Drug Targets 14(1) (2014) 91-103.
[140] Y. Yang, X. Sun, Y. Yang, X. Yang, H. Zhu, S. Dai, X. Chen, H. Zhang, Q. Guo, Y. Song, F. Wang, H. Cheng, X. Sun, Gambogic acid enhances the radiosensitivity of human esophageal cancer cells by inducing reactive oxygen species via targeting Akt/mTOR pathway, Tumour Biol 37(2) (2016) 1853-62.
[141] M. He, L. Ro, J. Liu, C.-C. Chu, Folate-decorated arginine-based poly(ester urea urethane) nanoparticles as carriers for gambogic acid and effect on cancer cells, Journal of Biomedical Materials Research Part A 105(2) (2017) 475-490.
[142] R. Doddapaneni, K. Patel, I.H. Owaid, M. Singh, Tumor neovasculature-targeted cationic PEGylated liposomes of gambogic acid for the treatment of triple-negative breast cancer, Drug Deliv 23(4) (2016) 1232-41.
[143] G. Haran, R. Cohen, L.K. Bar, Y. Barenholz, Transmembrane ammonium sulfate gradients in liposomes produce efficient and stable entrapment of amphipathic weak bases, Biochimica et Biophysica Acta (BBA) - Biomembranes 1151(2) (1993) 201-215.
[144] V. Joguparthi, B.D. Anderson, Liposomal delivery of hydrophobic weak acids: Enhancement of drug retention using a high intraliposomal pH, Journal of Pharmaceutical Sciences 97(1) 433-454.
[145] G. World Health Organization, Switerland, World Malaria Report 2015, 2015.
[146] C. Caminade, S. Kovats, J. Rocklov, A.M. Tompkins, A.P. Morse, F.J. Colón-González, H. Stenlund, P. Martens, S.J. Lloyd, Impact of climate change on global malaria distribution, Proceedings of the National Academy of Sciences of the United States of America 111(9) (2014) 3286-3291.
[147] E.L. Flannery, A.K. Chatterjee, E.A. Winzeler, Antimalarial drug discovery approaches and progress towards new medicines, Nat Rev Micro 11(12) (2013) 849-862.
[148] A.A. Ali, N.A. Charoo, D.B. Abdallah, Pediatric drug development: formulation considerations, Drug Development and Industrial Pharmacy 40(10) (2014) 1283-1299.

[149] P. Schlagenhauf, M. Adamcova, L. Regep, M.T. Schaerer, S. Bansod, H.-G. Rhein, Use of mefloquine in children - a review of dosage, pharmacokinetics and tolerability data, Malaria Journal 10(1) (2011) 292.
[150] N.J. White, Antimalarial drug resistance, Journal of Clinical Investigation 113(8) (2004) 1084-1092.
[151] L.H. du Plessis, C. Helena, E. van Huysteen, L. Wiesner, A.F. Kotzé, Formulation and evaluation of Pheroid vesicles containing mefloquine for the treatment of malaria, Journal of Pharmacy and Pharmacology 66(1) (2014) 14-22.
[152] T.K.M. Mbela, E. Deharo, A. Haemers, A. Ludwig, Biopharmaceutics: submicron oil-in-water emulsion formulations for mefloquine and halofantrine: effect of electric-charge inducers on antimalarial activity in mice, Journal of Pharmacy and Pharmacology 50(11) (1998) 1221-1225.
[153] N.I.o.H. (NIH), Best Pharmaceuticals for Children Act (BPCA) Priority list of needs in pediatric therapeutics for 2014. .
<https://bpca.nichd.nih.gov/prioritization/status/Documents/Priority_List_07082014.pdf>, 2014).
[154] P. Dey, S. Maiti, Orodispersible tablets: A new trend in drug delivery, Journal of natural science, biology, and medicine 1(1) (2010) 2-5.
[155] Y. Tahara, K. Toko, Electronic Tongues–A Review, IEEE Sensors Journal 13(8) (2013) 3001-3011.
[156] G.S. Duffó, E.Q. Castillo, Development of an artificial saliva solution for studying the corrosion behavior of dental alloys, CORROSION 60(6) (2004) 594-602.
[157] C.S. Rae, I. Wei Khor, Q. Wang, G. Destito, M.J. Gonzalez, P. Singh, D.M. Thomas, M.N. Estrada, E. Powell, M.G. Finn, M. Manchester, Systemic trafficking of plant virus nanoparticles in mice via the oral route, Virology 343(2) (2005) 224-235.
[158] S. Strauch, E. Jantratid, J.B. Dressman, H.E. Junginger, S. Kopp, K.K. Midha, V.P. Shah, S. Stavchansky, D.M. Barends, Biowaiver monographs for immediate release solid oral dosage forms: mefloquine hydrochloride, Journal of Pharmaceutical Sciences 100(1) (2011) 11-21.
[159] Astree Analyzer hardware user's guide, Alpha MOS, Toulouse, France, 2011, pp. 15-128.
[160] P.T. Ingvarsson, M. Yang, H. Mulvad, H.M. Nielsen, J. Rantanen, C. Foged, Engineering of an inhalable DDA/TDB liposomal adjuvant: A quality-by-design approach towards optimization of the spray drying process., Pharmaceutical Research 30(11) (2013) 2772-2784.
[161] M.B. Jiménez-Díaz, S. Viera, J. Ibáñez, T. Mulet, N. Magán-Marchal, H. Garuti, V. Gómez, L. Cortés-Gil, A. Martínez, S. Ferrer, M.T. Fraile, F. Calderón, E. Fernández, L.D. Shultz, D. Leroy, D.M. Wilson, J.F. García-Bustos, F.J. Gamo, I. Angulo-Barturen, A new in vivo screening paradigm to accelerate antimalarial drug discovery, PloS one 8(6) (2013) e66967.
[162] P. Khadka, J. Ro, H. Kim, I. Kim, J.T. Kim, H. Kim, J.M. Cho, G. Yun, J. Lee, Pharmaceutical particle technologies: An approach to improve drug solubility, dissolution and bioavailability, Asian Journal of Pharmaceutical Sciences 9(6) (2014) 304-316.
[163] T. Yang, F.-D. Cui, M.-K. Choi, J.-W. Cho, S.-J. Chung, C.-K. Shim, D.-D. Kim, Enhanced solubility and stability of PEGylated liposomal paclitaxel: In vitro and in vivo evaluation, International journal of pharmaceutics 338(1–2) (2007) 317-326.
[164] L. Hu, X. Tang, F. Cui, Solid lipid nanoparticles (SLNs) to improve oral bioavailability of poorly soluble drugs, Journal of Pharmacy and Pharmacology 56(12) (2004) 1527-1535.
[165] C. Kirby, J. Clarke, G. Gregoriadis, Effect of the cholesterol content of small unilamellar liposomes on their stability in vivo and in vitro, Biochemical Journal 186(2) (1980) 591-598.

[166] C.D. Medley, J. Kay, Y. Li, J. Gruenhagen, P. Yehl, N.P. Chetwyn, Quantification of residual solvents in antibody drug conjugates using gas chromatography, Analytica Chimica Acta 850 (2014) 92-96.
[167] D.L.P. Joanne T. Walker, and James Segretario Quantitation of Residual Dimethylsulfoxide in a Drug Substance (Bisnaf ide) by Reversed-Phase High-Performance Liquid Chromatography, Journal of Chromatographic Science 34 (1996) 513-516.
[168] W. Ciesielski, W. Jedrzejewski, Z.H. Kudzin, R. Skowroński, J. Drabowicz, A new method for the iodometric determination of sulphoxides, Talanta 35(12) (1988) 969-972.
[169] T.I.C.f.H. (ICH), Impurities: guidance for residual solvents Q3C(R6), The International Council for Harmonisation (ICH), 2016.
[170] S. Modi, B.D. Anderson, Determination of drug release kinetics from nanoparticles: overcoming pitfalls of the dynamic dialysis method, Molecular pharmaceutics 10(8) (2013) 3076-3089.
[171] S. Souza, A review of in vitro drug release test methods for nano-sized dosage forms, Advances in Pharmaceutics 2014 (2014) 12.
[172] S.A. Abouelmagd, B. Sun, A.C. Chang, Y.J. Ku, Y. Yeo, Release kinetics study of poorly water-soluble drugs from nanoparticles: Are we doing it right?, Molecular pharmaceutics 12(3) (2015) 997-1003.
[173] V. Kannan, P. Balabathula, L.A. Thoma, G.C. Wood, Effect of sucrose as a lyoprotectant on the integrity of paclitaxel-loaded liposomes during lyophilization, Journal of Liposome Research 25(4) (2015) 270-278.
[174] A. Chaudhury, S. Das, R.F.S. Lee, K.-B. Tan, W.-K. Ng, R.B.H. Tan, G.N.C. Chiu, Lyophilization of cholesterol-free PEGylated liposomes and its impact on drug loading by passive equilibration, International journal of pharmaceutics 430(1–2) (2012) 167-175.
[175] G. Mattheolabakis, T. Nie, P.P. Constantinides, B. Rigas, Sterically Stabilized Liposomes Incorporating the Novel Anticancer Agent Phospho-Ibuprofen (MDC-917): Preparation, Characterization, and In Vitro/In Vivo Evaluation, Pharmaceutical Research 29(6) (2012) 1435-1443.
[176] M. de Vrese, A. Stegelmann, B. Richter, S. Fenselau, C. Laue, J. Schrezenmeir, Probiotics—compensation for lactase insufficiency, The American Journal of Clinical Nutrition 73(2) (2001) 421s-429s.
[177] W.F. Wolkers, H. Oldenhof, F. Tablin, J.H. Crowe, Preservation of dried liposomes in the presence of sugar and phosphate, Biochimica et Biophysica Acta (BBA) - Biomembranes 1661(2) (2004) 125-134.
[178] E.M. Merisko-Liversidge, G.G. Liversidge, Drug nanoparticles: formulating poorly water-soluble compounds, Toxicologic Pathology 36(1) (2008) 43-48.
[179] H. Mu, R. Holm, A. Müllertz, Lipid-based formulations for oral administration of poorly water-soluble drugs, International journal of pharmaceutics 453(1) (2013) 215-224.
[180] Y. Yun, Y.W. Cho, K. Park, Nanoparticles for oral delivery: Targeted nanoparticles with peptidic ligands for oral protein delivery, Advanced Drug Delivery Reviews 65(6) (2013) 822-832.
[181] J. Renukuntla, A.D. Vadlapudi, A. Patel, S.H.S. Boddu, A.K. Mitra, Approaches for enhancing oral bioavailability of peptides and proteins, International journal of pharmaceutics 447(1–2) (2013) 75-93.

[182] G. Fricker, T. Kromp, A. Wendel, A. Blume, J. Zirkel, H. Rebmann, C. Setzer, R.-O. Quinkert, F. Martin, C. Müller-Goymann, Phospholipids and lipid-based formulations in oral drug delivery, Pharmaceutical Research 27(8) (2010) 1469-1486.
[183] Y. Zhu, M. Wang, J. Zhang, W. Peng, C.K. Firempong, W. Deng, Q. Wang, S. Wang, F. Shi, J. Yu, X. Xu, W. Zhang, Improved oral bioavailability of capsaicin via liposomal nanoformulation: preparation, in vitro drug release and pharmacokinetics in rats, Archives of Pharmacal Research 38(4) (2015) 512-521.
[184] T. Meyer, C. Surber, L.E. French, E. Stockfleth, Resiquimod, a topical drug for viral skin lesions and skin cancer, Expert Opinion on Investigational Drugs 22(1) (2013) 149-159.
[185] J.P. Adler-Moore, R.T. Proffitt, Amphotericin B lipid preparations: what are the differences?, Clinical Microbiology and Infection 14 (2008) 25-36.
[186] W.-L. Tang, W.-H. Tang, S.-D. Li, Cancer theranostic applications of lipid-based nanoparticles, Drug Discovery Today 23(5) (2018) 1159-1166.
[187] S. Moghassemi, A. Hadjizadeh, Nano-niosomes as nanoscale drug delivery systems: An illustrated review, Journal of Controlled Release 185 (2014) 22-36.
[188] C. Théry, L. Zitvogel, S. Amigorena, Exosomes: composition, biogenesis and function, Nature Reviews Immunology 2 (2002) 569.
[189] J.S. Lee, J. Feijen, Polymersomes for drug delivery: Design, formation and characterization, Journal of Controlled Release 161(2) (2012) 473-483.
[190] J.F. Lovell, C.S. Jin, E. Huynh, H. Jin, C. Kim, J.L. Rubinstein, W.C.W. Chan, W. Cao, L.V. Wang, G. Zheng, Porphysome nanovesicles generated by porphyrin bilayers for use as multimodal biophotonic contrast agents, Nature Materials 10 (2011) 324.
[191] M.S. Valic, G. Zheng, Rethinking translational nanomedicine: insights from the ‘bottom-up’ design of the Porphysome for guiding the clinical development of imageable nanomaterials, Current Opinion in Chemical Biology 33 (2016) 126-134.